Design of Hemispherical End Magnetorheological Finishing Tool for Diamagnetic and Paramagnetic Materials and its Experimental Investigations

A Dissertation submitted

in partial fulfilment of the requirements for

the degree of

Master of Engineering

in

Production Engineering

by

Harsh Kansal

Registration No.: 801585011

Under the Supervision of

Dr. Anant Kumar Singh

Assistant Professor

MECHANICAL ENGINEERING DEPARTMENT

THAPAR UNIVERSITY, PATIALA

June, 2017

CERTIFICATE

I hereby declare that the thesis entitled "**Design of Hemispherical End Magnetorheological Finishing Tool for Diamagnetic and Paramagnetic Materials and its Experimental Investigations**" is an authentic record of my work carried out as requirements for the award of the degree of **Master of Engineering** in **Production Engineering** at **Thapar University, Patiala** under the supervision of **Dr. Anant Kumar Singh**, Assistant Professor, Mechanical Engineering Department, Thapar University, Patiala during July, 2015 to July, 2017. No part of the matter embodied in this report has been submitted to any other university or institute for the award of any degree.

Harsh Kansal

Date: 31-JULY-2017

Harsh Kansal

It is certified that the above statement made by the student is correct to the best of my knowledge and belief.

31/07/2017

Dr. Anant Kumar Singh
Assistant Professor
Mechanical Engineering Department
Thapar University, Patiala - 147004

Dedicated to
My Grandparents
And
Parents.

Acknowledgements

I take this opportunity to express my profound gratitude and deep regards to my supervisor **Dr. Anant Kumar Singh** for his exemplary guidance, monitoring and constant encouragement which helped me in completing this work.

It has been a blessing for me to spend many opportune moments under the guidance of the perfectionist at the acme of professionalism. The present work is testimony to his activity, inspiration and ardent personal interest, taken by him during the course of his work in its present form. I am grateful to **Dr. S. K. Mohapatra**, Sr. Professor and Head, Mechanical Engineering Department for providing the facilities for the successful completion of this work.

I would like to express my sincere gratitude to all who directly or indirectly helped me for the successful completion of this report.

HARSH KANSAL

Abstract

Magnetorheological nano-finishing tool is a new advance finishing tool which is used to finish the flat surfaces of non-ferromagnetic (diamagnetic and paramagnetic) and ferromagnetic workpiece at the nano-meter level. Magnetorheological polishing fluid is used as finishing medium in this process. There is high need of nano-finishing of diamagnetic materials and paramagnetic materials such as copper, aluminium, etc. in various industries. Having excellent property of being light weight, nano-finished aluminium has wide applications in aerospace and automobile industries. Some industries like laser, aerospace, dentistry and metal optics etc. widely use highly finished copper mirrors. As these are soft and chemically reactive material, its surface finishing at nano level is difficult task. To fulfill this need, a new magnetorheological technique for precise finishing of diamagnetic materials and paramagnetic materials has been developed. Permanent magnets have been used for design and fabrication of the new tool namely hemispherical end magnetorheological finishing (HEMRF) tool. The finishing tool along with magnetorheological polishing fluid and workpiece has been modelled as well as simulated in Maxwell Ansoft V13 (student version) software to analyse the magnetic flux density distribution in the working gap. Experimentation has been performed to examine the performance of newly developed finishing tool to finish the flat surface of aluminium and copper workpieces. Magnetorheological polishing fluid is filled in the working gap of 1.5 mm that contains the cutting edged abrasives which results in material removal from the workpiece surface forming micro chips. The detailed study of the finishing process using statistical design of experiments for nano-finishing of copper is conducted. The performance of finishing process has been evaluated with the identified significant process parameters. Modeling of surface roughness with the effect of magnetic normal force at different finishing cycles has been proposed for the newly developed finishing process. Surface characteristics of both polished and unpolished workpiece are analyzed with the atomic force microscopy (AFM) and scanning electron microscopy (SEM). The results obtained from finite element analysis and experimentation assures that the newly developed hemispherical end magnetorheological finishing process (HEMRF) is capable to nano-finish of diamagnetic materials such as copper alloy etc.

Keywords: *Diamagnetic materials; Hemispherical; Modelling; Magnetorheological; Nano-finishing; Paramagnetic materials; Permanent magnets; Simulation; Surface roughness.*

Contents

List of Figures

List of Tables

Nomenclature

C	percentage concentration of carbonyl iron particles,%
CIP	carbonyl iron particles
M	abrasive mesh size
N	rotational speed of the tool, r.p.m
S	percentage concentration of abrasive particles i.e. Silicon carbide %
SiC	Silicon carbide abrasive particles
R_a	arithmetic average of the absolute values of the roughness profile heights over the evaluation length, nm
R_q	root mean square average of the roughness profile heights over the evaluation length, nm
R_z	average maximum height of the roughness profile, nm
$R_{a\ initial}$	initial value of surface roughness parameter R_a, nm
$R_{a\ final}$	final value of surface roughness parameter R_a, nm
$\%\Delta R_a$	percentage reduction in surface roughness parameter R_a, %

Greek Symbols

χ_m	magnetic susceptibility of carbonyl iron particles (CIPs), m^3/kg
μ_{mr}	relative permeability of the MR polishing fluid, H/m
μ_0	magnetic permeability of free space, H/m
σ	yield stress of copper in shear, MPa
τ	magnetorheological polishing fluid shear stress, MPa

Acronyms

BEMRF	Ball end magnetorheological finishing
FE	Finite element
HEMRF	Hemispherical end magnetorheological finishing
MR	Magnetorheological
MRAFF	Magnetorheological abrasive flow finishing
MRAH	Magnetorheological abrasive honing

Chapter 1

Introduction

1.1 Introduction

Surface finishing is an expensive but still an important phase of overall production processes. The final finishing operations are the most labour demanding area in the manufacturing of precision, which often require as much as 15% of the total manufacturing cost [Gorana et al., 2004]. The alignment, dimensional accuracy and quality of surface finish are obtained by the use of finishing processes.

The different types of traditional finishing processes are known as grinding, lapping, honing etc. The traditional finishing processes are less compatible regarding the shape and size of the workpiece material for finishing. Heat is generated in large amount during the grinding may results in different types of defects such as micro-crack, micro-cutting etc. This may result in the failure of the material. Lapping is usually carried out to finish flat surfaces, whereas honing is usually carried out to finish cylindrical (external and internal) surfaces. The lesser control over the forces during the traditional finishing processes often results in surface finish with many flaws [Shaw, 1996]. The fatigue life of the material of the workpiece is more affected by the poorly finished surface [Bayoumi et al., 1995]. As such the traditional finishing processes are not capable of producing the 3D surface finish which results in expensive equipment and long processing time. In order to overcome the drawbacks, the advanced finishing processes are developed for finishing of 3D surfaces in the level of nanometer surface finish.

1.2 Traditional Finishing Processes

To finish the surface of workpiece, several finishing processes such as lapping, honing, grinding, etc. are available. These are basic finishing processes which are generally used for pre-machined surfaces. These processes have limitation that forces applied for finishing operation is not controllable that is why it may lead to defects in the surface of workpiece. Moreover, finishing obtained from these processes is not the desired one to fulfill the requirement of high level nano-finishing. Various commonly used traditional finishing processes are given below.

1.2.1 Lapping

Lapping is one of the low speed, low pressure operation that results in tremendous accuracy, modification of small imperfections in shape, improvement in surface finish and also exceptionally close fitted structure. Generally used lapping process is flat surface lapping [Lynah et al., 1989]. The two surfaces are rubbed together in case of lapping with the help of abrasive particles (silicon carbide, aluminum oxide etc.) as shown in Fig. 1.1. The downward force exerted on the pressure plate helps the abrasive to be in contact with the rotating back up wheel for the finishing.

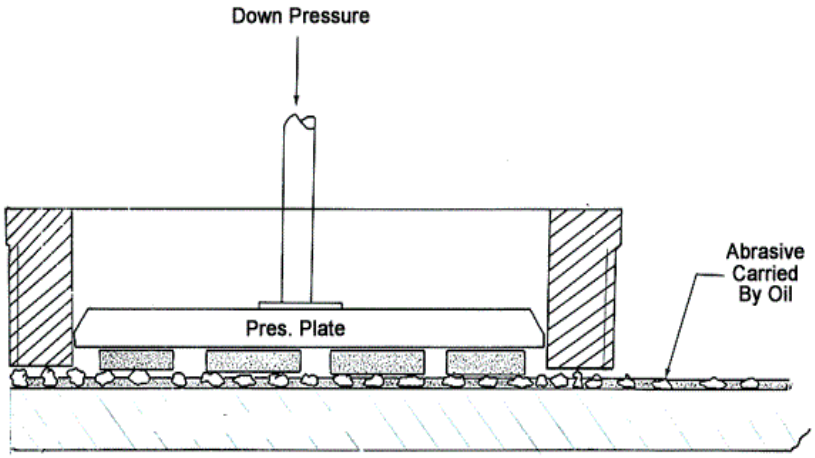

Figure 1.1: Lapping Process [W.1]

1.2.2 Honing

Honing is one of the most important methods for finishing and polishing of the component. The main purpose of honing process is used to remove the material and to generate a required surface finish [Khanna and Lal, 2010]. In order to produce a better surface finish where there is a high requirement of geometric and form accuracy the honing process is used [Schnitzler, 2001]. With the help of this process a narrow dimensional, geometric tolerances and low value of roughness of workpiece surfaces can be attained. It is normally used after the boring or drilling for the finishing of the component [Tolinski, 2008]. The mechanism of honing process for the finishing of internal surface of a hallow cylinder as shown in Fig. 1.2. The honing tool consists of honing stone (generally made from silicon carbide, cubic boron nitride etc.). The rotational and reciprocation movement of the honing stone is used for the finishing of cylinder of an internal combustion engine, air bearing

spindle, gears etc. Limitation of the honing process is that it can be used only for cylindrical surfaces and also have low finishing rate.

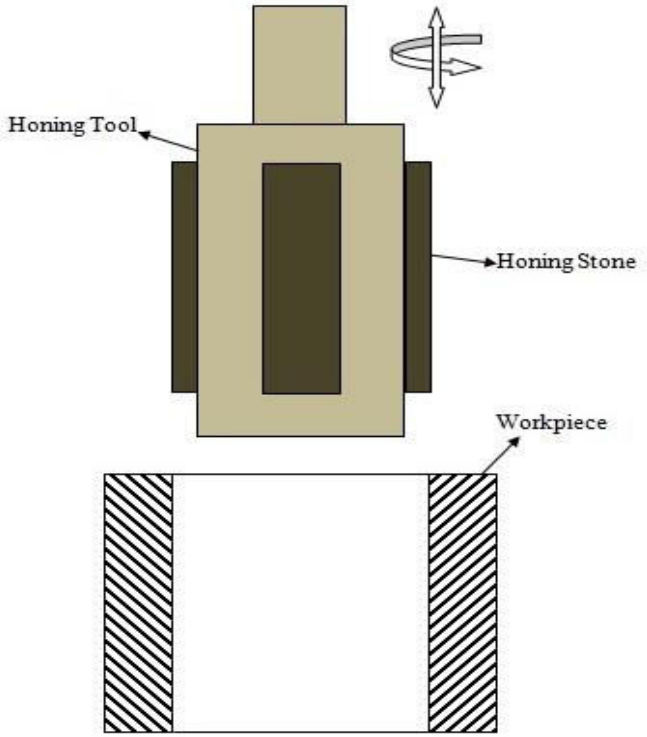

Figure 1.2: Mechanism of honing process [Schmitt and Bahre, 2014]

1.2.3 Grinding

Grinding is a finishing process in which material removal is done by relative movement of grinding wheel (having abrasive particles) on surface to be finish as shown in Fig. 1.3. Grinding process can finish the surface value up to roughness value of 1 µm. Grinding is one of the easiest available among various machining processes for finishing of the different types of material and which can also be difficult to machine by any other finishing processes ranging from simple rubber to the hardest material [Khanna and Lal, 2010]. Most extensively used abrasive finishing process is grinding that uses the abrasive particles which to forms a spongy body bonding together in order to finish the component [Shaw, 1996]. Grinding wheel get blunt after some time and needs to be regrind at regular intervals. It is done by diamond tool. It removes the fractured abrasives from the bond. Process of regrinding of grinding wheel is quite expensive and time consuming. Normal force acting in grinding operation is high that leads to the sub surface damage.

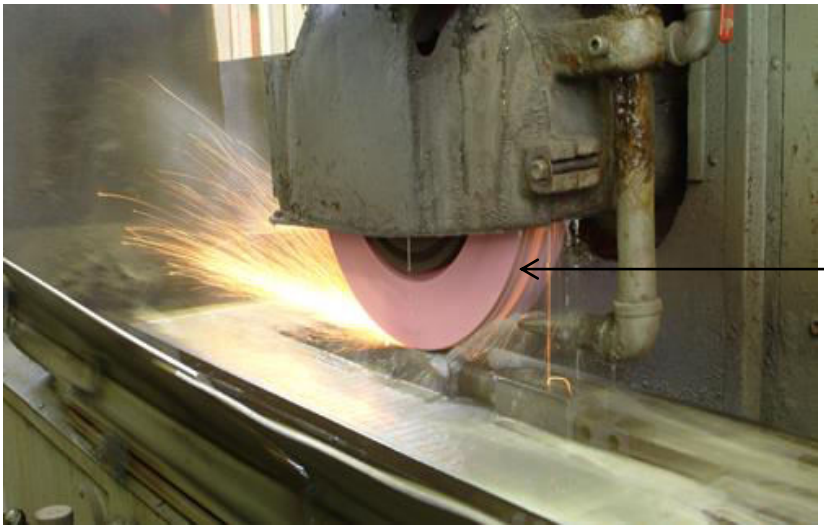

Figure 1.3: Grinding process [W.2.]

1.3 Advanced Finishing Processes

Processes which are used to finish the surface precisely upto a nanometer value of the surface roughness without any surface defects are called advance finishing processes. In these processes finishing action is done by small abrasive particles. Force acting on workpiece surface is quite small as it is applied by abrasive particles so there is less chance of surface rupture or fracture. It also leads to increase of tool life.

Advanced finishing processes are divided in two categories:

1) Without external control of forces.
2) With external control of forces.

1.3.1 Advanced Finishing Processes without External Control of Forces

These are the finishing processes which are used for ultrafine finishing of surfaces but finishing force exerted on surface of workpiece due to the abrasives particles cannot be controlled. Force exerting on surface of workpiece is not uniform. Some of the examples of advance finishing processes without external control of forces are given below:

1.3.1.1 Abrasive Flow Machining Process (AFM)

Abrasive flow machining process is the finishing process which is used to deburr and polish internal surfaces of cylindrical objects. AFM process is of three type 1-way AFM, 2-way AFM and orbital AFM. A 2-way AFM process is shown in Fig. 1.4; in which finishing is performed by abrasive particles (in a visco elastic polymeric medium) which are allowed to reciprocate up and down with the help of two vertically opposed pistons. Good abrasion is

obtained inside the cylinder where fluidic medium is allowed to flow through narrow passage. AFM process can finish the surface as good as 0.05 µm. [Jain et al., 1999]

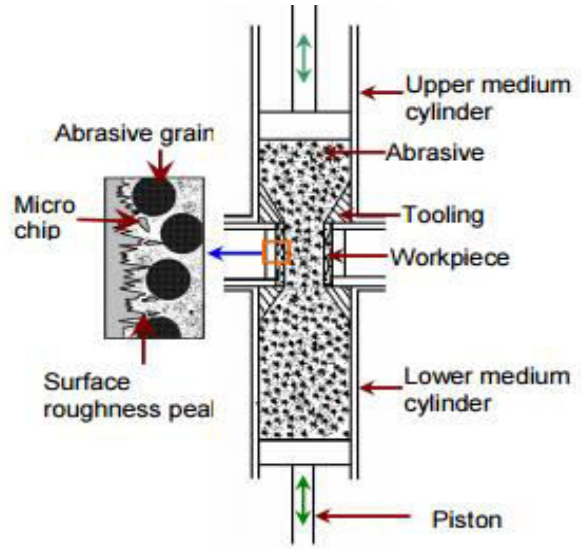

Figure 1.4: 2-way Abrasive Flow Machining process experimental setup [Jain et al., 1999]

1.3.1.2 Elastic Emission Machining

This method has the capability to surface finish the workpiece at the atomic level by mechanical action and produces a physically undisturbed surface. In this process ultrafine abrasive particle strikes the individual atom and separate out from the parent surface as shown in Fig. 1.5.

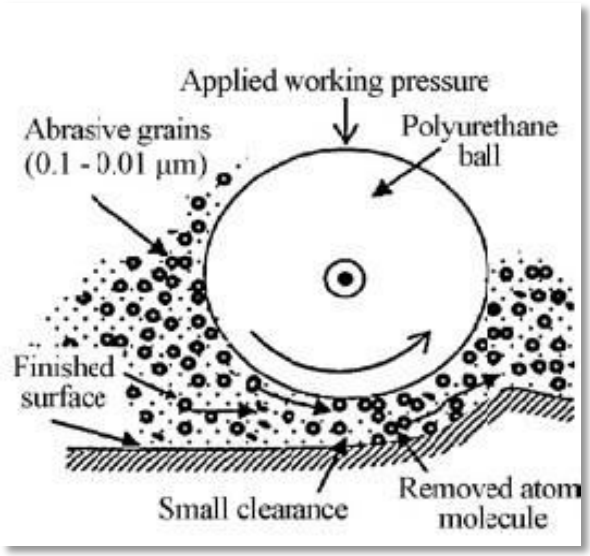

Figure 1.5: Elastic Emission Machining Process [Jain, 2009]

It has been found that the process of material elimination is a surface energy phenomenon in which every abrasive particle eliminates a number of atoms after making contact with the workpiece surface [Mori et al., 1987].

1.3.1.3 Chemo-mechanical Machining

Chemo-Mechanical polishing involves a chemical reaction between the workpiece and silica slurry, the rejoinder reaction product so obtained is removed by mechanical action [Nanz et. al, 1995] and results in a defect free surface [Komanduri, 1997]. This process includes the combination of both mechanical and chemical actions. It gives the higher average polishing rate (200nm/min), and keeps changing with polishing time [Jain, 2009]. A schematic of chemo-mechanical polishing process is shown in Fig.1.6.

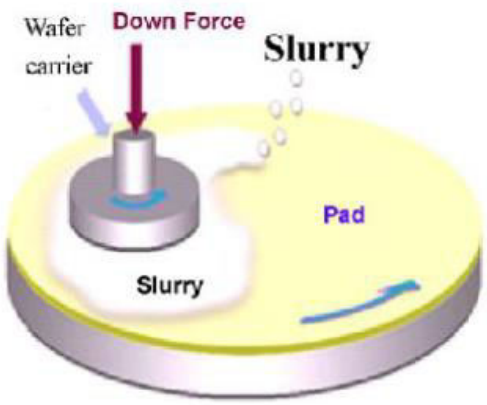

Figure 1.6: Chemo-mechanical polishing process [Nanz et al., 1995].

This process is used in semiconductor manufacturing industries and electronic industry for polishing of silicon, optical and glass disk etc [Jain, 2009]. It is used as surface finishing process that excludes the problem of surface damaging, brittle fracture, and abrasion scratching etc. due to abrasives. This process is limited to the finishing of flat surfaces only.

1.3.2 Advanced Finishing Processes with External Control of Forces

Several advance finishing operations have been developed in which force exerted on surface of workpiece can be controlled by controlling current given to electromagnet coil or by changing the working gap between the workpiece and tool. Such finishing processes make use of a special kind of smart fluid called magnetorheological (MR) fluid. MR polishing fluid is special kind of fluid which is made up of carbonyl iron particles (magnetic pariticles) and Silicon carbide abrasive particles (SiCs) with base fluid (grease, paraffin oil). In the presence

of magnetic field (created by permanent magnet or electromagnet coil), CIPs get aligned in a straight line due to dipolar moment. Due to magnetic field MR polishing fluid stiffens. SiCs get entrapped in between chain of CIPs and workpiece. Thus SiCs particles perform finishing action with their relative movement along the workpiece.

In finishing processes with external control of forces, forces acting on workpiece for finishing action can be controlled by varying the current given to the electromagnet coil. With the change in the electric current, the magnetic flux density in the finishing area due to which normal force acted by the abrasives on the workpiece changes [Jain, 2009]. Also, as the current increases, magnetic flux due to electromagnet coil increases. Due to more magnetic flux, MR polishing fluid gets stiffer and gives good finishing action. Several advance finishing processes with external control of forces are listed below.

- Magnetorheological Jet Finishing Process.
- Magnetorheological Abrasive Flow Finishing (MRAFF) Process.
- Ball end MR Finishing (BEMRF) Process
- Magnetic Float Polishing
- Magnetorheological abrasive honing process (MRAH)

1.3.2.1 Magnetorheological Jet Finishing Process

The Magnetorheological jet finishing have been newly developed for finishing of parts with a freeform optics, steep concave, cavities etc. The experimental setup of magnetorheological jet finishing is as shown in Fig. 1.7.

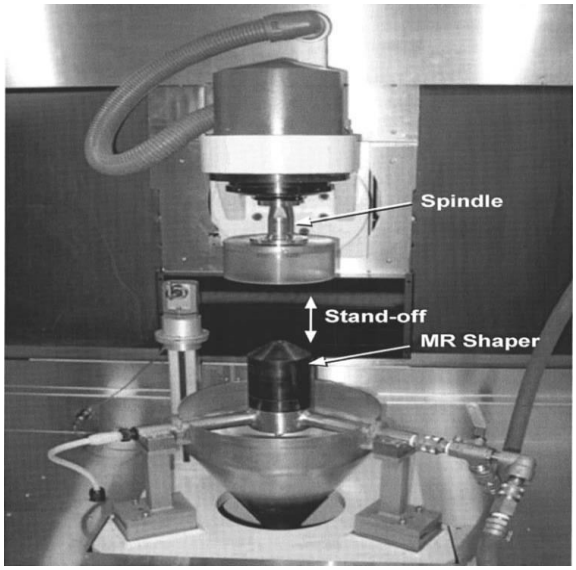

Figure 1.7: Experimental setup of magnetorheological jet finishing

[Kordonski et al., 2006]

This type of finishing process is a modification of MRF process in which MR fluid mixed with magnetic abrasive is jetted into the internal surface of the work material and is magnetized by an axial magnetic field when it flows out of the nozzle. The magnetic abrasive particles finish the internal surface of the work material more precisely. The jet snapshot image of magnetic abrasive jet finishing is as shown in Fig. 1.8. The jet of water loses its coherence when passes through the nozzle. When the magnet is off, the jet of MR fluid passes through nozzle losses its coherence due to its high viscosity.

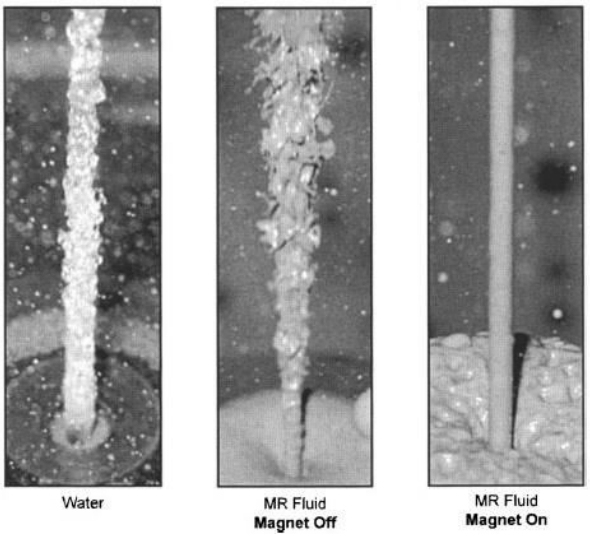

Figure 1.8: Jet snapshot image (velocity- 30 m/s, nozzle diameter- 2 mm)
[Kordonski et al., 2006]

Kordonski et al., (2006) performed their experiment on fused glass silica with newly developed magnetorheological jet finishing process. The finishing was done by MR fluid (usually mixed with magnetic abrasive particles). The experimentation was performed both on flat and concave shaped workpiece. The result concluded that the surface roughness of flat and concave shaped work material reduces to 0.013 µm and 0.040 µm.

1.3.2.2 Magnetorheological Abrasive Flow Finishing (MRAFF) Process

Magnetorheological abrasive flow finishing process is the recently invented finishing process. In Abrasive flow finishing process, the finishing medium acts as amenable stage and overcomes shape constraint intrinsic in almost all the traditional processes. In order to overcome the limitation of an abrading forces produced during the abrasive flow finishing processes process along with the combination of magnetorheological finishing for controlling the rheological properties, a newer finishing process was introduced known as magnetorheological abrasive flow finishing process [Seok et al., 2007] as shown in Fig. 1.9.

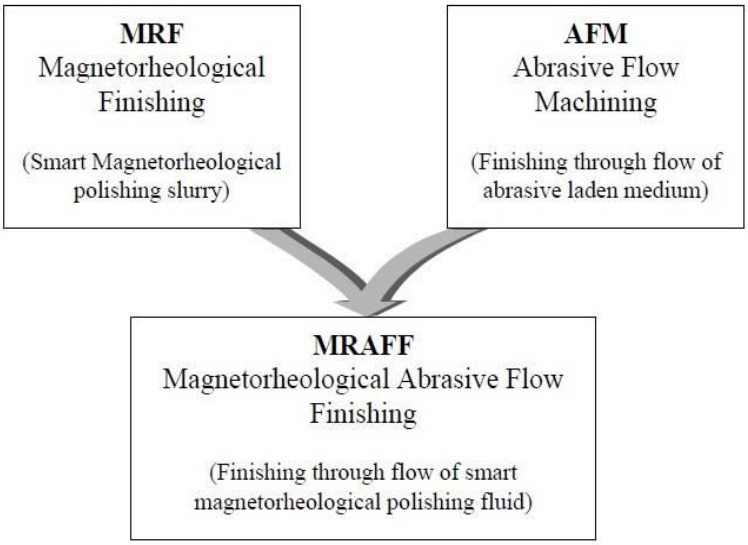

Figure 1.9: Development of magnetorheological abrasive flow finishing process [Jha and Jain, 2006]

MRAFF process consisted of CIPs particles, abrasive particles along with the base media. Due to the increase in magnetic field, the CIPs particles formed a chain over the abrasive particle for the precise finishing. The amount of material sheared from the peaks of the workpiece surface by an abrasive grains depends on the bonding strength provided by the magnetic field induced structure of MR-polishing fluid and the extrusion pressure applied by a piston. The level to which the magnetic particles stiffened is strongly dependent on the external magnetic field for controlling the viscosity of the fluid [Kordonski et al., 1999]. The MRAFF process is mainly used for the finishing of complex internal and external geometry, optical flats, spheres etc. A schematic diagram showing MRAFF process is shown in Fig. 1.10.

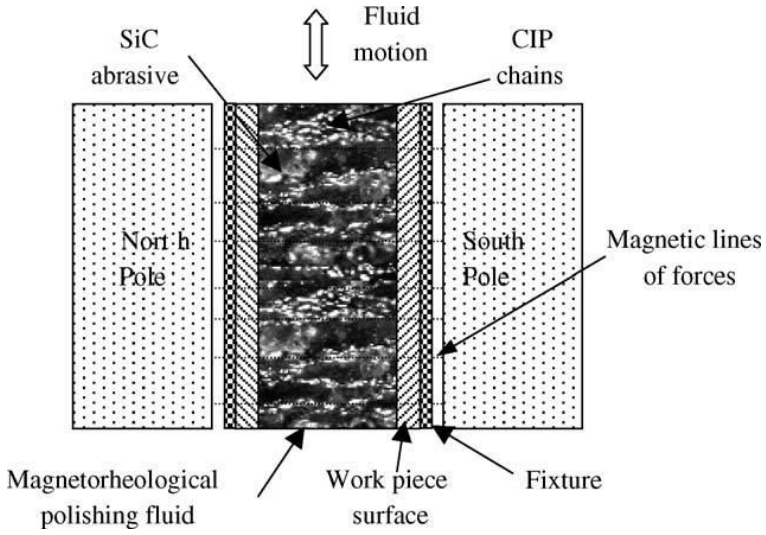

Figure 1.10: Schematic Diagram showing MRAFF Process [Jha and Jain, 2006]

1.3.2.3 Ball End Magnetorheological Finishing (BEMRF) Process

It is the finishing process which is used to precisely finish 3-D surface with the help of MR polishing fluid. A core is rotated over the workpiece surface and MR polishing fluid is allowed to flow through core. Magnetic field is produced by electromagnet coil wounded over the core. In the presence of magnetic field, MR polishing fluid gets stiff enough and forms a ball shaped structure which performs the finishing action. Due to this ball shaped structure this process is called ball end magnetorheological finishing process (BEMRF). Normal force acting on workpiece surface by MR polishing fluid can be controlled by changing electromagnet current given to the coil. [Singh et al., 2012] The setup of ball end magnetorheological finishing process is given in Fig. 1.11.

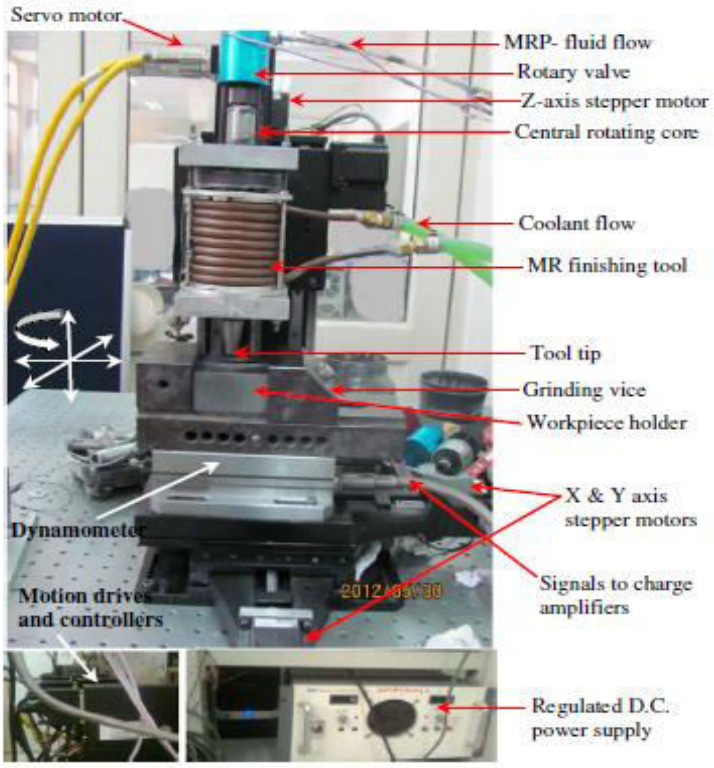

Figure 1.11: Ball End Magnetorheological Finishing process [Singh et al., 2012]

1.3.2.4 Magnetic Float Polishing

The various types of finishing processes have been developed for finishing of either flat surfaces, cylindrical surfaces or their combinations leading to complex 3-D surfaces. Magnetic float polishing process is used for the precise finishing of the bearing rollers and ceramics balls with the help of fine abrasive particles. The experimental setup and mechanism of magnetic float polishing process is shown in Fig. 1.12.

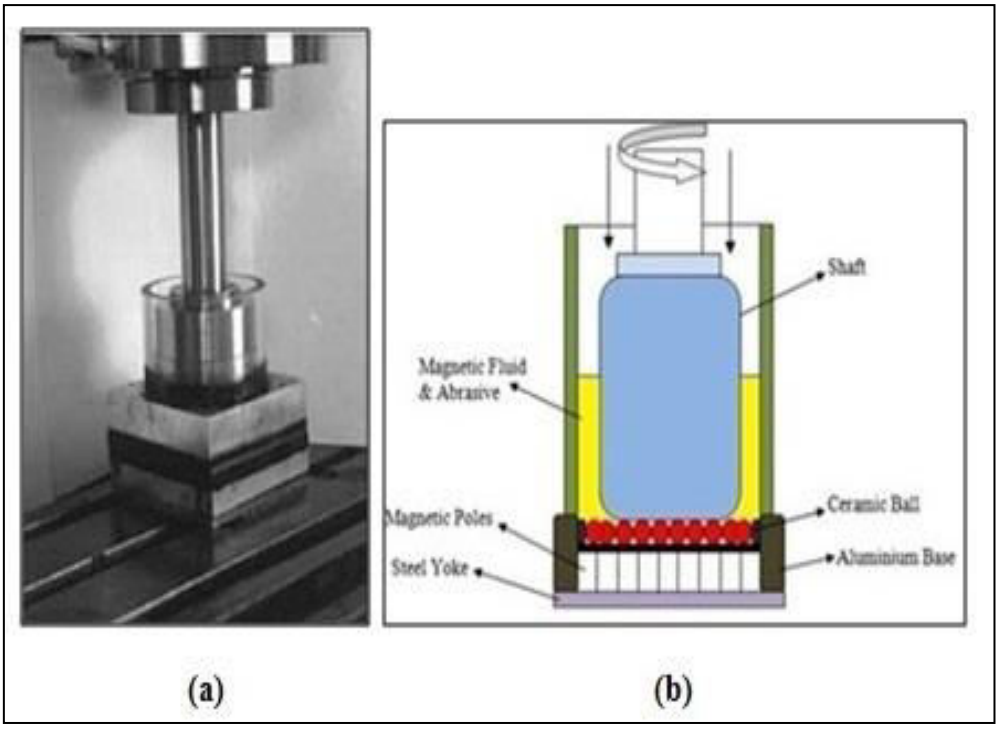

Figure 1.12: (a) Photograph of the experimental setup used in finishing Si_3N_4 balls by small batch Magnetic float polishing apparatus (b) Mechanism of Magnetic Float Polishing process. [Komanduri *et al*., 1999]

MFP finishing process is based upon the ferro-hydrodynamic behaviour of magnetic fluid that rise a non-magnetic float and abrasive particles suspended in it during the application of magnetic field. The drive shaft is moved downward to contact the spherical balls and press them downward to reach the desired force level. The balls are polished by means of a relative motion between the balls and the abrasive particles under the influence of the force [Jha and Jain, 2005].

1.3.2.5 Magnetorheological Abrasive Honing (MRAH) Process

Magnetorheological abrasive honing process is a finishing process which is used to finish external surface of cylindrical objects. Cylindrical workpiece is attached with spindle and allowed to rotate in MR polishing fluid as shown in Fig. 1.13. MR polishing fluid flows over the workpiece surface and is pushed up and own with the help of plunger. Magnetic field is produced by external permanent magnet which is placed across outer cylinder. Under the influence of magnetic field, CI particles present in MR polishing fluid undergoes dipolar interaction and form a chain like structure. Due to rotatory and reciprocatory motion of MR polishing fluid abrasive present in MR polishing fluid apply normal and tangential force on surface of workpiece which results in removal of workpiece and performs finishing action.

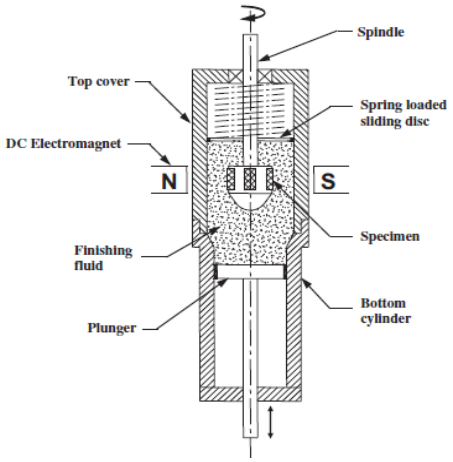

Figure 1.13: Magnetorheological Abrasive Honing Process [Sadiq and Shunmugam, 2010]

1.4 Advantages of using Magnetorheological Fluids in Finishing Operations

Using MR polishing fluids in finishing operations have the following advantages over conventional finishing processes.

- Finishing forces exerted on the surface of workpiece can be regulated by controlling the magnetizing current as per the properties of workpiece surfaces. These are not possible in conventional finishing processes.
- MR based finishing is capable to reduce surface roughness upto nano level.
- MR finishing processes are used to precisely finish the surfaces of any shape.
- Closer tolerances can be achieved.
- Decreasing the wear and friction losses.
- Used for finishing of internal and external surfaces.
- Reduces the surface defects (such micro cracks, cavity etc.).

1.5 Applications of Magnetorheological Finishing Processes

- Optical industries
- Aerospace industries
- Automobile industries
- Medical industries
- Defense sector

Chapter 2

Literature Review

2.1 Literature Review

Researchers have developed many conventional and advance ultrafine finishing processes as per the requirement of surface finishing at various level and applications. These have been developed from traditional to ultrafine finishing processes. Traditional finishing processes are developed such as flexible abrasive tools, honing, ball burnishing, grinding, etc. However, the requirement of ultrafine finishing of surface was still an issue due to various reasons like high temp, intended abrasive particles and uncontrollable finishing forces etc. For these problems several advance finishing processes were developed. In this chapter, the literature review of various authors in the field of advanced finishing processes (with/without the help of magnetic properties) have been discussed and their brief observations have been drawn from the authors work and are represented here for better understanding.

[Gheisari et al., 2014] developed a magnetorheological finishing process for ultra-precision finishing of Aluminum work material (cylindrical type). The MR fluid consisted of water based suspension of micron sized diamond particles. The process parameters were (current- 9A and working gap- 5 mm). The initial surface roughness of the work material was 170 nm. The experimentation was conducted in three sets. In first set, the work material speed varied from 250-1000 rpm. In second set, the process time varies from 20-100 min. In third case, the effect of a fast ram on the surface roughness was considered. The results concluded that with the increase in rotational speed (1000 rpm), the surface roughness value improved by 40 nm. With the increase in finishing time (90 min), the surface roughness value decreased by 42 nm whereas, when the fast ram (with 0.5 m/sec) was applied, the surface roughness value improved by 78 nm.

[Shankar et al., 2010] performed theoretical and experiment investigation on R-AFF process for comparing the performance of ΔRa and MR at different rotational on three types of work material namely Al alloy, Al alloy/SiC MMC with 10% SiC and Al alloy/SiC MMC with 15% SiC. The results concluded that the rotational abrasive flow finishing yields better

hardness and higher MRR as compared to the abrasive flow finishing in case of Al alloy/SiC (10%) MMC as illustrated in Fig. 2.1.

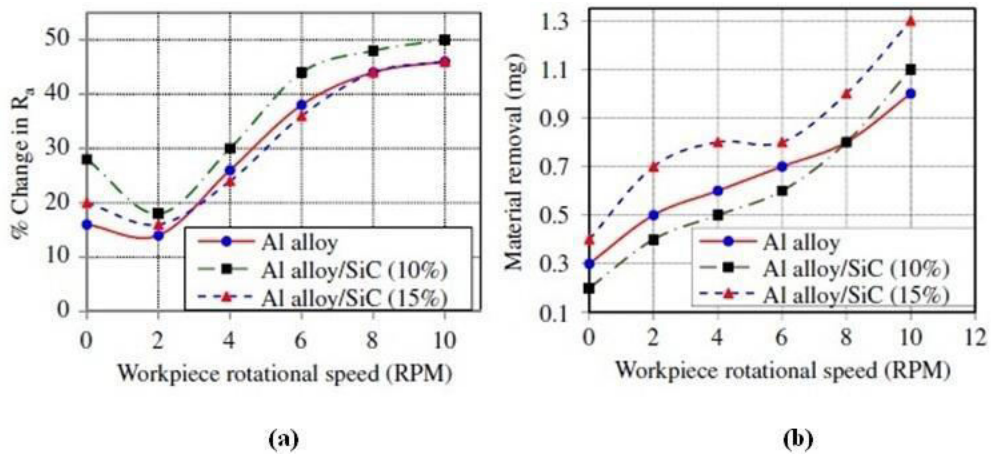

Figure 2.1: Effect of workpiece on rotational speed on (a) Ra (b) MR for the three workspaces (speed-550 RPM, pressure- 6.25 MPa, M-10%) in AFF (RPM- 0) and in RAFF [Shankar et al., 2010]

[Seok et al., 2007] presented a study on the fabrication of curved surfaces by using a magnetorheological fluid finishing process. In this research paper the fabrication method of curved surfaces depending on the silicon-based micro structures by magnetorheological finishing process was studied. The explanations were made between the procedures of analysis and evaluation of surface characteristics of the workpiece. The effect of the magnetic field around the tool a assembly was investigated using a finite element method.

[Saraeian et al., 2016] optimized the MAF process parameters working gap, abrasive size and rotation speed for finishing of AISI321 steel by applying full factorial method at three level. The MAF fluid was prepared with CIPs, Sic abrasive and SAE40 oil. The finishing was done on workpiece 50 mm lengths for 20 min. The three level for rotation speed (355, 500, 1000 rpm), working gap (0.5, 1, 2mm) and abrasive size (100, 200, 300 mesh) was used. The best result was achieved at 1mm gap, 500 rpm and with abrasive size 100 mesh. Working gap is the most effective parameter for finishing followed by rotation speed.

[Singh et al., 2013] compared the theoretical and experimental experiments on MRR with different working gaps by using ball-end MR finishing tool for finishing ferromagnetic material. The theoretical observation was carried out by using the mathematical formulas for calculating the normal forces at different working gap. The finishing was carried out with MR polishing fluid (usually a mixture of 20% SiC abrasive powder, 20% CIPs and 60% base

medium). The results concluded that the surface roughness decrease to 0.028 µm with 0.66 mm working gap as illustrated in Fig. 2.2.

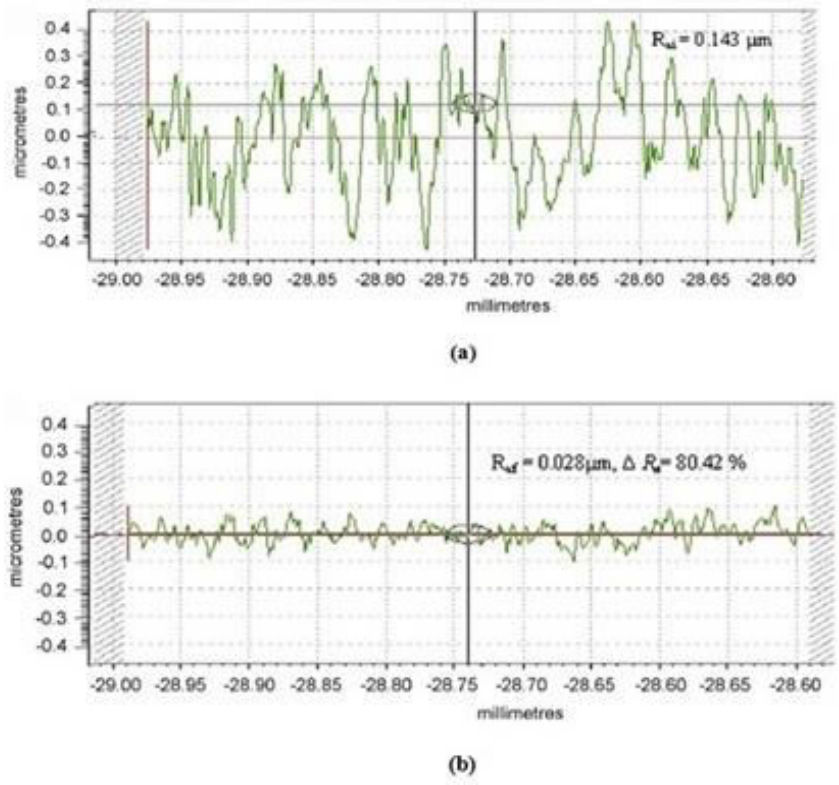

Figure 2.2: Surface roughness profile (a) initial (b) after BEMRF at working gap 0.66 mm with Fn- 16.35 N [Singh et al., 2013]

[Wang and Hu, 2005] compared the performance of surface roughness and MRR with finishing time by using a magnetic assisted finishing process for finishing of Ly12 aluminum alloy, 316L stainless steel and H62 brass. The experimentation was carried out with 4 different types of abrasive particle were Al_2O_3/Fe (20% Al_2O_3), TiC/Fe (20% TiC), TiC/Fe (35% TiC), TiC/Fe (7% TiC) along with a finishing fluid (stearinic acid and transformer oil). The results concluded that the value of MRR increases whereas the surface roughness value decreases with increase in finishing time.

[Sadiq and Shunmugam, 2010] performed their experiment on magnetorheological abrasive based honing process for finishing of stainless steel (SS 316L) and mild steel (AISI 1020) at a different magnetic flux density with the rotation speed of 310 RPM. The result concluded that a very little change in Ra (6.7% at 0T, no change at 0.65T) was observed during finishing of the mild steel material, whereas a larger improvement in surface finish (43.5% at 20 min) and (41.7% at 0.65T) was observed in case of stainless steel.

[Niranjan et al., 2014] studied on the workpiece surface roughness by changing the MR fluid with new composition of fluid called bidisperse MR fluid. MRP fluid was prepared with different compositions and compared with each other for best results. They uses two different grades of CIP's (CS & HS grade). The average particle size of CIP's of CS & HS are 6–7 μm and 1.8–2.3 μm, respectively and SiC abrasive particles size 19 μm. The best results are obtained with this composition CIP 16 vol. % CS grade, 4 vol. % HS grade, 25 vol. % SiC abrasive.

[Sidpara and Jain, 2013] performed an experiment to measure the forces on the freeform surface in real time. The rotational speed of the tool, angles of curvature of the workpiece and feed rate on tangential, normal and axial forces which are the parameters of the process were given by the researchers. As compared to other forces, it was found that the normal force was more dominant. Model of tangential force and normal force acting on the workpiece was also proposed to improve the understanding of the workpiece abrasive particles interaction in the MR polishing fluid which was based on finishing process. Experimental and theoretical results were compared to validate the proposed models. From the results it was concluded that both normal and tangential forces decreases with increases in the angle of curvature ($\theta = 5^o$, 15^o and 25^o) and increases with the increase in rotations.

[Saraswathamma et al., 2015] studied the effect of input parameters (machine process parameters and fluid composition parameters) using BEMRF process on the silicon wafer. The authors used cerium oxide as abrasives and deionized water as carrier medium. Experimental plan was prepared using statistical design of experiments. Magnetizing current, working gap and core rotational speed were used as process parameters in the design and percentage reduction in surface roughness was considered as response. Using ANOVA, effect of each parameter was analyzed. It was observed that maximum contribution was made by the working gap followed by magnetizing current and core rotational speed. The average Ra of silicon wafer decreased from 457nm to 89.8nm.

[Cheng et al., 2008] worked on wheel shaped polishing tool for finishing of K9 glass mirror by the use of MR fluid (usually a mixture of 57.34% silicon oil, 33.84% carbonyl iron powder, 6% cerium agent and 2.82% stabilizing agent). Two sets of experimental studies were conducted (with/without abrasive particles). Initial roughness value was Ra- 1.52 nm. The results concluded that roughness value after 10 min was Ra- 0.61 nm and the surface roughness decreased to 0.47 nm (with time- 20 min, voltage- 2V, viscosity- 8.9 Pa).

[Singh et al., 2012] performed their experiments on ball end MR finishing tool for finishing of ferromagnetic magnetic material with different projections (such as flat, 30^o, 45^o and 50^o curve surface) as illustrated in Fig. 2.3. The finishing was carried out with MR fluid (usually a mixture of 20% CIPs, 20% SiC abrasive powder and 60% visco plastic base medium. The results concluded that the surface roughness of flat, 30^o, 45^o and 50^o curve surface reduces to 19.7 nm, 30.4 nm, 71.0 nm and 123.7 nm. With the process parameters (speed- 500 RPM, current- 4 Amp, time- 30 min and working gap- 0.66 mm), the results concluded that the surface roughness reduces from 142.9 nm to 19.7 nm after 120 min of a time interval as illustrated in Fig. 2.4 and Fig. 2.5.

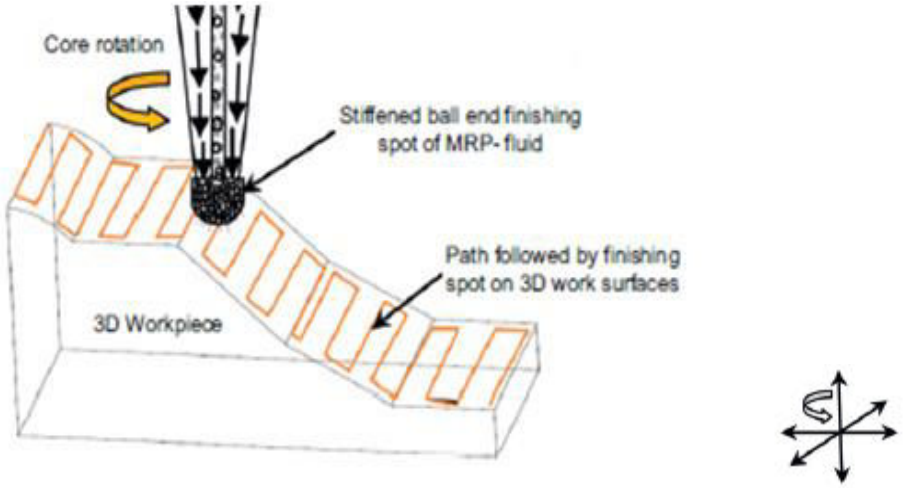

Figure 2.3: Schematic of a ball end MR finishing process of the typical 3D workpiece surfaces [Singh et al., 2012]

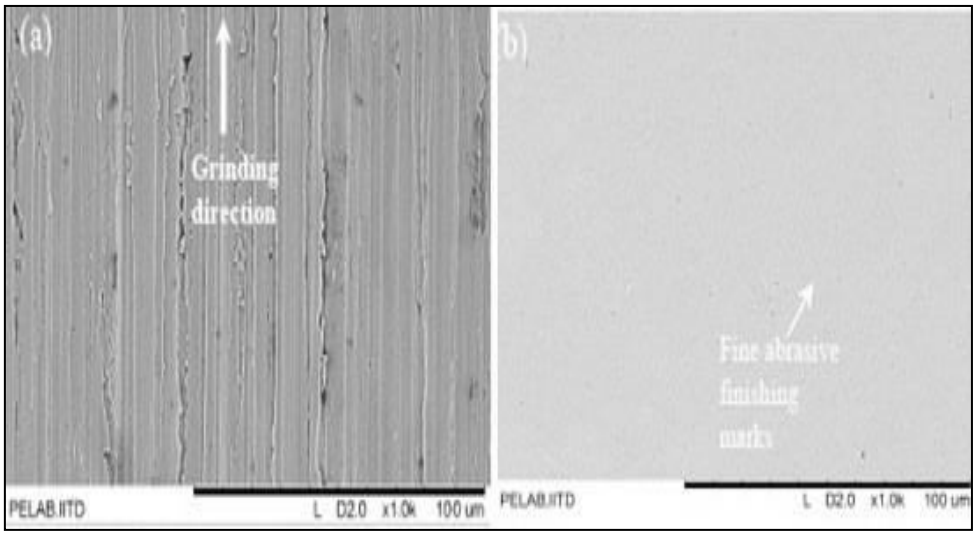

Figure 2.4: SEM micrograph at 1000x (a) initial surface and (b) finished surface after ball end MR finishing with 120 min of finishing time [Singh et al., 2012]

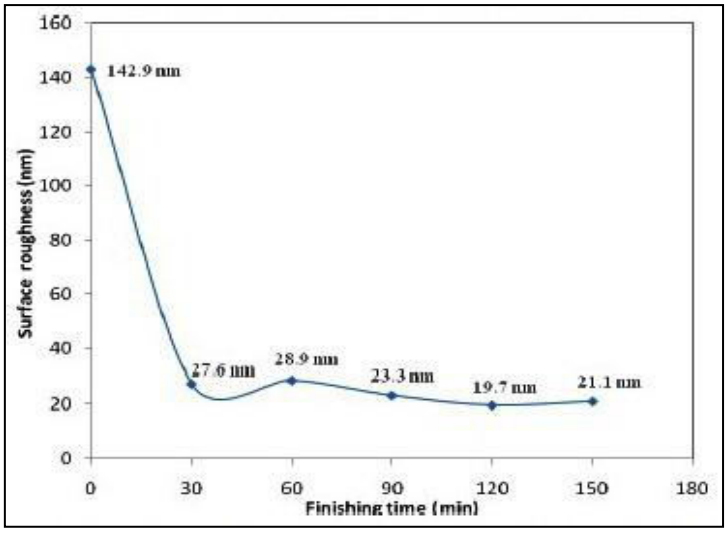

Figure 2.5: Effect of finishing time on surface roughness value of ferromagnetic workpiece [Singh et al., 2012]

[Wang and Lee, 2009] worked on magnetic finishing process for precise finishing of cylindrical type SKD-110 mild steel. The finishing medium included silicone gel, steel grid (SG) and silicon carbide. The results concluded that the surface roughness with magnetic field shows better results. With the increase in the quantity of SiC particles, the surface roughness decreases, whereas MRR increases.

[Singh et al., 2004] worked on magnetic abrasive process in order to determine the effect of process variable on the surface finish by using a mixture of 75% iron and 25% SiC with different parameters. It is concluded that the value of surface roughness ΔRa was better within the parameters of voltage-11.5 V, working gap-1.25 mm, speed-180 RPM improving the surface roughness values as shown in Fig. 2.6.

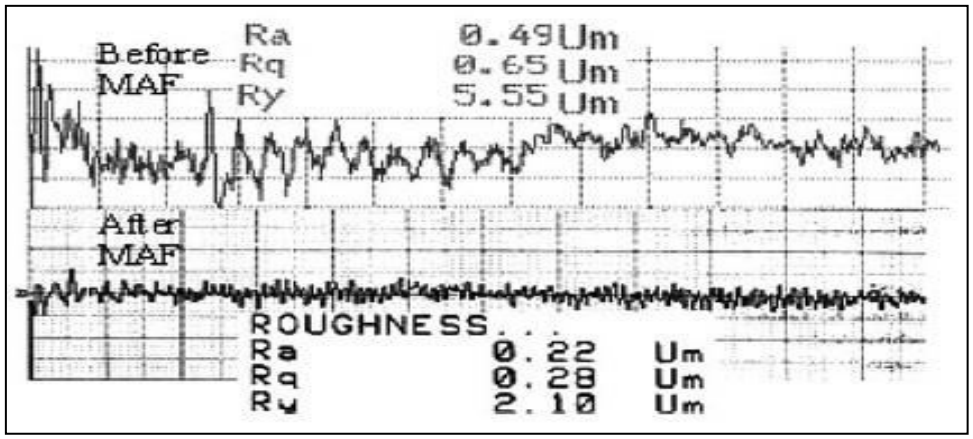

Figure 2.6: Surface roughness values before and after finishing [Singh et al., 2004]

Cheng et al., 2010] developed a dual axis MRF tool with internal magnet for finishing of BK7 mirror. The finishing was carried out with the help of MR polishing fluid (includes 10% CeO_2 abrasive particles). The mathematical modeling was carried out in order to calculate material removal. The process parameters were (magnetic field strength- 860KA/m and polishing time- 1 min). The results obtained by the experimentation showed that the value of surface roughness decreases from 328.42 nm to 42.93 nm.

[Jha and Jain, 2006] evaluated the effect of different grades of CIPs particles (CS and HS) on the surface finish by using MRAFF process for finishing of stainless steel material. MR polishing fluid (a mixture of 20% SiC abrasive powder, 20% CIPs and 60% visco plastic base medium) with which the finishing was done. The results concluded that higher improvement in surface roughness between 0.32-0.09 µm was made by using CIPs (CS) with SiC-800 mesh size as illustrated in Table 2.1.

Table 2.1: Surface roughness results [Jha and Jain, 2006]

Expt. No.	CIP dia. (D_{CIP}) (µm)	SiC dia. (D_{SiC}) (µm)	D_{CIP}/ D_{SiC}	Initial Ra (µm)	Final Ra (µm)	ΔRa^a (µm)	%ΔRa
1.	18.0 (CS)	19.00	0.95	0.32	0.09	-0.23	-17.87
2.	18.0 (CS)	12.67	1.42	0.28	0.17	-0.11	-39.28
3.	18.0 (CS)	7.50	2.40	0.31	0.23	-0.08	-25.80
4.	3.5 (HS)	19.00	0.18	0.26	0.23	-0.03	-11.54
5.	3.5 (HS)	12.67	0.28	0.28	0.24	-0.04	-14.28
6.	3.5 (HS)	7.50	0.47	0.25	0.24	-0.01	-4.00

[Das et al., 2010] worked on rotational magnetorheological abrasive flow finishing process for finishing of stainless steel work material. The finishing was carried out with the help of MR polishing (usually contains 26.6% Fe powder, 13.5% SiC abrasive with base fluid). The preliminary experimentation along with design of experiment and response surface regression analysis were also carried out in order to determine the effect of abrasive particle size, rotational per minute of magnet and finishing time on the surface roughness. The results concluded that with the increase in RPM (up to 150) and finishing time (1600 sec) the surface roughness found to be better upto 20%, whereas with the decrease in abrasive particle size, the surface roughness founds to be better upto 14%.

[Niranjan and Jha 2014] worked on BEMRF for finishing of mild steel. The authors made use of bidisperse MRP fluid. The results concluded that the surface roughness value decreases to Ra- 0.1406 µm, Rq- 0.1967 µm and Rz- 1.1403 µm as illustrated in Fig. 2.7.

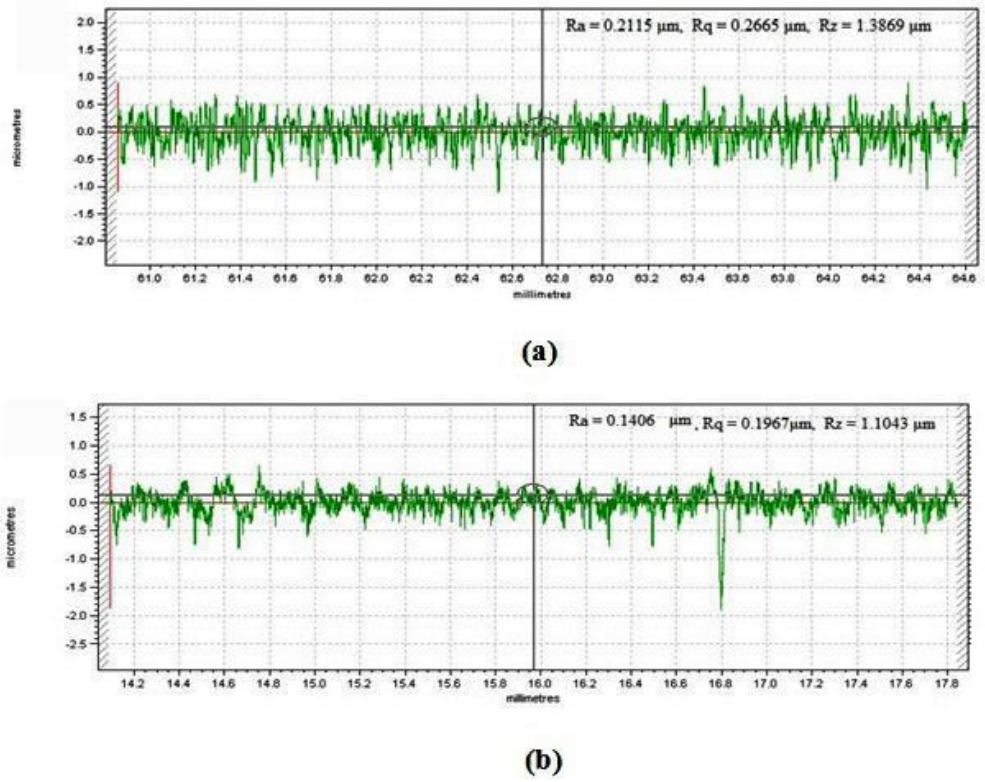

Figure 2.7: (a) Surface roughness profile before finish (b) Surface roughness profile after finish using bidisperse MR fluid (sample 3) [Niranjan and Jha, 2014]

[Kang et al., 2012] designed and developed a newly built magnetic abrasive finishing (with double dipole tip set) for finishing of austenite 304 stainless steel tubes. The mixed type magnetic abrasive consists of (80% iron particles and 20% magnetic abrasive) along with a soluble type barrel finishing compound. The process parameters were (magnetic flux- 1.26-1.29 T, speed- 500-30000 rpm, processing time- 10 to 20 min and workpiece pole tip clearance- 0.3 mm). The initial surface roughness of 304 stainless steel was 2-3 µm. The results concluded that at 10000 rpm the surface roughness decreased to 0.1 µm (for 10 min) whereas, the surface roughness at 10000 rpm decreased to 0.01 µm (20 min).

[Judal et al., 2013] developed a new vibration assisted magnetic abrasive finishing process for finishing of aluminium workpiece. The finishing was carried out with the help of steel grit and Al_2O_3 abrasive. The effect of different process parameters such as magnetic flux density, rotational speed, size of abrasive particles and frequency on the material removal rate

was investigated. The result concluded that with the increase in rotation speed and magnetic flux density and frequency of vibration, the value of material removal rate increases. The surface roughness value Ra decreased by 0.18 µm.

2.2 Comparison of Capabilities of Different Finishing Processes

The comparison of results produced by various surface finishing processes in micro/nano meter level reading is reported in this section. The advanced finishing processes provide better surface finish than the traditional finishing processes mainly <50 nm (Ra value) while finishing over the different substrate material. Cheng et al., [2010] developed a dual axis MRF tool for finishing of BK7 mirror. The finishing was carried out with the help of MR fluid (includes 10% CeO_2 abrasive particles). The results concluded that the surface roughness value decreases to 42.93 nm. Singh et al., [2012] worked on ball end magnetorheological finishing process for finishing fused silica glass. The finishing was carried out with the help of MR polishing fluid (usually a mixture of 20% CIPs and 10% CeO_2 abrasive powder) improve the surface finish value upto 0.14 nm as illustrated in Fig. 2.8. Some other surface finishing (Ra value) results obtained by different finishing processes as illustrated in Table 2.2.

Table 2.2: Comparison of results obtained by different finishing processes [Jha and Jain, 2005]

Sr No.	**Finishing Process**	**Substrate**	**Ra Value (nm)**
1.	Honing	-	50-1500
2.	Grinding	-	250-6250
3.	Lapping	-	130-750
4.	Abrasive Flow Machining with SiC abrasive	Hardened steel	50
5.	Magnetic Abrasive Finishing	Stainless steel	8 approx.
6.	Magnetic Float Polishing with CeO_2	Si_3N_4	4
7.	MR Finishing Process with CeO_2	Flat BK7 glass	0.8 (RMS)

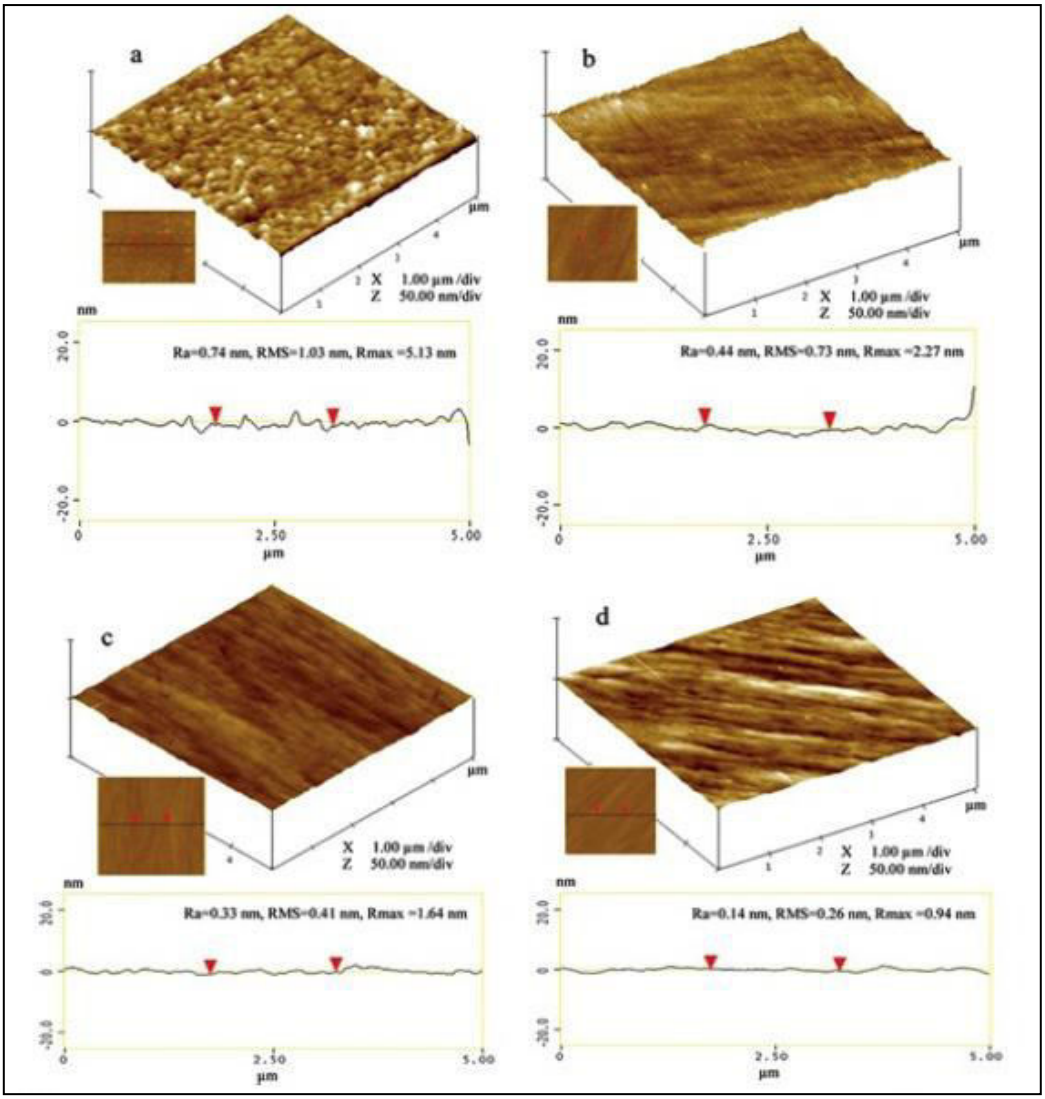

Figure 2.8: Atomic force microscope images for workpiece surface: (a) initial, (b) after 30 min of finishing at current 4 A, gap 1.5 mm, rotational speed 400 RPM, (c) after 90 min of finishing at current 2.4 A, gap 1.5 mm, rotational speed 400 RPM, and (d) after 150 min of finishing time at current 2.4 A, gap 1.5 mm, rotational speed 400 RPM [Singh et al., 2012]

2.3 Research Gap

From the literature survey, it is found that the advanced finishing processes due to its better surface finishing tendency and more preferable over the traditional finishing process. The magnetorheological finishing process has the potential to finish the surfaces to nanometer surface roughness value. Therefore, advantage of the magnetorheological finishing technique can be taken and explore further possibilities to work in the area of magnetorheological finishing (MRF) process which would finish the surfaces with controlled magnetic field.

- Most of the MR finishing processes make use of electromagnetic coil for generating magnetic field which may cause heating problem. Heating of finishing tool results in decrease in viscosity of MR polishing fluid attached with tool which further results decrease in performance of MR polishing fluid. Alternate to this problem can be the usage of permanent magnet for generating magnetic field.
- Finite Element simulation of MR polishing fluid assisted with permanent magnet finishing process for non ferrous workpiece has not been carried out.
- Work on paramagnetic and diamagnetic materials has not been significantly done using MR finishing processes.
- Mathematical modeling of MR polishing fluid assisted with permanent magnet finishing process has not been carried out.

2.4 Research Objectives

Most of the MR finishing processes [Jha and Jain, 2004; Kordonski and Shorey, 2007; Singh et.al. 2011; Sadiq and Shunmugam, 2009] make use of electromagnetic coil for generating magnetic field which may cause heating problem. Heating of finishing tool results in decrease in viscosity of MR polishing fluid attached with finishing tool. Also continuous finishing for longer period can not be performed with MR finishing tool using electromagnet. This is one of the limitations of MR polishing fluid based finshing processes as for this a proper chiller appratus is to be used to cool the electromagnet area. This problem can be eliminated with the use of permanent magnets for generating magnetic field. Also, by using permanent magnets, simplification of the finishing setup is there and reduction in cost of finishing appuratus as well as running cost.

Based on the research gaps identified through the literature survey, following are the research objectives

- Design and fabrication of new finishing tool using permanent magnets along with MR polishing fluid.
- Finite Element simulation of proposed MR finishing tool.
- Experiments on non ferrous materials such as aluminum and copper.
- To optimize the process parameters to obtain the best finishing.
- To analyze the material removal mechanism and surface characteristics with the developed tool, the scanning electron microscopy and atomic force microscopy is to be carried out.

- Mathematical modeling of the magnetic forces and surface roughness.

2.5 Methodology

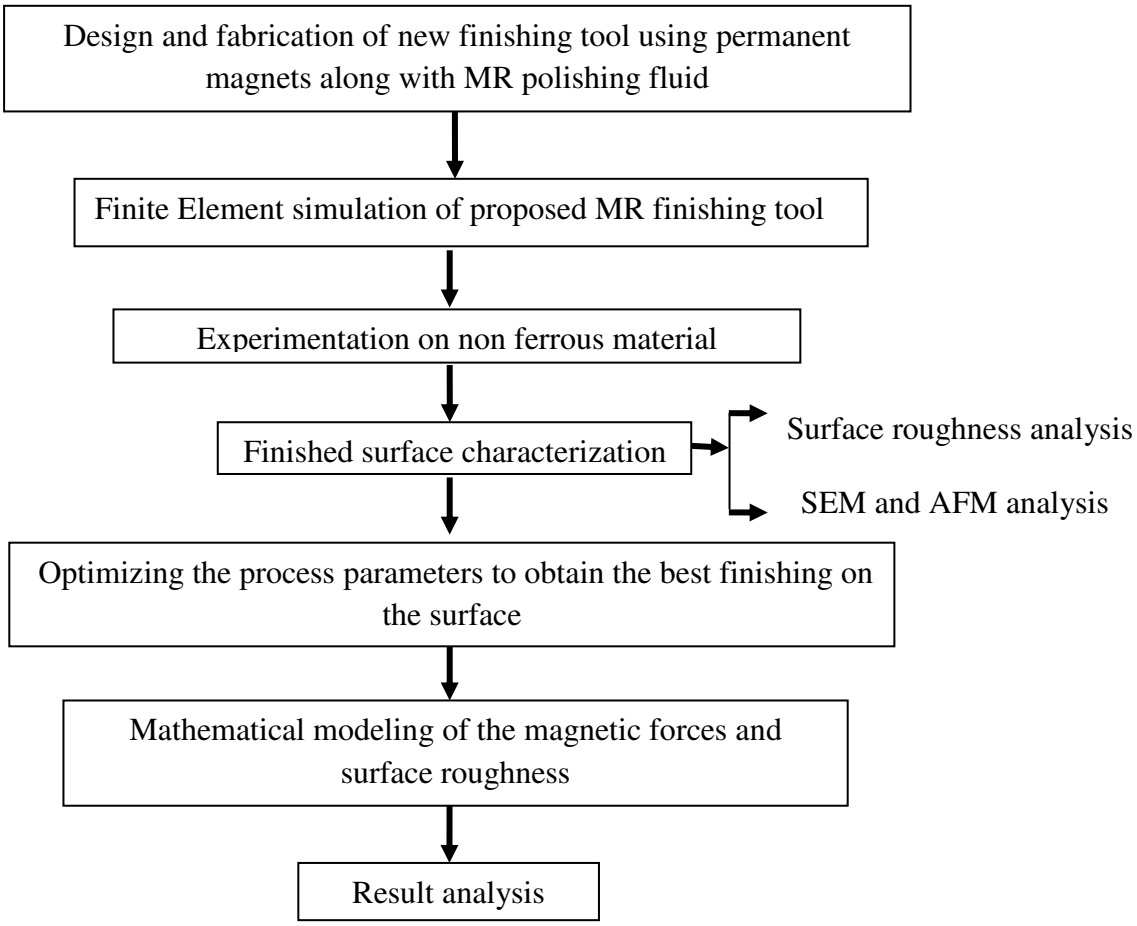

Figure 2.9: Methodology for the present work

Hence, a new finishing tool using permanent magnets along with MR polishing fluid has been developed to overcome the research gaps. The developed process has advantages over other finishing processes in terms of reduced finishing time, lesser operating cost and simplified setup.

Chapter 3

Design and Fabrication of the New Finishing Tool for Diamagnetic and Paramagnetic Materials

3.1 Design of the New Finishing Tool

Strength of magnetic field is the foremost requirement in magnetorheological (MR) fluid based finishing processes. As more the magnetic field, stiffer is the MR polishing fluid and more firmly it holds the abrasives on workpiece surface. MR polishing fluid chains should have enough strength so that it overcomes the shear strength of roughness peaks of workpiece material. Induction of higher magnetic field in the working area is very much important. Therefore, an appropriate finishing tool using permanent magnets is designed to fulfill the aforesaid requirement. To analyze the performance of proposed design of finishing tool, the study of magnetic field distribution in working area has been done. The finishing tool along with MR polishing fluid and diamagnetic copper alloy workpiece has been modeled and simulated in Maxwell Ansoft V13 software. From the finite element (FE) magnetostatic simulation, distribution of magnetic flux density has been examined in the working region.

Two cylindrical permanent magnets have been used to design the finishing tool. One is hollow cylindrical permanent magnet (named as magnet 1) and other is solid cylindrical permanent magnet (named as magnet 2) as shown in Fig. 3.1. Firstly the magnet 1 and rotating shaft of stainless steel are modeled. One end of the rotating shaft is modeled in such a way that it has a tight fit with internal diameter of magnet 1 as shown in Fig.3.1 (a). A rotating shaft made of stainless steel is modeled which is used to rotate finishing tool over the copper alloy workpiece. Further the magnet 2 is modeled to get attached with the magnet 1 as shown in Fig. 3.1 (b). Magnet 2 has been used in the setup for uniform finishing. Magnet 1 is used to affix the magnet 2 and the rotating shaft. Fig. 3.1(a) shows the modeling of rotating shaft and hollow cylindrical permanent magnet (magnet 1). Fig.3.1 (b) shows the magnetic model of discrete view of solid cylindrical permanent magnet (magnet 2) and joined model of the rotating shaft and hollow cylindrical permanent magnet (magnet 2). Finally all the parts

have been joined together to make the complete finishing tool as shown in Fig. 3.1 (c). Diameter of the magnet being 30 mm and total height of the combined magnet is 35 mm.

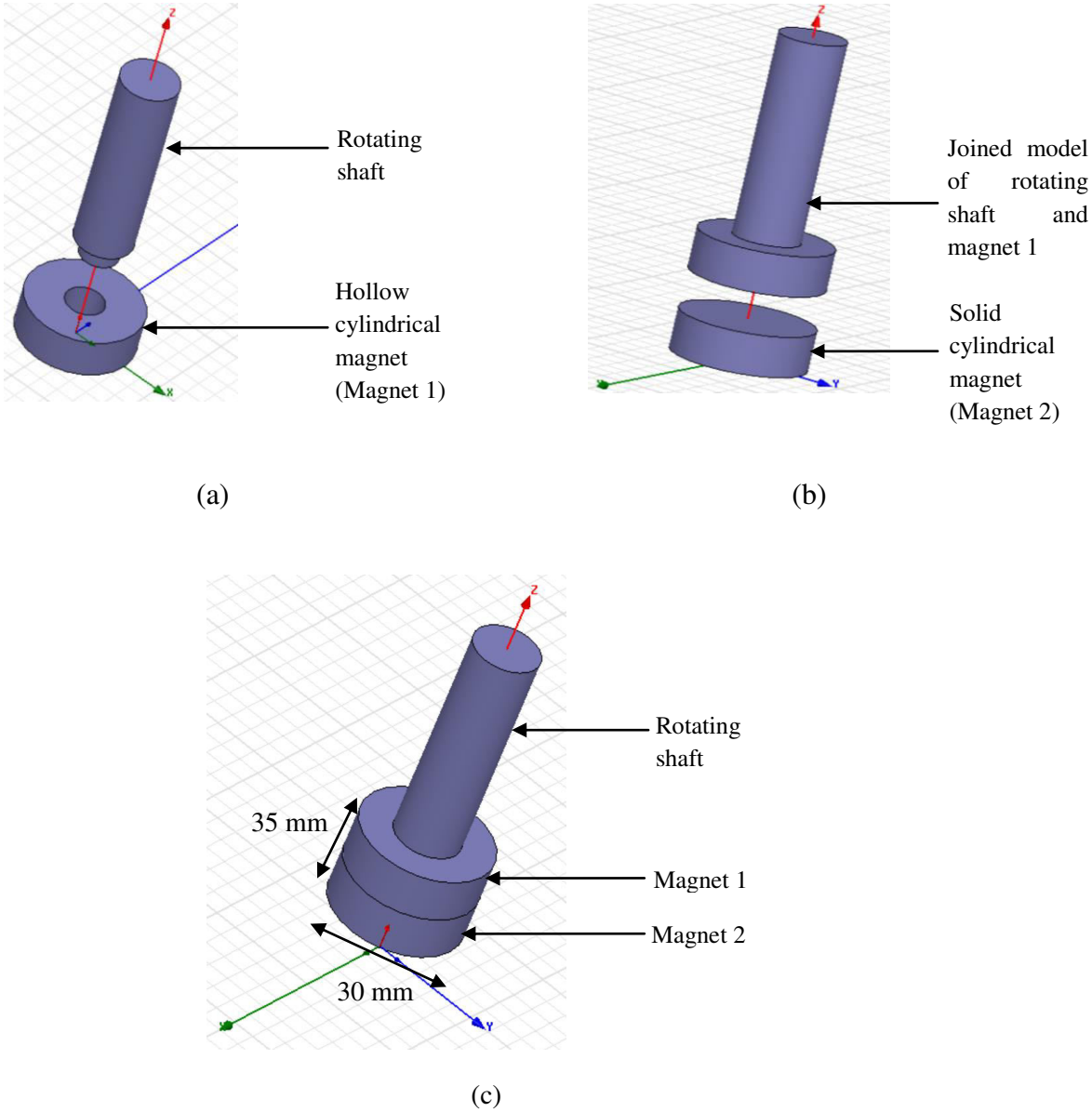

Figure 3.1: Magnetic model of (a) rotating shaft and hollow cylindrical permanent magnet, (b) solid cylindrical permanent magnet and joined model of the rotating shaft and hollow cylindrical permanent magnet and (c) final permanent magnet finishing tool.

Magnetorheological (MR) polishing fluid with relative permeability 5 is then modeled under the magnet 2 with thickness of 1.5 mm (working gap). Below the 1.5 mm thickness of MR polishing fluid, the workpiece material with relative permeability 1 (approx.) is also modeled. Modeling has been done for two materials i.e. paramagnetic aluminium and

diamagnetic copper. In real practice MR polishing fluid gets stiffened on the bottom surface of the finishing tool due to the magnetic field produced by combined effect of two permanent magnets and performs finishing onto the surface of workpiece by its rotation.

3.2 Selection of the Workpiece Materials

3.2.1 Paramagnetic Aluminium Alloy

Having excellent property of being light weight, nano-finished aluminum has wide applications in aerospace and automobile industries. Also aluminum alloy has wide applications especially in the field of micro-electronics and optics because of light weight, high corrosion resistance high conductivity, constant reflectance over the entire visible spectrum range and longer wear as well as fatigue life [Newswander et al., 2013; Ranjan et al., 2017].

Paramagnetic materials have relative permeability of slightly above 1. Atoms of these materials in the absence of an external magnetic field have a net magnetic moment as the orbital and spin moments do not cancel. The net external field observed is either zero or very close to zero since moments are oriented randomly. The net magnetic moments of atoms are induced by an external field in diamagnetic materials, but in paramagnetic materials the magnetic moments always exist. The increase the total field is experienced as these moments tend to align with the external field in the presence of an external magnetic field [Ida, 2000]. This property of paramagnetic material played vital role in the present experiments. Abrasive particles are gripped outwards from the magnet onto the workpiece surface, which is the basic necessity for the MR polishing fluid assisted finishing.

3.2.2 Magnetic Field Analysis of the Finishing Tool with Aluminium

Magnetorheological (MR) polishing fluid with relative permeability 5 is then modeled under the magnet surface with thickness of 1.5 mm (working gap). Below the 1.5 mm thickness of MR polishing fluid, the aluminum workpiece with relative permeability 1.000021 is modeled. In real practice MR polishing fluid gets stiffen on the bottom surface of the finishing tool due to the magnetic field produced by combined effect of two permanent magnets and performs finishing onto the surface of aluminum alloy workpiece by its rotation. The magnetic model of the finishing tool along with MR polishing fluid and aluminum workpiece is shown in Fig. 3.2. The complete developed magnetic model is then simulated in Maxwell Ansoft V13 software for magnetic flux density analysis. Materials assigned to the magnetic model components and their relative permeability is stated in Table 3.1.

The entire setup is simulated in Maxwell Ansoft V13 software to analyse the magnetic flux distribution in it. Figure 4.3 gives the magnetic flux density distribution of the setup obtained through finite element analysis in Maxwell Ansoft V13 software. As it can be observed in the Fig. 3.3 that MR polishing fluid region is red in colour that signifies presence of maximum magnetic flux in the region of MR polishing fluid. Green colour in the workpiece shows the presence of magnetic flux in that region i.e. in workpiece and surroundings. Blue colour region in shaft and surroundings show the minimum magnetic flux region.

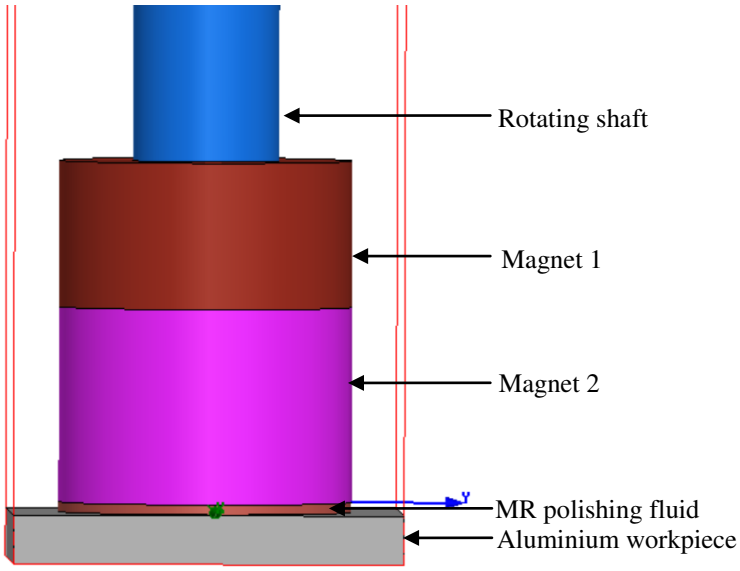

Figure 3.2: Magnetic model of permanent magnets finishing tool along with MR polishing fluid and aluminium workpiece.

Table 3.1: Materials assigned to the magnetic model components

Components	**Material**	**Relative Permeability**
Magnet 1	NdFe 35	1.1
Magnet 2	NdFe 35	1.1
Rotating shaft	Stainless Steel	1
MR Polishing fluid	MR fluid	5
Paramagnetic workpiece	Aluminium	1.000021

Distribution of magnitude of magnetic flux density along vertical length from finishing tool surface to workpiece surface i.e. in MR polishing fluid region is examined from

finite element simulation and is shown in Fig. 3.4. It can be observed in Fig. 3.4 that maximum flux density is present on the outer surface of finishing tool and goes on decreasing as approaching to the aluminum alloy workpiece surface. It is very important requirement for finishing of workpiece surface in fluid based finishing processes. Therefore, the higher magnetic flux density gradient on the bottom surface of finishing tool ensured the MR polishing fluid get attached with its bottom surface and can perform finishing on the surface of aluminum workpiece with proper relative motion.

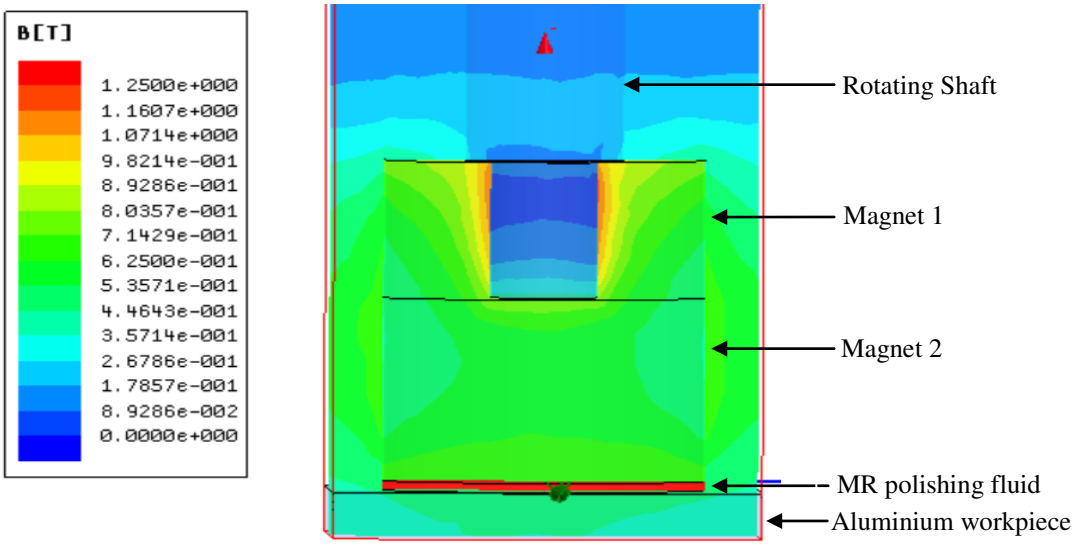

Figure 3.3: Finite element analysis result of the finishing tool along with MR polishing fluid and aluminium workpiece.

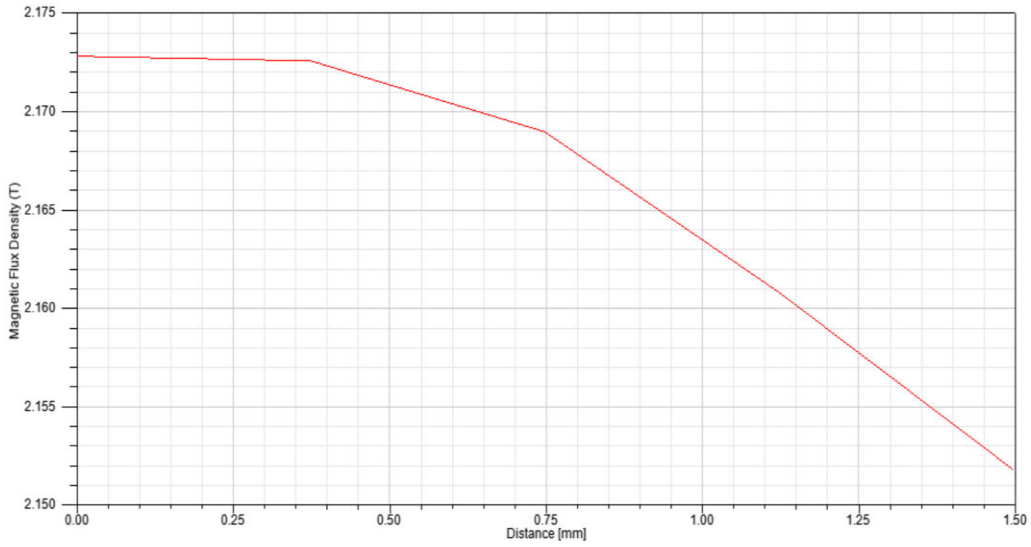

Figure 3.4: Distribution of magnetic flux density along the vertical length in MR polishing fluid region from the outer finishing tool surface to aluminium alloy workpiece surface.

3.2.3 Diamagnetic Copper Alloy

Copper and its alloys are most important materials in electronics and electrical industries because it has good properties like high electrical and thermal conductivity and mechanical workability. Being good conductor in electrical and electronics industries, it has its wide applications in oil and gas lines, and heat conductors, heat exchangers laser cutting and engraving, and laser welding systems for directing the beam of laser etc. Precisely finished copper electrodes are also used in electric discharge machining (EDM) for the machining of different complex shaped materials with high surface finish [Torres et al., 2016; Balasubramanian and Senthilvelan, 2014]. In EDM, replica of electrode is formed on the workpiece surface, due to which there is necessity of high surface finish of electrode. Highly finished copper surface is also used as metallic mirrors for different plasma diagnostics [Bardamid et al., 1998 and Voitsenya et al., 1996]. Some industries like laser, aerospace, dentistry etc. widely use metallic mirrors. Copper is the most suitable material for metallic mirrors due to ease in manufacturing, high reflectivity, high thermal conductivity and light weight.

When the diamagnetic material is placed near a permanent magnet, the magnet induced equivalent magnetic field in the diamagnetic material. But, inside the diamagnetic material, magnetic flux density is lower than the external magnetic field. Due to magnetization of the diamagnetic material, the magnet and the equivalent magnetic field oppose each other and due to this opposition the diamagnetic material is repelled from the magnetic field in the same way that two magnets repel each other when their magnetic flux densities oppose each other. However, for all diamagnetic materials this repelling force is extremely small [Ida, 2000]. This property of diamagnetic material played vital role in the present experiments.

3.2.4 Magnetic Field Analysis of the Finishing Tool with Copper

Strength of magnetic field is the foremost requirement in magnetorheological (MR) fluid based finishing processes. As more the magnetic field, stiffer is the MR polishing fluid and more firmly it holds the abrasives on workpiece surface. MR polishing fluid chains should have enough strength so that it overcomes the shear strength of roughness peaks of workpiece material. Induction of higher magnetic field in the working area is very much important. To analyze the performance of tool during finishing, the study of magnetic field distribution in working area has been done. The finishing tool along with MR polishing fluid

and diamagnetic copper alloy workpiece has been modeled and simulated in Maxwell Ansoft V13 software. From the finite element (FE) magnetostatic simulation, distribution of magnetic flux density has been examined in the working region.

As the tool consists of two cylindrical permanent magnets, Magnetorheological (MR) polishing fluid with relative permeability 5 is then modeled under the magnet 2 with thickness of 1.5 mm (working gap). Below the 1.5 mm thickness of MR polishing fluid, the diamagnetic material i.e. copper with relative permeability 0.999991 (from the library of Maxwell Ansoft) is also modeled. In real practice MR polishing fluid gets stiffen on the bottom surface of the finishing tool due to the magnetic field produced by combined effect of two permanent magnets and performs finishing onto the surface of copper alloy workpiece by its rotation. The complete developed magnetic model is then simulated in Maxwell Ansoft V13 software for magnetic flux density analysis.

The magnetic flux density distribution is an important significant parameter in MR fluid based finishing processes because the strength of MR polishing fluid depends mainly upon the distribution of magnetic flux density. Since the proposed finishing tool is based on MR fluid, therefore the analysis of magnetic flux density distribution becomes vital factor to achieve the required process performance. The materials assigned to the designed model with MR polishing fluid thickness of 1.5 mm are given in Table 3.2. The developed finishing tool with stiffened MR polishing fluid is rotated on the surface of copper alloy workpiece to finish its surface.

Table 3.2: Materials assigned to the magnetic model components.

Components	**Material**	**Relative Permeability**
Magnet 1	NdFe 35	1.10
Magnet 2	NdFe 35	1.10
Rotating shaft	Stainless Steel	1.00
MR Polishing fluid	MR fluid	5.00
Diamagnetic workpiece	Copper	0.999991

The entire setup of finishing tool along with MR polishing fluid is simulated in Maxwell Ansoft V13 software to analyse the distribution of magnetic flux density in it. Figure 4.11 shows the distribution of magnetic flux density of the finishing setup through a plane obtained from finite element analysis performed in Maxwell Ansoft V13 software. It

can be observed in the Fig. 3.5 that MR polishing fluid region is red in colour which signifies presence of maximum magnetic flux in that region. Green colour in the workpiece signifies the presence of moderate magnetic flux in that region. Blue colour region in shaft and surroundings show the minimum magnetic flux region.

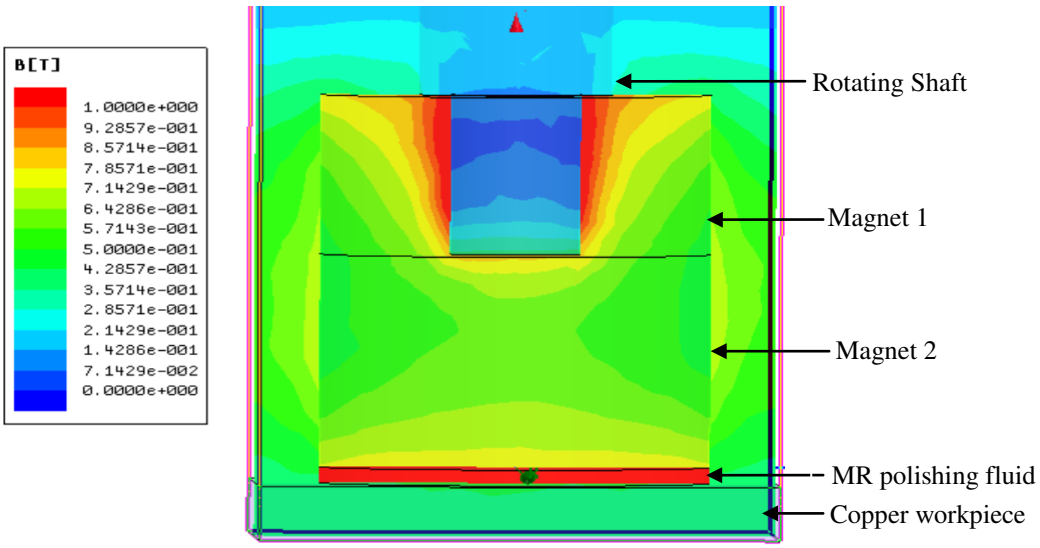

Figure 3.5: Finite element analysis result of the finishing tool along with MR polishing fluid and copper workpiece.

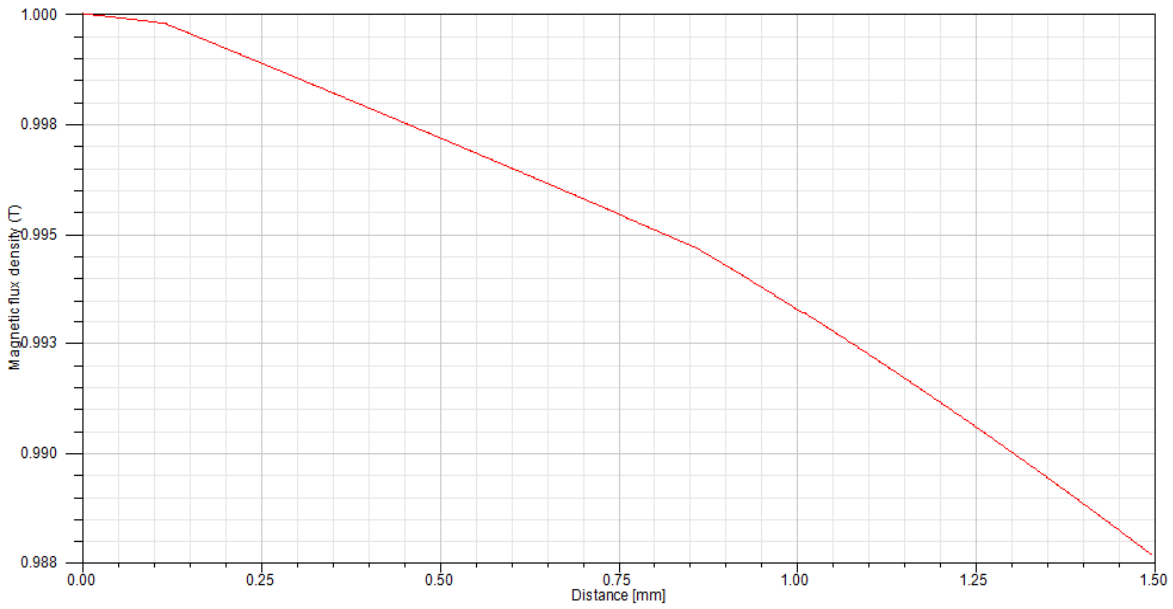

Figure 3.6: Distribution of magnetic flux density along the vertical length in MR polishing fluid region from the outer finishing tool surface to copper alloy workpiece surface.

Distribution of magnitude of magnetic flux density along vertical length from finishing tool surface to workpiece surface i.e. in MR polishing fluid region is examined from finite element simulation and is shown in Fig. 3.6. It can be observed in Fig. 3.6 that maximum flux density is present on the outer surface of finishing tool and goes on decreasing as approaching to the copper alloy workpiece surface. It is very important requirement for finishing of workpiece surface in fluid based finishing processes. Therefore, the higher magnetic flux density gradient on the bottom surface of finishing tool ensured the MR polishing fluid getting attached with its bottom surface and can perform finishing on the surface of copper workpiece with proper relative motion.

3.3 Fabrication of the Finishing Tool

The finishing tool has been fabricated by using two cylindrical magnets (NdFeB 35) and a rotating stainless steel shaft. Diameter of the magnet being 30 mm and total height of the combined magnet is 35 mm. Both cylindrical permanent magnets are of same diameter and are made in such a way that opposite poles facing same face so that the both magnets can stick together with good bonding strength. Magnet 2 can be changed according the required geometry to be finished. Hence, it makes the design of the finishing tool flexible for finishing the workpieces with different geometries.

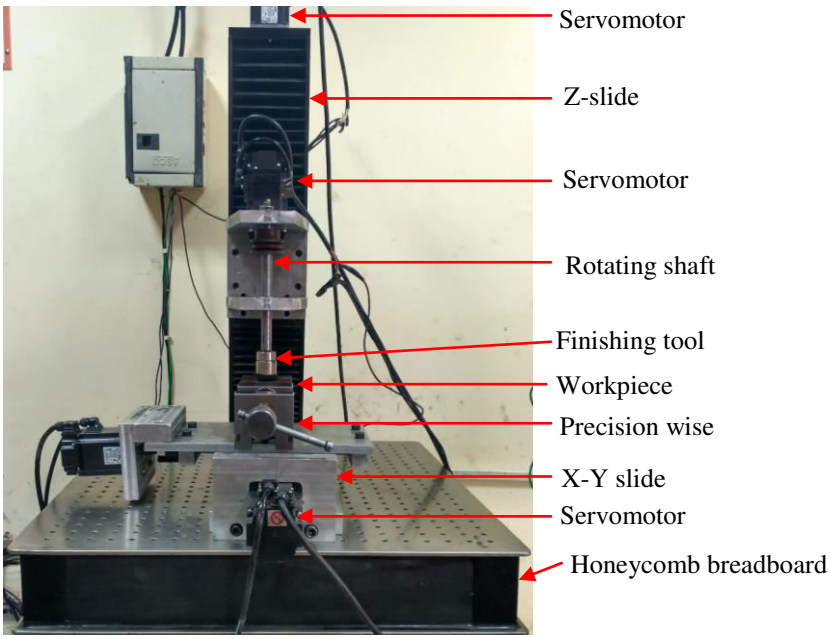

(a)

(b)

Figure 3.7: (a) Experimental setup of the magnetorheological finishing tool (b) Enlarged view of the magnetorheological finishing tool with stiffened MR polishing fluid.

The finishing tool is fabricated in the same way as modeled in Maxwell Ansoft V13 software for finite element analysis. The complete magnetorheological finishing setup for finishing the diamagnetic copper alloy workpiece is shown in Fig. 3.7 (a). The rotating shaft is moved linearly with C-shaped aluminium bracket which is mounted over the Z-slide. Enlarged view of the finishing tool with stiffened MR polishing fluid is shown in Fig. 3.7 (b). Stiffeness of MR polishing fluid with the effect of magnetic field can be observed at the bottom end surface of finishing tool in Fig. 3.7 (b). Its clearly visible that the MR polishing fluid has taken the hemispherical shape. Hence the tool has got its name 'Hemispherical End MagnetRheological Finishing' process (HEMRF).

Experimentation has been performed by the newly designed finishing tool on the workpieces. Position of the workpiece beneath the surface of the finishing tool can be precisely adjusted by linear X-Y slide as shown in Fig. 3.7 (a). The working gap of 1.5 mm thickness is maintained for MR polishing fluid between the bottom face of finishing tool and the workpiece surface by moving the Z-slide.

Chapter 4

Preliminary Experiments to Examine the Performance of HEMRF Tool

To check the feasibility and workability of the newly designed hemispherical end magnetrheological finishing (HEMRF) tool, preliminary experimentation has been performed on paramagnetic alluminium alloy workpiece and diamagnetic copper alloy workpiece.

4.1 Experimentation on Paramagnetic Alluminium Workpiece

The most important and costly stage of a production system is surface finishing. For precise and accurate components, it is the most demanding area of labour. Nearly 15% of the overall manufacturing cost is involved in finishing [Gorana et al., 2004]. Also nano-finished materials have great demand in various industries like aerospace, automobile and biomedical industries etc.. The surface characteristics are the most prominent factor for increasing the durability and reliability of various components [Bedi and Singh, 2015]. Precisely finished surfaces have various benefits like closer tolerance mating, less maintenance and better functionality [Grover and Singh, 2017]. Having excellent property of being light weight, nano-finished aluminum has wide applications in aerospace and automobile industries. Also aluminum alloy has wide applications especially in the field of micro-electronics and optics because of light weight, high corrosion resistance high conductivity, constant reflectance over the entire visible spectrum range and longer wear as well as fatigue life [Newswander et al., 2013; Ranjan et al., 2017]. In abrasive based polishing process, ductile materials like aluminium is highly challenging to generate nano metric surface finish [Ranjan et al., 2017].

In the present section, preliminary experimentation has been carried out on flat workpiece of aluminum alloy workpiece using HEMRF. Finite element simulation of the finishing tool along with magnetorheological polishing fluid and aluminum workpiece has been done. Distribution of magnetic flux density is observed in the working gap (distance between finishing tool surface and aluminum alloy workpiece surface).

4.1.1 Experimental Setup

The complete magnetorheological finishing setup for finishing the aluminium alloy workpiece is shown in Fig. 4.1. The rotating shaft is moved with C-shaped aluminium bracket which is mounted over the Z-slide. Stiffening of MR polishing fluid on the bottom surface of the finishing tool will help in finishing of the workpiece. The working gap of 1.5 mm thickness is maintained for MR polishing fluid between the bottom face of finishing tool and workpiece surface.

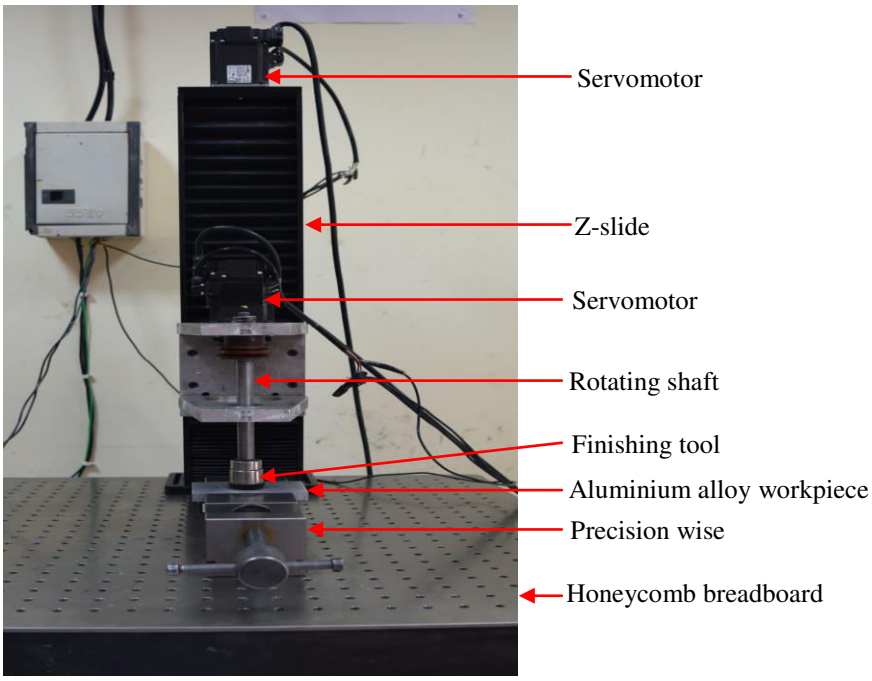

Figure 4.1: Experimental setup of the magnetorheological finishing tool.

Experimentation has been performed by the newly designed finishing tool HEMRF on the aluminum alloy workpiece. Position of aluminum alloy workpiece beneath the surface of the finishing tool has been adjusted and held in vice precisely as shown in Fig. 4.1. The working gap of 1.5 mm thickness is maintained for MR polishing fluid between the bottom face of finishing tool and workpiece surface by moving the Z-slide. MR polishing fluid is prepared by thoroughly mixing of carbonyl iron (CI) particles, silicon carbide (SiC) particles in base fluid with the help of mixing chamber. Composition of MR polishing fluid is made with 17 % carbonyl iron (CI) of particles mesh size 400, 23% silicon carbide (SiC) of particles mesh size 600 and 800 (two fluids were made separately) and 60 % base fluid (80 % paraffin oil and 20 % grease). These compositions have been selected on the basis of trial experiments. Mesh size 600 of SiC particles are taken for finishing of the workpiece,

thereafter mesh size 800 SiC particles used for the final polishing of workpiece surface. The workpiece of aluminum alloy of size 50 mm × 35 mm × 5 mm has been selected for experimentation. Electron dispersive spectography (EDS) of aluminum alloy has been performed and chemical composition of the aluminum alloy workpiece is reported in Table 4.1.

Table 4.1: Chemical composition of aluminium alloy

Sr. No.	Material	Percentage by Weight (%)
1.	Aluminium (Al)	71.13
2.	Carbon (C)	18.50
3.	Oxygen (O)	10.37

Newly designed finishing tool is rotated over the aluminum alloy workpiece to finish its surface. Working gap between the finishing tool surface and the workpiece surface plays an important role in MR fluid based finishing processes. Working gap of 1.5 mm thickness is maintained between finishing tool surface and aluminium alloy workpiece surface. The thickness of 1.5 mm of MR polishing fluid has been decided on the basis of trial experiments. It is maintained in such a way that no erosion of aluminum alloy workpiece occurs and only surface can be polished.

Table 4.2: Experimental parameters and conditions used for different sets of finishing

Sr. No.	Parameters	Set 1	Set 2
1.	CIPs Size	400 mesh	400 mesh
2.	Abrasives Size	600 mesh	800 mesh
3.	Finishing tool rotation speed	750 rpm	750m

Experimentation has been performed in four sets each with 5 minutes. First two cycles of finishing are performed with abrasives mesh size of 600 and the last two cycles of nano-finishing is performed with comparatively fine abrasives of 800 mesh size. Experimental parameters used for nano-finishing of aluminium alloy workpiece are reported in Table 4.2. Tool roation speed is kept same i.e. 750 r.p.m for all the cycles of finishing.

4.1.2 Results and Discussion for Finishing on Aluminium Workpiece

The newly developed finishing tool using permanent magnets has been designed for finishing of non ferrous workpiece. Magnetorheological (MR) polishing fluid stick to the bottom surface of finishing tool and gives repulsive force to the abrasive particles towards the surface of aluminium alloy workpiece. The repulsive force moves the active abrasives towards the workpiece surface. This result in active silicon carbide (SiC) abrasive particles embed on to the roughness peaks of workpiece. These active abrasive particles are strongly gripped by carbonyl iron (CI) particles chains and rotate with the rotation of finishing tool. Fig. 4.2 (a) shows the roughness peaks on the workpiece surface before the finishing cycle. Due to the rotational motion of gripped SiC particles and tangential cutting force applied by them on to the peaks of workpiece surface, peaks material gets removed in the form of micro chips as shown in Fig. 4.2 (b).

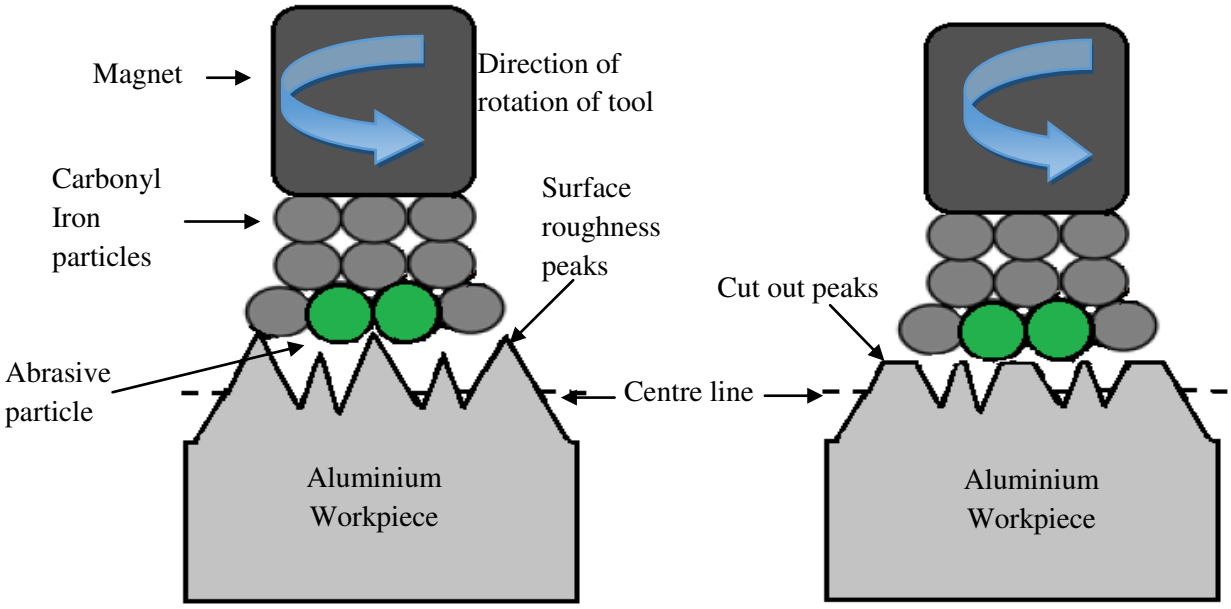

Figure 4.2: Mechanism of finishing performed by magnetorheological finishing tool.

Experimentally the magnitude of magnetic flux between the bottom tool surface and workpiece surface i.e. in the working gap was obtained using guassmeter. Magnetic flux density in the working gap at different points along the vertical direction were noted and plotted as shown in Fig. 4.3. On comparing with finite element magnetostatic simulation results for magnetic flux density along vertical length from finishing tool surface to

workpiece surface (Fig. 3.4) and actual magnetic flux density noted (Fig. 4.3), it can be observed that same decreasing trend is followed by the magnetic flux density in the working gap. This signifies that the decreasing trend of magnetic flux density of the working gap is helpful for the finishing of workpiece as MR polishing fluid gets proper relative motion.

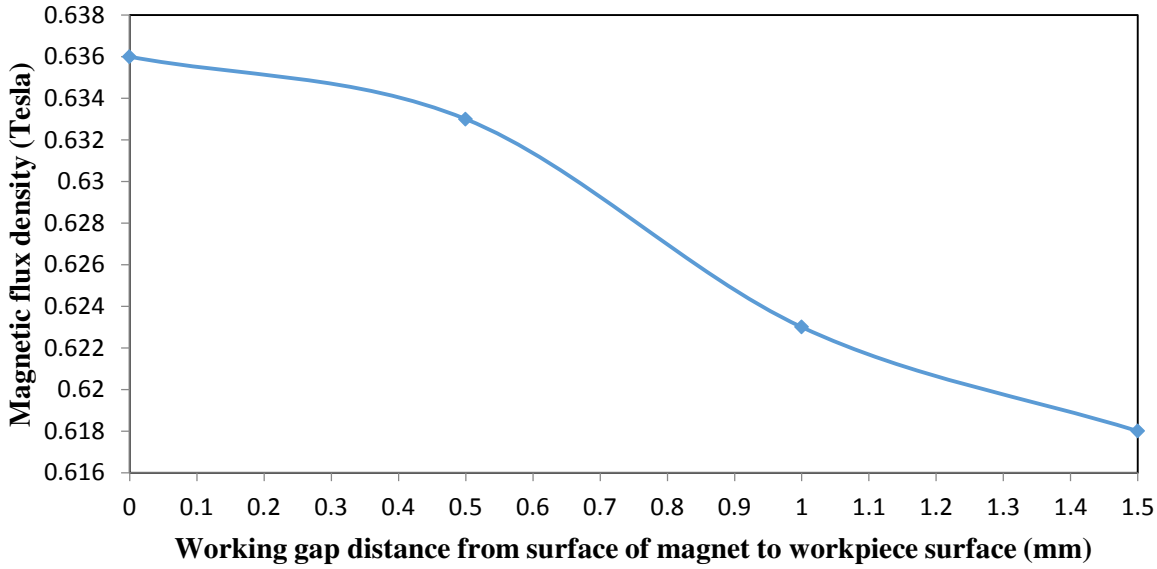

Figure 4.3: Experimentally measured magnetic flux density in MR polishing fluid region from the bottom surface of finishing tool to top surface of aluminium alloy workpiece.

While experimentation, surface roughness parameters (R_a, R_q and R_z) have been measured with Mitutoyo Surftest SJ- 400 instrument. Initially aluminium alloy workpiece is made ready for experimentation by grinding. Before experimentation, the parameters of surface roughness are found as R_a= 718.2 nm, R_q= 981 nm and R_z= 4905 nm. Surface roughness profile of the initial ground surface is shown in Fig. 4.4 (a). Working gap is maintained between the aluminium alloy workpiece and finishing tool of 1.5 mm.

In first cycle of experiment (set 1 in Table 4.2), aluminium alloy workpiece has been finished for 5 minutes. The sharp-ended grinding marks get removed in this first set of finishing. After the first set of experimentation, surface roughness of the workpiece was R_a = 316.8 nm, R_q= 381.6 nm and R_z= 1662 nm. Successive polishing was done on the workpiece as same workpiece was used for all experiments. The initial roughness value for next experiment is the value of surface roughness obtained after previous experiment. The second experiment was performed again with the parameters mentioned in set 1 of Table 4.2 for the further finishing time of 5 minutes. After the second cycle, due to decrement in the surface roughness of the workpiece, final surface roughness value was found to be R_a = 152.1 nm, R_q= 226.2 nm and R_z= 1233 nm.

Third finishing cycle of 5 minutes was performed with parameters of set 2 as mentioned in Table 4.2. After the third cycle, due to decrement in the surface roughness of the workpiece, final surface roughness value was found to be R_a = 93.6 nm, R_q= 134 nm and R_z= 702 nm. Fourth i.e. last finishing cycle of 5 minutes was performed with parameters of set 2 as mentioned in Table 4.2. After this cycle surface roughness of the workpiece was decreased to R_a = 62.7 nm, R_q= 97.2 nm and R_z= 459 nm. Roughness profile of final finished surface is obtained from Mitutoyo Surftest SJ-400 machine as shown in Fig. 4.4 (b). With the parameters mentioned in the Table 4.3, the four cycles of finishing have been performed with 5 minutes each. Surface roughness parameters have been recorded after each set of finishing.

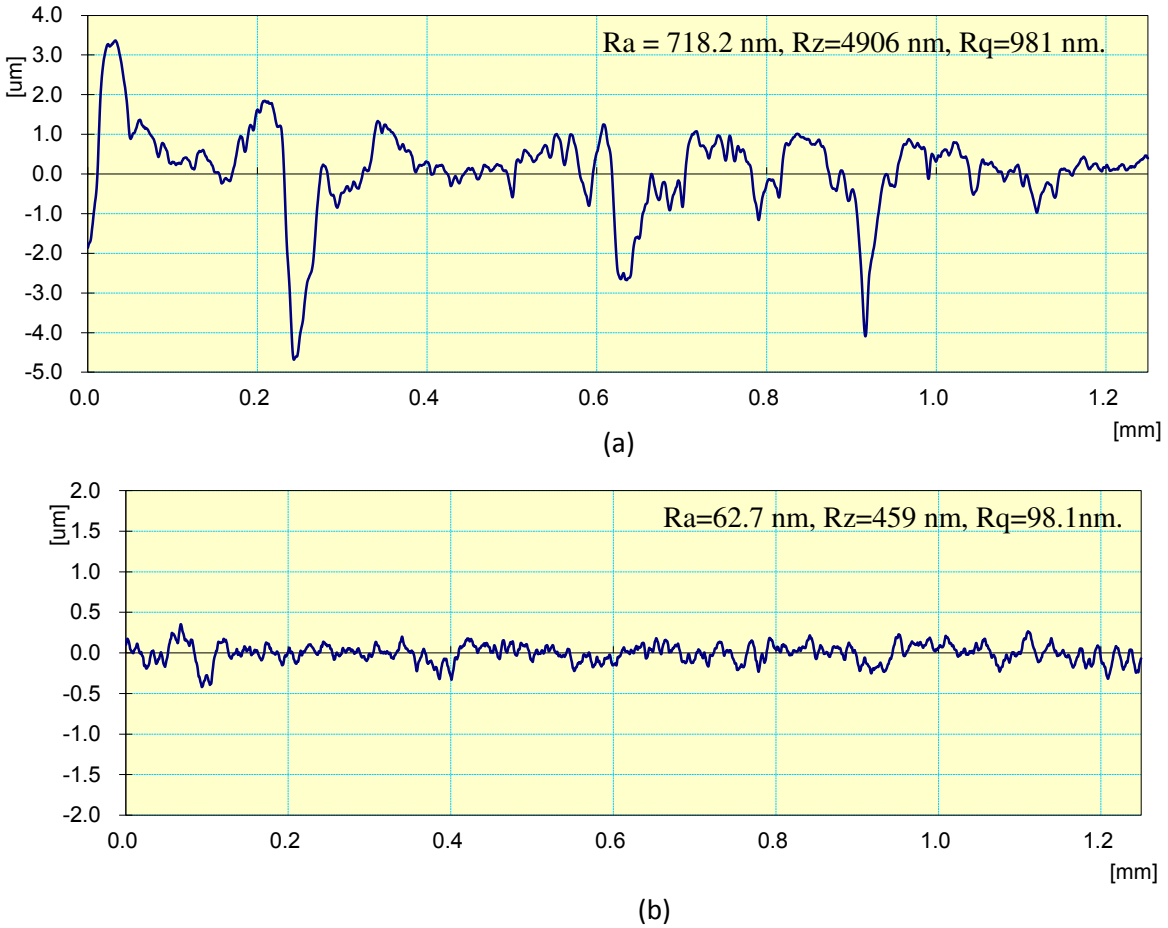

Figure 4.4: Surface roughness profiles of Aluminium alloy workpiece (a) initial and (b) final after finishing of 20 minutes.

The trend of decrease in surface roughness value R_a in percentage with respect to each cycle time is plotted in Fig. 4.5. Initially, the percentage reduction in R_a value is more i.e. 55.8 % because of shearing of peak edges of the surface. Later on it decreases to 38.8 % as

after 15 minutes, the peaks gets flattened and it becomes difficult to shear out the flattened surface by abrasives because of higher shear modulus of flattened surface [Zhong, 2008].

When MR polishing fluid is applied on the magnet between the working gap, the chains of carbonyl iron particles (CIPs) were formed with abrasives embedded in it. CIPs attract each other with greater magnetic force and provide more bonding strength for holding the abrasive particles together firmly. This restricts the lateral displacement motion of abrasive particles due to the presence of CIPs around them and preventing its rolling motion during the finishing cycle. On interaction with the roughness peaks, the abrasives are capable of yielding chips by shearing out peaks. In this case, first two cycles of finishing resulted in improvement in R_a from 718.2 nm to 152.1 nm. In the third and fourth cycle when smaller sized abrasives were used, polishing of the workpiece surface was finished up to R_a 62.7 nm with levelling of most of the peaks and valleys.

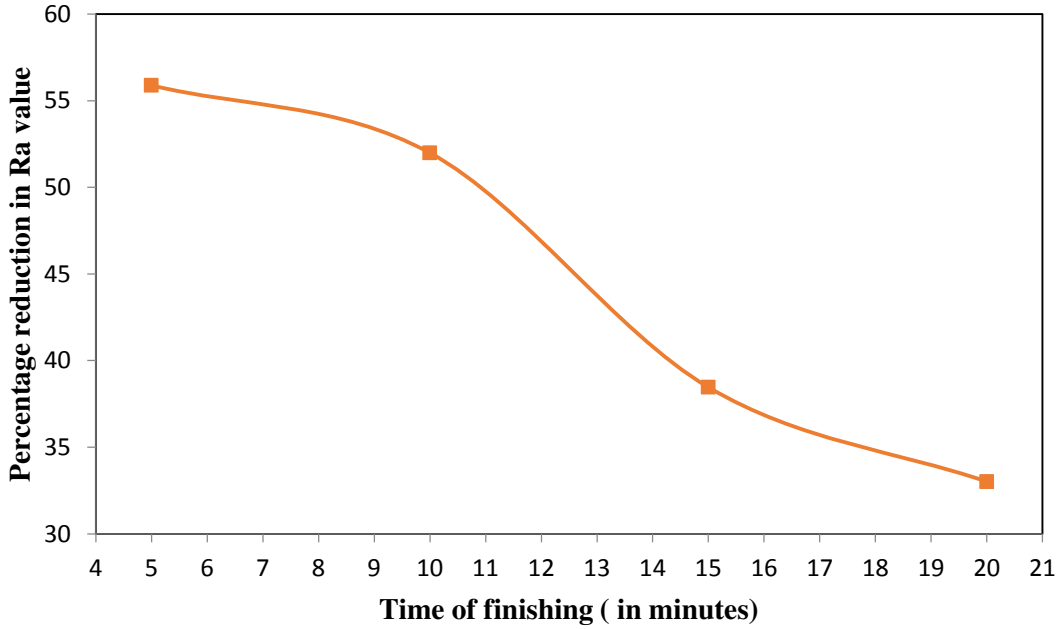

Figure 4.5: Percentage reduction in Ra value with respect to time of finishing.

The normal magnetic force is applied on active abrasives and its rotation on workpiece surface resulted in finishing due to abrasion action. The significant change in surface roughness value and improved surface quality of the workpiece demonstrates the finishing capability of newly developed finishing tool. Reduction in Ra values is observed under scanning electron microscopy (SEM) which shows that the most of the peaks got

sheared. The surface gets flattened with small sharp peaks and few valleys left out are clearly visible in Fig. 4.6 (a) and Fig. 4.6 (b).

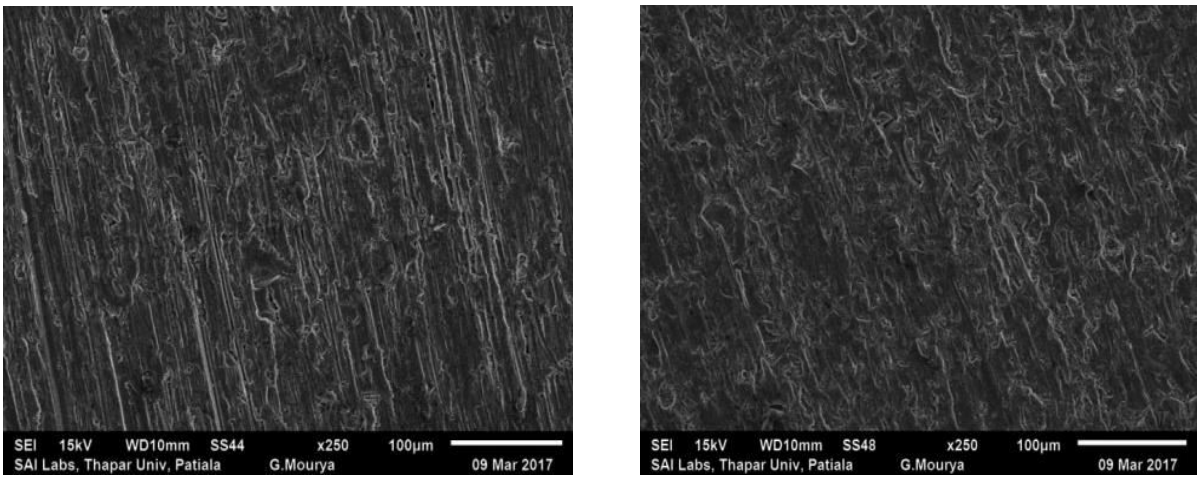

(a) (b)

Figure 4.6: Scanning electron microscopy (SEM) of aluminium alloy workpiece (a) before and (b) after 20 minutes of finishing cycle.

4.2 Experimentation on Diamagnetic Copper Workpiece

Due to its properties of being soft and highly conductive material, copper can be used as interconnect material in electronics industries requiring high level of planarization [Ein and Starosvetsky, 2007]. Copper and its alloys are most important materials in electronics and electrical industries because it has good properties like high electrical and thermal conductivity and mechanical workability. Highly finished copper surface is also used as metallic mirrors for different plasma diagnostics [Bardamid et al., 1998; Voitsenya et al., 1996]. Some industries like laser, aerospace, dentistry etc. widely use metallic mirrors. Copper is the most suitable material for metallic mirrors due to ease in manufacturing, high reflectivity, high thermal conductivity and light weight. Copper, being a soft material, requires precise control of finishing forces to achieve the nano-level finish surface [Khan and Jha, 2016]. Achieving the nano-level surface finish is still challenging, time consuming and labor extensive task. Finishing of soft materials such as paramagnetic and diamagnetic materials is also difficult with the developed advanced finishing processes because during finishing, abrasives get embedded into the surface of soft material and the polished area get covered by abrasives [Barletta et al., 2007].

In the present section, using HEMRF experimentation has been performed on flat workpiece of diamagnetic copper alloy workpiece. Finite element simulation of the finishing tool along with magnetorheological polishing fluid and copper workpiece has also been done.

4.2.1 Experimental Setup

The magnetorheological finishing setup used for the finishing of the diamagnetic copper alloy workpiece is HEMRF. Position of copper alloy workpiece beneath the surface of the finishing tool can be precisely adjusted by linear X-Y slide as shown in Fig. 4.7. The working gap of 1.5 mm thickness is maintained for MR polishing fluid between the bottom face of finishing tool and workpiece surface by moving the Z-slide. MR polishing fluid is prepared by thoroughly mixing of magnetic carbonyl iron (CI) particles, silicon carbide (SiC) abrasives particles in base fluid with the help of mixing chamber. Composition of MR polishing fluid is made with 23% silicon carbide (SiC) of particles size 600 mesh and 800 mesh (two fluids were made separately), 17% carbonyl iron particle (CIP) of 400 mesh and 60% base fluid (20% grease and 80% paraffin oil). These compositions have been selected on the basis of trial experiments. 600 mesh size of SiC particles is taken for finishing of the workpiece, thereafter size of SiC particles used for the final polishing of workpiece surface is 800 mesh. The workpiece of copper alloy of size 50 mm × 40 mm × 5 mm has been selected for experimentation. Electron dispersive spectography (EDS) of copper alloy has been performed and chemical composition of the copper alloy workpiece is reported in Table 4.3.

Table 4.3: Chemical composition of copper alloy.

Sr. No.	**Material**	**Percentage by Mass (%)**
1.	Copper (Cu)	71.51
2.	Aluminium (Al)	1.21
3.	Carbon (C)	23.18
4.	Oxygen (O)	4.10

Newly designed finishing tool is rotated over the copper alloy workpiece to finish its surface. Working gap between the finishing tool surface and the workpiece surface plays a vital role in MR fluid based finishing processes. Working gap of 1.5 mm thickness is

maintained between finishing tool surface and copper alloy workpiece surface. The thickness of 1.5 mm of MR polishing fluid has been decided on the basis of trial experiments. It is maintained in such a way that no erosion of copper alloy workpiece occurs and only surface can be polished. When MR polishing fluid is applied on the magnet between the working gap, the chains of carbonyl iron particles (CIPs) were formed with abrasives embedded in it. Hence, the active abrasives which are in contact with the workpiece surface perform the finishing action.

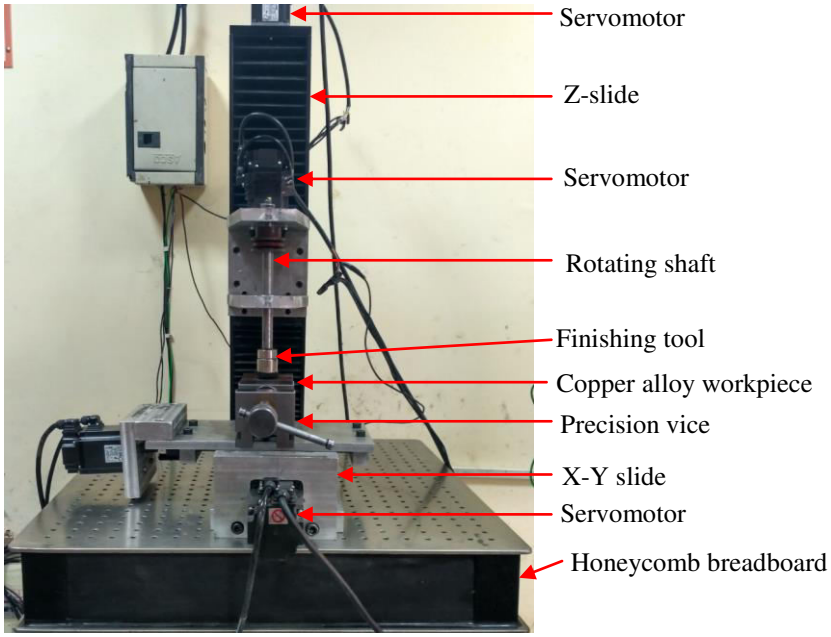

Figure 4.7: Experimental setup of hemispherical end magnetorheological finishing.

Table 4.4: Experimental parameters and conditions used for three different sets of finishing

Sr. No.	**Parameters**	**Set 1**	**Set 2**	**Set 3**
1.	CIPs Size	400 mesh	400 mesh	400 mesh
2.	Abrasives Size	600 mesh	600 mesh	800 mesh
3.	Finishing tool rotation speed	750 rpm	750 rpm	750 rpm

Experimentation has been performed in three sets each with 2.5 minutes. First two sets of finishing are performed with abrasives size of 600 mesh and the last set of nano-finishing is performed with comparatively fine abrasives of size 800 mesh. Experimental parameters used for nano-finishing of copper alloy workpiece are reported in Table 4.4.

4.2.2 Results and Discussion for Finishing on Copper Workiece

Magnetorheological (MR) polishing fluid stick to the bottom surface of finishing tool and gives repulsive force to the abrasive particles towards the surface of diamagnetic copper alloy workpiece. The repulsive force moves the active abrasives towards copper alloy workpiece surface. This result in active silicon carbide (SiC) abrasive particles embed on to the roughness peaks of copper alloy workpiece. These active abrasive particles are strongly gripped by carbonyl iron (CI) particles chains and rotate with the rotation of finishing tool. Due to the rotational motion of gripped SiC particles and tangential cutting force applied by them on to the peaks of workpiece surface, peaks material gets removed in the form of micro chips as shown in Fig. 4.8. As copper is diamagnetic material, its repulsive properties are helpful in the mechanism of finishing. Due to this repulsion force, CI particles get repelled from the copper workpiece surface and get attracted towards tool magnet surface. As a result abrasive particles are gripped outwards from the magnet onto the workpiece surface, which is the basic necessity for the MR polishing fluid assisted finishing.

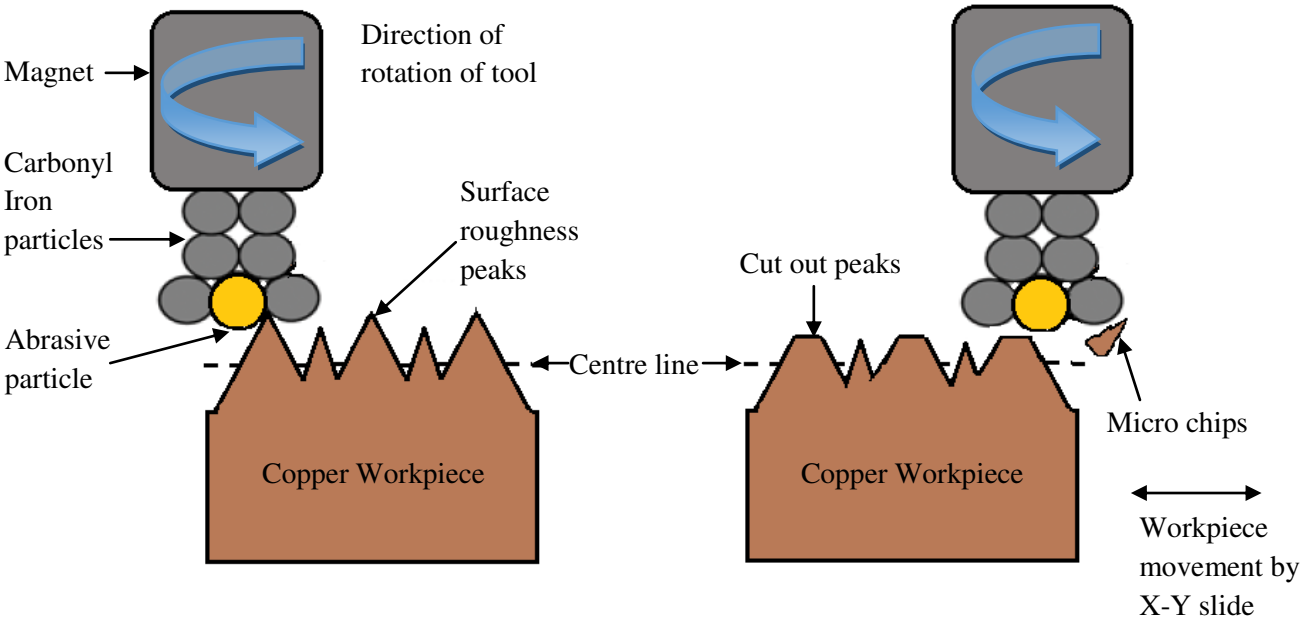

Figure 4.8: Mechanism of finishing performed by the proposed magnetorheological finishing tool

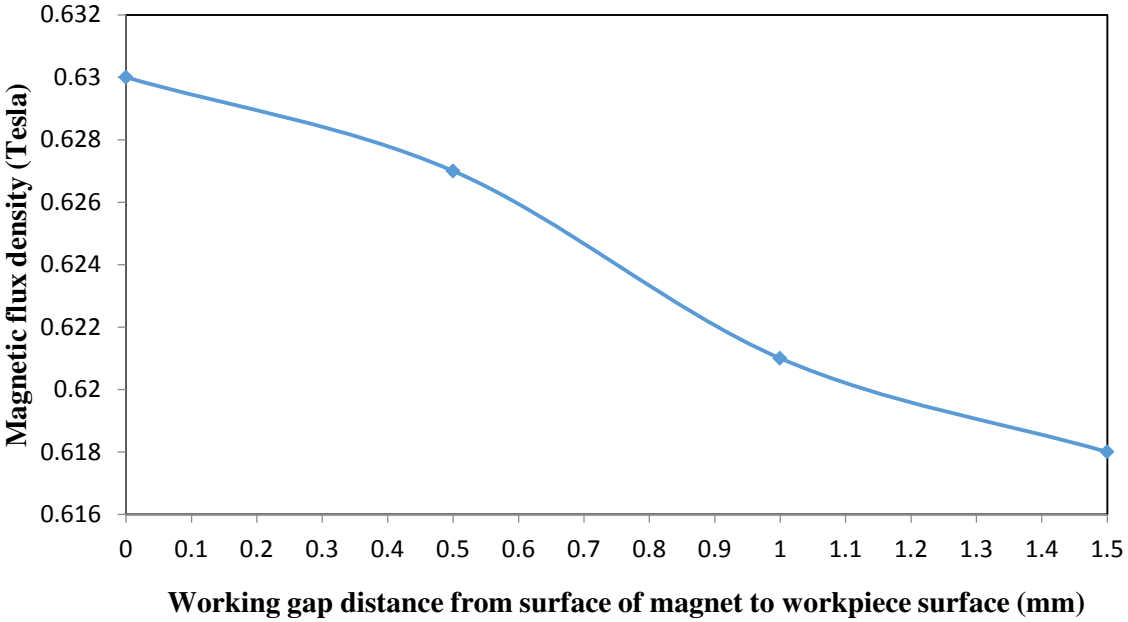

Figure 4.9: Experimentally measured magnetic flux density in MR polishing fluid region from the bottom surface of finishing tool to top surface of copper alloy workpiece.

Experimentally the magnitude of magnetic flux between the bottom tool surface and workpiece surface i.e. in the working gap was obtained using guassmeter. Magnetic flux density in the working gap at different points along the vertical direction were noted and plotted as shown in Fig. 4.9. On comparing with finite element magnetostatic simulation results for magnetic flux density along vertical length from finishing tool surface to workpiece surface (Fig. 3.6) and actual magnetic flux density noted (Fig. 4.9), it can be observed that same decreasing trend is followed by the magnetic flux density in the working gap. This signifies that the decreasing trend of magnetic flux density of the working gap is helpful for the finishing of copper workpiece as MR polishing fluid gets proper relative motion.

While experimentation, surface roughness parameters (R_a, R_q and R_z) have been measured with Mitutoyo Surftest SJ- 400 instrument. Initially copper alloy workpiece is made ready for experimentation by grinding. Before experimentation, the parameters of surface roughness are found as R_a= 273.6 nm, R_q= 347.2 nm and R_z= 1769 nm. Surface roughness profile of the initial ground surface is shown in Fig. 4.10 (a). Working gap of 1.5 mm is maintained between the finishing tool and copper alloy workpiece.

In first cycle of experiment (set 1 in Table 4.4), copper alloy workpiece has been finished for 2.5 minutes with a finishing tool rotational speed of 750 rpm. The sharp-ended

grinding marks get removed in this first set of finishing. After the first set of experimentation, surface roughness of the workpiece was Ra = 108.9 nm, Rq= 136.5 nm and Rz= 845.3 nm. For all experiments same workpiece was used and successive polishing was done on it. The surface roughness obtained after previous experiment was taken as initial roughness value for next experiment.

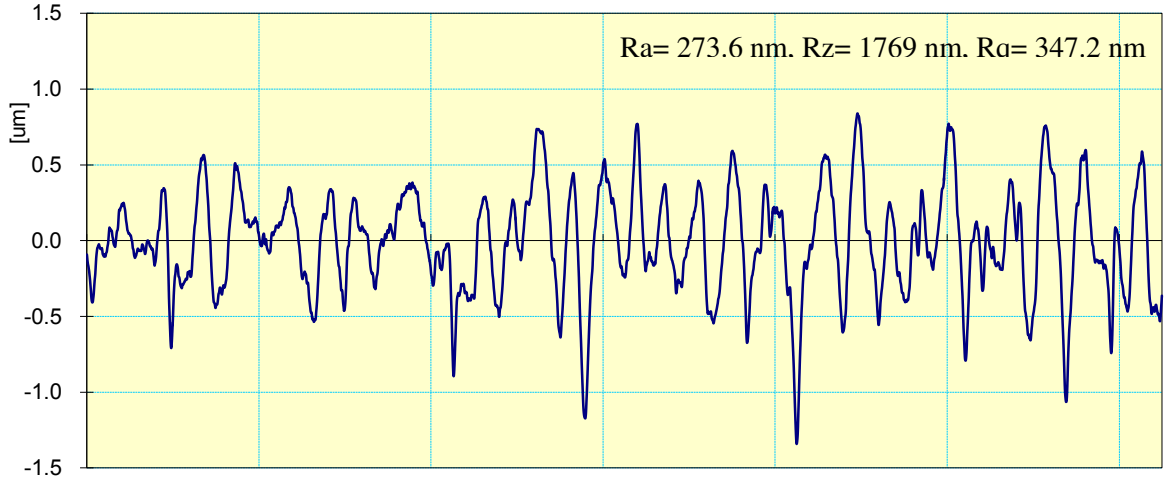

(a)

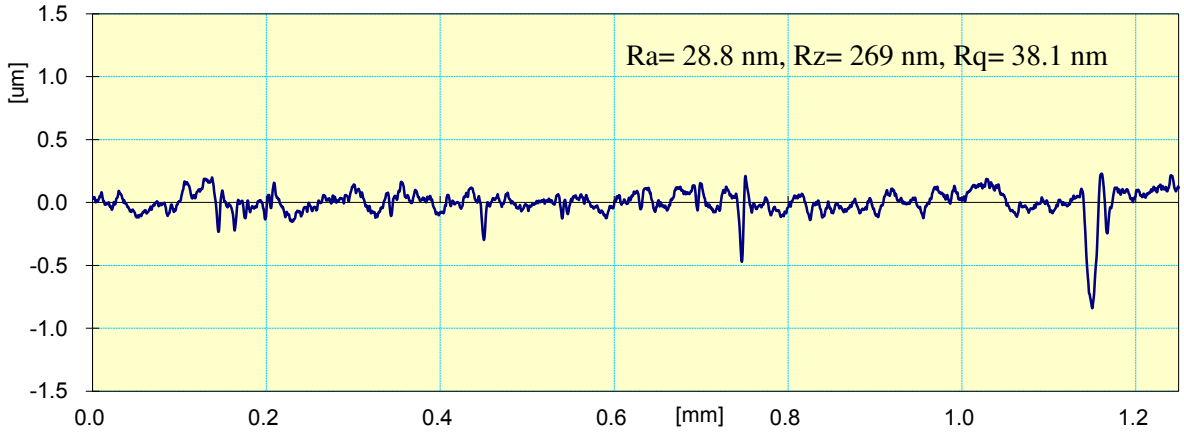

(b)

Figure 4.10: Surface roughness profiles of copper alloy workpiece (a) initial and (b) final after finishing of 7.5 minutes.

The second experiment was performed with the parameters mentioned in set 2 (Table 4.4) for the further finishing time of 2.5 minutes. After this cycle, the surface roughness of the workpiece decreased to Ra = 48.6 nm, Rq= 71.6 nm and Rz= 367.7 nm. Third i.e. the last finishing cycle of 2.5 minutes was performed with parameters of set 3 as mentioned in Table

4.4. After this cycle surface roughness of the workpiece was decreased to Ra = 28.8 nm, Rq= 38.1 nm and Rz= 269 nm. Roughness profile of final finished surface is obtained from Mitutoyo Surftest SJ-400 machine as shown in Fig. 4.10 (b). With the parameters mentioned in the Table 4.4, the three sets of finishing have been performed with 2.5 minutes each cycle. Surface roughness parameters have been recorded after each set of finishing. The decrease in surface roughness parameters i.e. R_a, R_q and R_z during complete experimentation at different cycle time is shown in Fig. 4.11.

The trend of decrease in surface roughness value Ra in percentage with respect to each cycle time is plotted in Fig. 4.12. Initially, the percentage reduction in Ra value is more i.e. 60.19% because of shearing of peak edges of the surface. Later on it decreases to 40.74% as after 5 minutes, the peaks get flattened and it is difficult to shear out the flattened surface by abrasives because of higher shear modulus of flattened surface. When MR polishing fluid is applied on the magnet between the working gap, the chains of carbonyl iron particles (CIPs) were formed with abrasives embedded in it. CIPs attract each other with greater magnetic force and provide more bonding strength for holding the abrasive particles together firmly. This restricts the lateral displacement motion of abrasive particles due to the presence of CIPs around them and preventing it from the rolling motion during the finishing cycle. On interaction with the roughness peaks, the abrasives are capable of shearing peaks and yielding chips. In this case, first two cycles of finishing resulted in improvement in Ra from 273.6 nm to 48.6 nm.

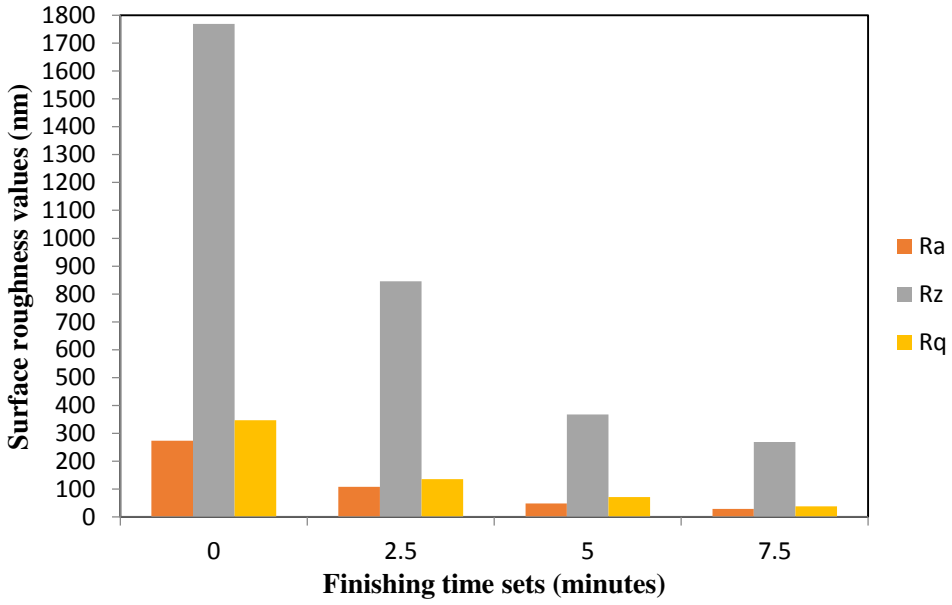

Figure 4.11: Surface roughness parameters versus finishing time.

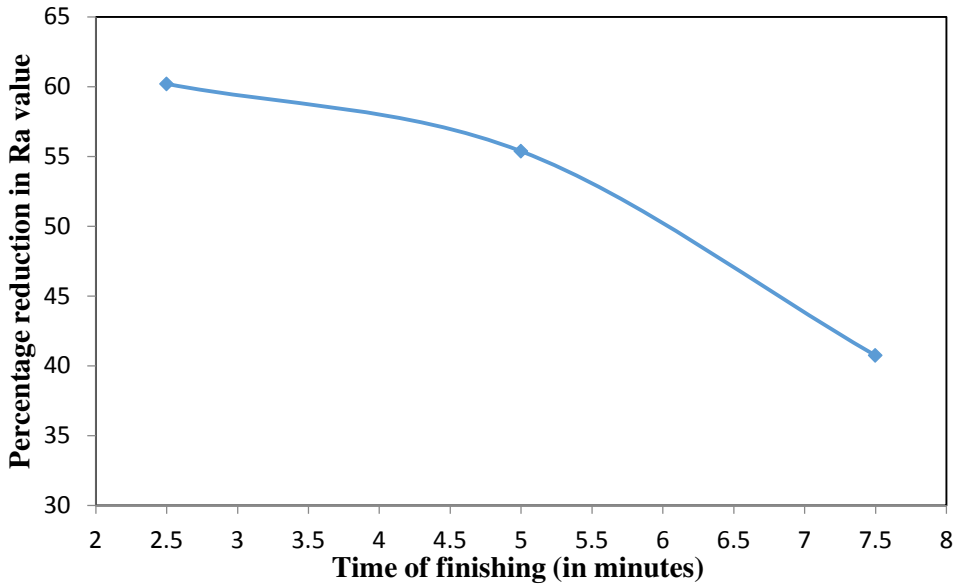

Figure 4.12: Percentage reduction in Ra value with respect to time of finishing.

In the third cycle when smaller sized abrasives were used, polishing of the workpiece surface was finished up to Ra 28.8 nm with leveling of most of the peaks and valleys as observed under scanning electron microscopy (SEM) (Fig. 4.13). The most of the peaks got sheared which showed reduction in Ra values significantly. The surface gets flattened with small sharp peaks and few valleys left out are clearly visible in Fig. 4.19. The surface obtained for this finishing cycle with low Ra is the actual finished surface with reduced peaks and grinding marks. The process parameters can be optimized for higher surface finish (lower Ra value) once complete understanding of the process mechanism has to be developed.

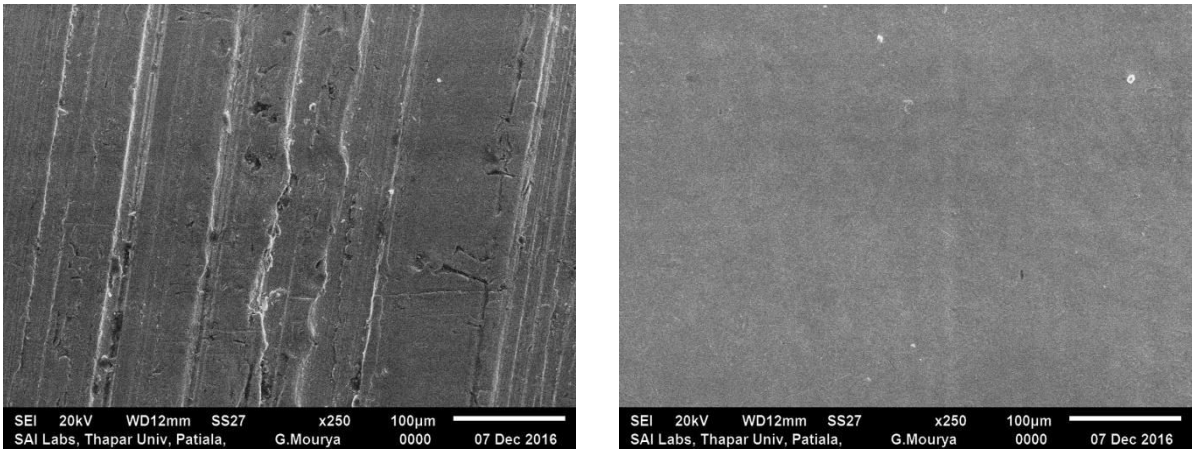

(a) (b)

Figure 4.13: Scanning electron microscopy (SEM) of copper alloy workpiece (a) before and (b) after 7.5 minutes of finishing cycle.

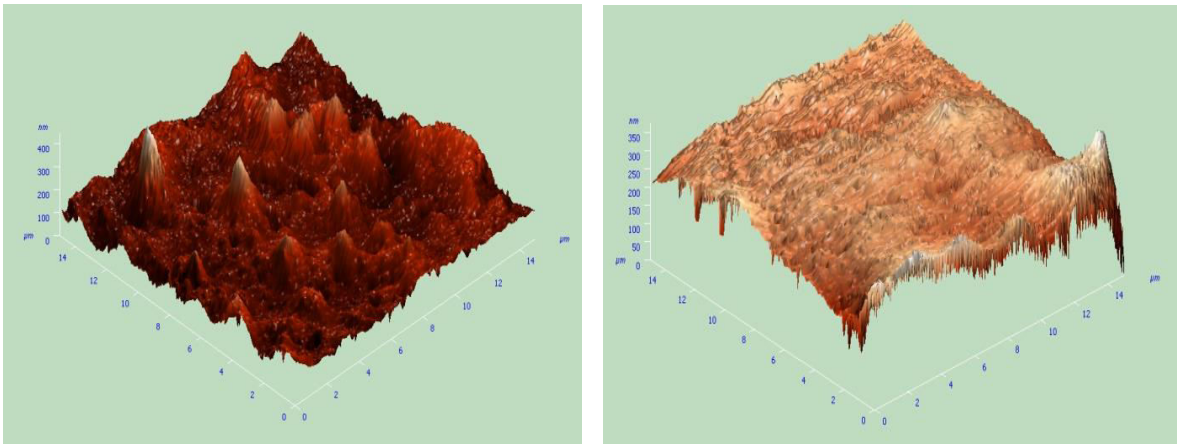

(a) (b)

Figure 4.14: Atomic force microscopy (AFM) results (a) before and (b) after finishing of 7.5 minutes.

The atomic force microscopy (AFM) images for the copper workpiece surface before and after 7.5 minutes of finishing by the newly developed magnetorheological finishing process is shown in Fig. 4.14. The normal magnetic force is applied on active abrasives and its rotation on workpiece surface resulted in finishing due to abrasion action. It can be seen from Fig. 4.14 (a) that the initial surface of the copper alloy workpiece is very rough as there are many high peaks and valleys. Figure 4.14 (b) shows the finished surface after 7.5 minutes of finishing cycle. It is clearly visible in Fig. 4.14 (b) that the surface quality improved significantly and the workpiece surface almost flattened with some small sharp peaks and few valleys left out. Upon the analysis of AFM image, the surface roughness values obtained are Ra = 18.48 nm, Rq= 26.4 nm and Rz= 194.85 nm. But surface roughness values obtained from the surface roughness tester are Ra = 28.8 nm, Rq= 38.1 nm and Rz= 269 nm. However, difference in the values of surface roughness is occurring because of the difference in the measuring scale in two different measuring processes. In case of surface roughness tester, the measurement of roughness was taken along a straight line for the distance of 1.25 mm whereas in case of AFM image analysis, the measurement of roughness was done on the surface area of square with edge 15 micron. The significant change in surface roughness value and surface quality demonstrates the finishing capability of newly developed finishing tool on diamagnetic workpiece.

4.3 Conclusions

A new finishing tool with permanent magnets is made for magnetorheological nanofinishing of paramagnetic and diamagnetic materials. The following conclusions were made which showed the presently developed permanent magnets tool is found suitable to finish the aluminium and copper workpiece surface.

- Surface roughness parameters i.e. R_a, R_q and R_z of the aluminum alloy workpiece get decreased from 718.2 nm, 981 nm and 4906 nm to 62.7 nm, 97.2 nm and 459 nm respectively in finishing time span of 20 minutes. Therefore, this new technique for nano-finishing of aluminum showed high productive rate.
- Surface roughness parameters i.e. Ra, Rq and Rz of the copper alloy workpiece get decreased from 273.6 nm, 347.2 nm and 1769 nm to 28.8 nm, 38.1 nm and 269 nm, respectively in finishing time span of 7.5 minutes. Therefore, this new technique for nano-finishing of diamagnetic materials showed high productive rate.
- Decrease in size of abrasives from 600 mesh size to 800 mesh size resulted in further decreases in surface roughness from 48.6 nm to 28.8 nm for copper and 152.1 nm to 62.7 nm for aluminium. Thus, size of the abrasives was found to be the critical parameter.
- Surface characteristics examined by atomic force microscopy (AFM) and scanning electron microscopy (SEM) of copper alloy workpiece and scanning electron microscopy (SEM) of aluminium alloy workpiece clearly signifies that most of the peaks have been removed and surface quality has been improved by the present magnetorheological fluid assisted finishing method.
- Results obtained from the experiments showed that the present new technique is capable for nano-finishing of paramagnetic materials such as aluminium which significantly useful in industries like aerospace and automobile industries. It is also useful especially in the field of micro-electronics and optics. Results obtained from the experiments on diamagnetic materials such as copper showed that the present new technique is capable for nano-finishing that is significantly useful in industries like aerospace, dentistry and laser etc. for metallic mirrors. It is also useful to nanofinish the copper electrodes of electric discharge machining and many other electronics components.

Chapter 5

Plan of Experiments using Response Surface Methodology

In the present section, the newly developed finishing tool i.e. Hemispherical end magnetorheological finishing (HEMRF) process has been used. In abrasive based polishing process, ductile materials like copper is highly challenging to generate nano metric surface finish [Ranjan et al., 2017]. The most difficult task is performing finishing in least time. Response surface methodology has been used to plan and analyze the effect of rotational speed of tool, abrasive mesh size, abrasive concentration and carbonyl iron particles on percentage change in surface roughness value. The experimental results are discussed and the best finishing conditions are identified using the experimental range of process parameters. The performance of finishing process with different MR polishing fluid compositions has been studied. The optimal process parameters are then identified from the results obtained from the experimental range of process parameters. In order to study the finished surface morphology, the scanning electron microscopy (SEM) is also conducted. The performance of finishing process has been evaluated with the identified significant process parameters. Also results of the optimal parameters are validated experimentally and using the Eq. of surface roughness reduction formed by response surface methodology.

5.1 Experimental Setup for the Finishing

Experimentation has been performed by the newly developed finishing tool hemispherical end magnetorheological finishing (HEMRF) tool on the copper alloy workpieces. The complete magnetorheological finishing setup for finishing the diamagnetic copper alloy workpiece is shown in Fig. 4.7. The shaft rotates in C-shaped aluminium bracket which is mounted over the Z-slide. Workpiece holder is mounted on X-Y slide mounted on the machine table and MR finishing tool assembly travel in vertical direction along Z-axis. Position of copper alloy workpiece beneath the surface of the finishing tool can be precisely adjusted by linear X-Y as shown in Fig. 4.7. The working gap of 1.5 mm thickness is maintained for MR polishing fluid between the bottom face of finishing tool and workpiece surface by moving the Z-slide.

Working gap between the finishing tool surface and the workpiece surface plays a vital role in MR fluid based finishing processes. Working gap of 1.5 mm thickness is maintained between finishing tool surface and copper alloy workpiece surface. The thickness of 1.5 mm of MR polishing fluid has been decided on the basis of trial experiments. It is maintained in such a way that no erosion of copper alloy workpiece occurs and only surface can be polished. Also, the finishing forces exerted by the finishing spot of the MR polishing fluid on the workpiece surface can be found to be higher at the lower working gap and relatively less at the higher working gap.

Table 5.1: Chemical composition of copper alloy workpiece

Sr. No.	**Material**	**Percentage by mass (%)**
1.	Copper (Cu)	91.51
2.	Aluminium (Al)	0.15
3.	Carbon (C)	7.48
4.	Oxygen (O)	0.85

MR polishing fluid is prepared by thoroughly mixing of carbonyl iron (CI) particles, silicon carbide (SiC) particles in base fluid with the help of mixing chamber. The base fluid consists of 20 % AP3 grease and 80 % paraffin oil. The workpiece of copper alloy of size 50 mm × 40 mm × 5 mm has been used for experimentation. Electron dispersive spectography (EDS) of copper alloy has been performed and chemical composition of the copper alloy workpiece is reported in Table 5.1.

5.2 Process Variables for the Experiment

List of controllable and uncontrollable variables that may have effects on nano-finishing of copper alloy workpiece are reported in Table 5.2. Out of these variables, those independent variables which affects the finishing process significantly has been selected for parametric study are described below.

Table 5.2: Process variables for the experimentation

Dependent uncontrollable variables	**Independent controllable variables**
Permanent magnets and magnetic field	Properties of the workpiece material
Ambient temperature	Initial surface roughness of the workpiece
	Speed of the tool rotation
	Abrasive type, mesh size and concentration
	Carbonyl iron particle size and concentration
	Percentage volume of base medium
	Viscosity of the fluid

5.2.1 Tool Rotation Speed

Speed of the tool rotation has a significant effect in the finishing of workpiece. The indentation force provided by the magnetizing field along with shearing force as provided by the rotation of the tool forms a resultant force on the active abrasive particles. The removal of material, in the form of micro chips, can be found owing to this resultant force. Experimental range for tool rotation was selected as 250 rpm to 1250 rpm. The levels of tool rotation were selected on the basis of "α" value for statistical design. The range of these values was chosen on the basis of preliminary experimentation.

5.2.2 Mesh Size of Abrasive Particles

Selection of suitable mesh size of abrasive particles is very important. Abrasives used for experimentation is silicon carbide (SiC). Generally, lesser mesh sized abrasive particles are used for finishing the workpiece yielding micro chips but larger mesh size of abrasive particles is used for polishing yielding nano chips from the workpiece surface. Experiments were conducted with the mesh size varying from 400 to 1200 mesh as per the design levels. The range of these values was chosen on the basis of preliminary experimentation as well as previous literature available.

5.2.3 Concentration of Abrasive Particles

Abrasive particles are added in the MR fluid in order to remove the material in the form of micro chips. The chipping off action is performed by the active abrasive particles at

the surface of the tool tip. These abrasive particles are gripped between the chains of CIPs. The amount of abrasive particles will have considerable effect on the cutting action performed by the tool. Experiments were conducted with the concentration in percentage volume varying from 10% to 30% as per the design levels. The range was selected on previous literature available.

5.2.4 Concentration of Carbonyl Iron Particles

Carbonyl iron particles (CIPs) are important element of MR polishing fluid. They are responsible for gripping the abrasive particles in the chain like structures formed by them when magnetic field is applied across them. For a particular level of abrasives, if the CIPs are too low, they might not be able to grip enough abrasive particles and if the CIPs are too high it may result in lower abrasive concentration thus leading to reduced cutting action. Experiments were conducted with concentration in percentage change varying from 10% to 30%, as per the design level. The range was selected on the basis of previous literature.

5.3 Design of Experiment

Systematic investigation of the effect of process variables on the percentage change in surface roughness value was done using the designed experiments. The setup shown in Fig. 5.1 was used for performing the designed experimentation. The initial surface roughness (R_{ai}) was approximately same for all the workpiece i.e. 198 nm. The workpiece is held in the precision vice tightly and then precision vice along with workpiece is fixed on X–Y movement linear slides driven by HMI (human machine interface) controlled servo motors. For the complete finishing of workpiece, reciprocating linear motion in Y- axis by servo motor was given. For the finishing, time span of 10 minutes was used for each experiment.

Response surface methodology is a collection of mathematical methods and statistical techniques that are used for analysis and modeling the engineering problems. The conditions at which experiments conducted are represented by the combination of different factor levels and measurement of responses is done for those combinations. Four factor three level full factorial designs with six central runs were to make combination of the factors and conduct the experiments. To explain the relationship between the process parameters and improvement in surface finish and to know the significance of the regression equation, *F-test* was conducted from the analysis of variance (ANOVA). Using the full factorial design,

investigation on percentage change in surface roughness value (% ΔR_a) is carried out to know the effects of four process variables.

Coded levels and actual values of the parameters used in the finishing process of copper alloy workpiece are listed in Table 5.3. Other experimental conditions and parameters used during the experimentation are reported in Table 5.4. As per the plan of experiment provided in the Table 5.5, randomly experiments were conducted on the workpiece.

Table 5.3: Coded levels and actual values of the parameters used in the finishing process

Sr. No.	**Parameter**			**Levels**		
		-2	**-1**	**0**	**1**	**2**
1.	Speed of the tool rotation in rpm (*N*)	250	500	750	1000	1250
2.	Abrasive mesh size (*M*)	400	600	800	1000	1200
3.	% abrasive concentration (*S*)	10	15	20	25	30
4.	% carbonyl iron particles (*C*)	10	15	20	25	30

Table 5.4: Experimental conditions and parameters used for the finishing

Sr. No.	**Parameters**	**Conditions**
1.	CIPs Size	600 mesh
2.	Finishing cycle time	10 minutes
3.	Working gap	1.5 mm

Table 5.5: List of plan of experiments

Run Order	**Std order**	**Parametric conditions**			
		N	**M**	**S**	**C**
14	1	500	600	25	25
4	2	1250	800	20	20
18	3	750	800	20	20
24	4	500	600	15	25
7	5	1000	600	25	25

9	6	750	800	20	20
20	7	500	600	25	15
13	8	500	1000	15	15
27	9	250	800	20	20
3	10	500	600	15	15
30	11	500	1000	25	25
21	12	1000	1000	25	15
8	13	750	800	20	20
5	14	750	800	30	20
6	15	1000	1000	15	25
28	16	750	800	20	20
23	17	750	400	20	20
17	18	750	800	20	30
29	19	750	800	20	10
22	20	1000	600	25	15
26	21	1000	600	15	25
10	22	1000	1000	15	15
2	23	1000	1000	25	25
16	24	500	1000	15	25
19	25	750	800	20	20
25	26	750	1200	20	20
12	27	750	800	20	20
15	28	500	1000	25	15
11	29	1000	600	15	15
1	30	750	800	10	20

The responses in terms of percentage change in roughness value (% Δ Ra) are presented in Table 5.6. Response surface for percentage change in R_a value is analyzed. Eq. 5.1 gives the formula to calculate percentage change in roughness value (% Δ R_a).

$$\Delta R_a\ (\%) = (R_{a\ initial} - R_{a\ final})\ \text{x}\ 100\ /\ R_{a\ initial} \qquad (5.1)$$

Table 5.6: Summary of the responses obtained from the experiments

Std order	**Parametric conditions**				**Percentage change in roughness value (% Δ R_a)**
	N	**M**	**S**	**C**	
1	500	600	25	25	72.1
2	1250	800	20	20	89.2
3	750	800	20	20	75.8
4	500	600	15	25	69.5
5	1000	600	25	25	83.1
6	750	800	20	20	81.4
7	500	600	25	15	72.6
8	500	1000	15	15	76.9
9	250	800	20	20	75.2
10	500	600	15	15	73.8
11	500	1000	25	25	70.2
12	1000	1000	25	15	88.5
13	750	800	20	20	79.3
14	750	800	30	20	82.9
15	1000	1000	15	25	67.6
16	750	800	20	20	82.2
17	750	400	20	20	63.9
18	750	800	20	30	68.3
19	750	800	20	10	80.1

20	1000	600	25	15	79.0
21	1000	600	15	25	72.3
22	1000	1000	15	15	79.7
23	1000	1000	25	25	83.1
24	500	1000	15	25	58.5
25	750	800	20	20	80.1
26	750	1200	20	20	79.2
27	750	800	20	20	81.7
28	500	1000	25	15	74.8
29	1000	600	15	15	74.9
30	750	800	10	20	61.4

The sequential model sum of squares was calculated to select the highest order polynomial where the additional terms are significant and the model is not aliased. Table 5.7 of sequential model sum of squares show how terms of increasing complexity contribute to the total model. The significance of adding quadratic terms to two factor interactions and linear term is highest, as it has high *F*- value and least *p*- value suggesting its suitability. Lack of fit for all possible models was calculated and is presented in Table 5.8. For the selected quadratic model, the lack of fit is insignificant.

On the basis of Tables 5.7 and 5.8, quadratic model was selected. Initially all the terms such as N, M, S, C, NM, NS, NC, MS, MC, SC, N^2, M^2, S^2 and C^2 were included in the response surface model. The ANOVA for this model is given in Table 5.9. The model *F*-value of 10.35 implies that the model is significant. There is only a 0.01% chance that this large Model F-Value could occur due to noise. If the values of Prob > F less than 0.05 then it indicates that the model is significant. The significant level (0.05) for a given hypothesis test is a value for which a *p –value* less than or equal to α is considered statistically significant.

Table 5.7: Sequential model sum of squares

Source	Sum of squares	DOF	Mean square	F-Value	Prob > F	Remarks
Mean	171143.4	1	171143.4			
Linear	932.9483	4	233.2371	8.407065	0.0002	
2FI	244.5088	6	40.75146	1.724196	0.1697	
Quadratic	296.4251	4	74.10627	7.282416	0.0018	Suggested
Cubic	113.1967	8	14.14958	2.511071	0.1212	Aliased
Residual	39.44417	7	5.634881			
Total	172770	30	5758.998			

Table 5.8: Lack of Fit Tests

Source	Sum of Squares	DF	Mean Square	F value	Prob>F	
Linear	658.82	20	32.94	4.74	0.0461	
2FI	414.31	14	29.59	4.26	0.0593	
Quadratic	117.89	10	11.79	1.7	0.2912	Suggested
Cubic	4.69	2	2.35	0.34	0.7287	Aliased
Pure Error	34.75	5	6.95			

Table 5.9: ANOVA for the percentage reduction in surface roughness value

Source	Sum of squares	DOF	Mean square	F-Value	Prob > F	Remarks
Model	1473.882	14	105.2773	10.34559	< 0.0001	significant
N	335.2538	1	335.2538	32.94535	< 0.0001	
M	47.32042	1	47.32042	4.650173	0.0477	
S	370.5204	1	370.5204	36.41101	< 0.0001	
C	179.8538	1	179.8538	17.67421	0.0008	

N^2	6.546458	1	6.546458	0.64332	0.435	
M^2	140.275	1	140.275	13.78481	0.0021	
S^2	125.1965	1	125.1965	12.30304	0.0032	
C^2	62.66074	1	62.66074	6.157665	0.0254	
NM	19.58063	1	19.58063	1.924186	0.1857	
NS	50.05563	1	50.05563	4.918961	0.0424	
NC	6.630625	1	6.630625	0.651591	0.4322	
MS	16.60563	1	16.60563	1.631833	0.2209	
MC	88.83063	1	88.83063	8.729377	0.0098	
SC	62.80563	1	62.80563	6.171903	0.0253	
Residual	152.6408	15	10.17606			
Lack of Fit	117.8875	10	11.78875	1.69606	0.2912	not significant
Pure Error	34.75333	5	6.950667			
Total	1626.523	29				

In the present study the significance level is taken as $\alpha = 0.05$. In this case N, M, S, NS, MS, SC, M^2, S^2 and C^2 are significant terms. *p*-values greater than 0.05 indicate that terms are not significant. If there are many insignificant terms, then the model reduction by removing insignificant terms may improve the model. The lack of fit is the variation of data around the fitted model. The lack of fit *F*-value of 1.70 implies there is a 29.12% chance that this large lack of fit *F*-value could occur due to noise.

Table 5.10: Other ANOVA parameters

Std. Dev.	3.19	R-Squared	0.9062
Mean	75.53	Adj R-Squared	0.8186
C.V.	4.22	Pred R-Squared	0.5518
PRESS	729.08	Adeq Precision	13.198

Other ANOVA parameters are given in Table 5.10. The predicted R^2 which is a measure of how good the model predicts a response value. The Predicted R^2 of 0.5518 is not as close to the Adjusted R^2 of 0.8186 as one might normally expect. This may indicate a large block effect or a possible problem with model or data. Things to consider are model reduction, response tranformation, etc. Adequate Precision measures the signal to noise ratio. A ratio greater than 4 is desirable. In the above model, this ratio of 13.198 indicates an adequate signal. This model can be used to navigate the design space.

Hence, Eq. in terms of actual factors is given as:

$$\%\Delta Ra \text{ reduction} = +20.64271 - 0.053075N + 0.10764M + 0.74292S + 1.78458C + 0.00000781667N^2 - 0.0000565365M^2 - 0.085458S^2 - 0.060458C^2 + 0.0000221250NM + 0.001415NS + 0.000515NC + 0.00101875MS - 0.00235625MC + 0.079250SC \quad (5.2)$$

The ANOVA analysis after dropping the insignificant terms is presented in Tables 5.11 and 5.12. The Model F-value of 13.40 implies the model is significant. There is only a 0.01% chance that a Model F-Value this large could occur due to noise. Values of Prob > F less than 0.0500 indicate model terms are significant. In this case N, M, S, NS, MS, SC, M^2, S^2 and C^2 are significant model terms. The Lack of Fit F-value of 1.72 implies the Lack of Fit is not significant relative to the pure error. There is a 28.63% chance that a Lack of Fit F-value this large could occur due to noise. Other ANOVA parameters after dropping insignificant terms are given in Table 5.13. The predicted R^2 of 0.5827 is not as close to the Adjusted R^2 of 0.8104 as one might normally expect. This may indicate a large block effect or a possible problem with model or data. The adequate precision value measures the signal to noise ratio. A ratio greater than 4 is desirable. The ratio of 12.926 indicates an adequate signal.

Table 5.11: ANOVA for the percentage reduction in surface roughness value after dropping insignificant terms

Source	**Sum of squares**	**DOF**	**Mean square**	**F-Value**	**Prob > F**	**Remarks**
Model	1424.519	10	142.4519	13.39866	< 0.0001	significant
N	335.2538	1	335.2538	31.53312	< 0.0001	

M	47.32042	1	47.32042	4.450838	0.0484	
S	370.5204	1	370.5204	34.85021	< 0.0001	
C	179.8538	1	179.8538	16.91659	0.0006	
M^2	152.1723	1	152.1723	14.31295	0.0013	
S^2	136.2911	1	136.2911	12.81919	0.002	
C^2	70.00984	1	70.00984	6.584948	0.0189	
NS	50.05563	1	50.05563	4.708105	0.0429	
MC	88.83063	1	88.83063	8.355183	0.0094	
SC	62.80563	1	62.80563	5.907338	0.0252	
Residual	202.0042	19	10.6318			
Lack of fit	167.2508	14	11.94649	1.718754	0.2863	not significant
Pure error	34.75333	5	6.950667			
Total	1626.523	29				

Table 5.12: Lack of Fit Tests after dropping insignificant terms

Source	**Sum of Squares**	**DF**	**Mean Square**	**F value**	**Prob>F**	
Linear	658.82	20	32.94	4.74	0.0461	
2FI	414.31	14	29.59	4.26	0.0593	
Quadratic	117.89	10	11.79	1.7	0.2912	Suggested
Cubic	4.69	2	2.35	0.34	0.7287	Aliased
Pure Error	34.75	5	6.95			

Table 5.13: Other ANOVA parameters after dropping insignificant terms

Std. Dev.	3.26	R-Squared	0.8758
Mean	75.53	Adj R-Squared	0.8104
C.V.	4.32	Pred R-Squared	0.5827
PRESS	678.81	Adeq Precision	12.926

Hence, final Eq. in terms of actual factors in reduced form is given as follows

$$\%\Delta Ra \text{ reduction} = -23.84583 - 0.01335N + 0.1474M + 1.66958S + 2.2825C - 0.0000582812M^2 - 0.08825S^2 - 0.06325C^2 + 0.001415NS - 0.00235625MC + 0.07925SC \quad (5.3)$$

The percentage contribution of the parameters used in the process in final surface roughness value R_a is mentioned in Table 5.14.

Table 5.14: Percentage contribution of the parameters used in the process in final surface roughness value R_a

Source	Sum of squares	Percentage contribution
N	335.254	21.9426
M	47.3204	3.09716
S	370.52	24.2508
C	179.854	11.7716
M^2	152.172	9.95979
S^2	136.291	8.92035
C^2	70.0098	4.5822
NS	50.0556	3.27618
MC	88.8306	5.81403
SC	62.8056	4.11067
Pure error	34.7533	2.27463

5.4 Results and Discussion

Using the results obtained after regression analysis of the responses, the results in terms of the effect of mesh size of the abrasives particles, abrasive particle concentration, rotational speed of tool and concentration of carbonyl iron particles on the percentage reduction of roughness value ($\%\Delta R_a$) of the surface have been observed and computed. The effects of these independent controllable variables on the $\%\Delta R_a$ value have been discussed as follows.

5.4.1 Effect of Speed of Tool Rotation (N)

The percentage change in surface roughness increases with an increase in speed of the tool rotation as observed in the Fig. 5.1. In Fig. 5.1, the effect of the speed of the tool rotation on the $\%\Delta R_a$ with different mesh size of the abrasive particles and at a constant value of 20% concentration of both abrasive particles and CIPs. Lowest $\%\Delta R_a$ is observed for mesh size 600 of abrasives. Surface roughness reduction value of 1000 mesh size of abrasives is slightly lower than that of 800 mesh size of abrasives. This occurred due to proper holding of abrasives of 800 mesh in the CIPs of 600 mesh size and providing significant cutting edges for the finishing.

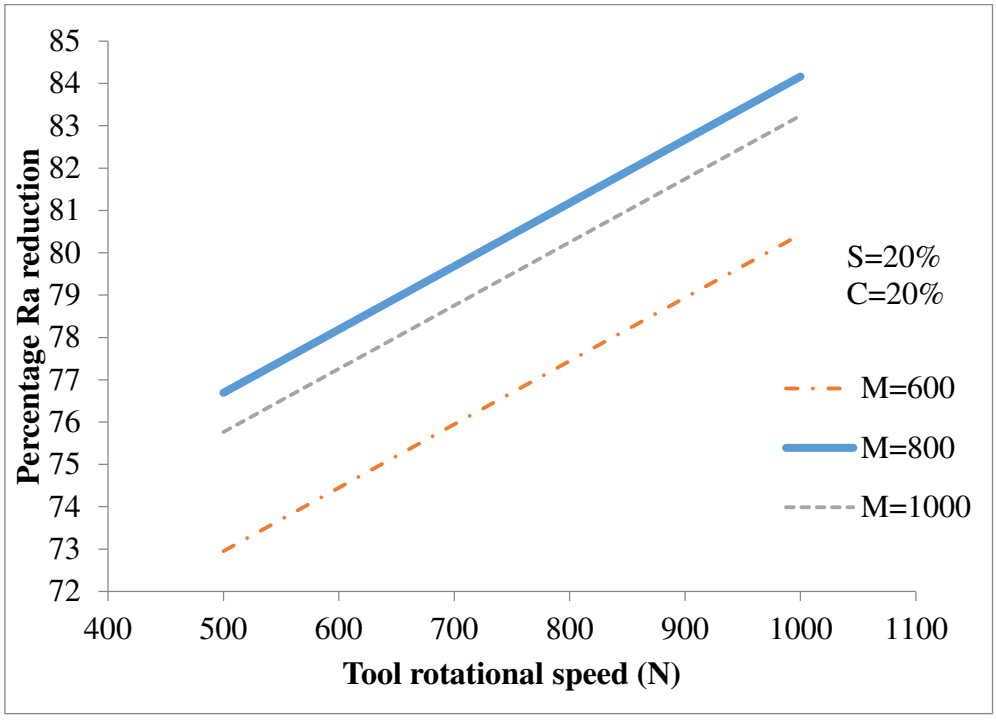

Figure 5.1: Effect of tool rotation speed on percentage change in roughness value.

5.4.2 Effect of Mesh Size of Particles of the Abrasive (M)

The effect of mesh size of particles of the abrasive on percentage change in value of surface roughness at different concentration of abrasive at a fix value of CIP concentration of 20% and tool rotation speed of 750 rpm is shown in Fig. 5.2. It is observed from the experimental result that as the mesh size of abrasive particles is increased, the $\%\Delta R_a$ increases initially and then decreases after a particular value. The decrement in $\%\Delta R_a$ after a particular value happens due to at higher mesh size the particle size decreases and with small size particles, there is less removal of material. Lowest reduction in surface roughness is

observed for mesh size 600 of abrasives. During finishing, the normal force acts on the abrasive particle due to which the abrasive particle penetrate the workpiece surface. Therefore bigger size particle remove more material initially as compared to small size particle. But for the proper finishing a moderate range of mesh size of the abrasive is required. Hence it is observed that reduction in surface roughness value with 1000 mesh size of abrasives is slightly lower than that with 800 mesh size of abrasives.

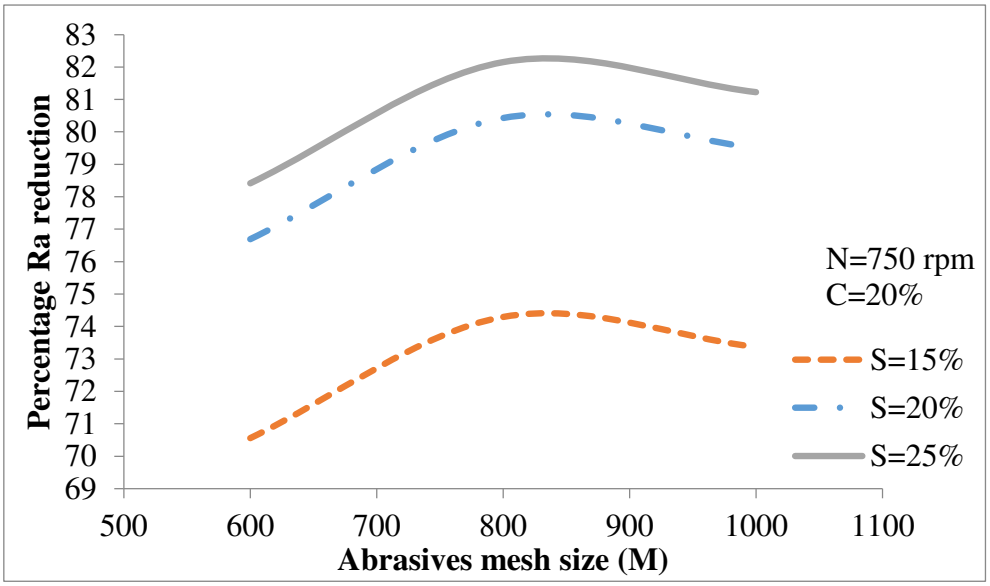

Figure 5.2: Effect of abrasive mesh size on percentage change in roughness value.

5.4.3 Effect of Abrasive Concentration (S)

Abrasives are the non magnetic particles and mainly responsible for the finishing. As the abrasive concentration increased in MR polishing fluid, higher number of abrasive particles performs cutting action. This results in increased finishing action. After a certain volume of abrasive concentration, further addition of abrasives reduces the magnetic permeability of the MR polishing fluid that weakens the CIP chains during the finishing. These weak chains get broken under shear flow and result in lower material removal from the roughness peaks which reduce the % ΔR_a at higher volume concentration of abrasives.

In the Fig. 5.3, it can be observed that there is slight decrease in % ΔR_a after 24% of abrasive concentration. Also with the increase in speed of tool rotation keeping abrasive mesh size at 800 and CIP concentration as 20%, increase in reduction of surface roughness is shown in Fig. 5.3.

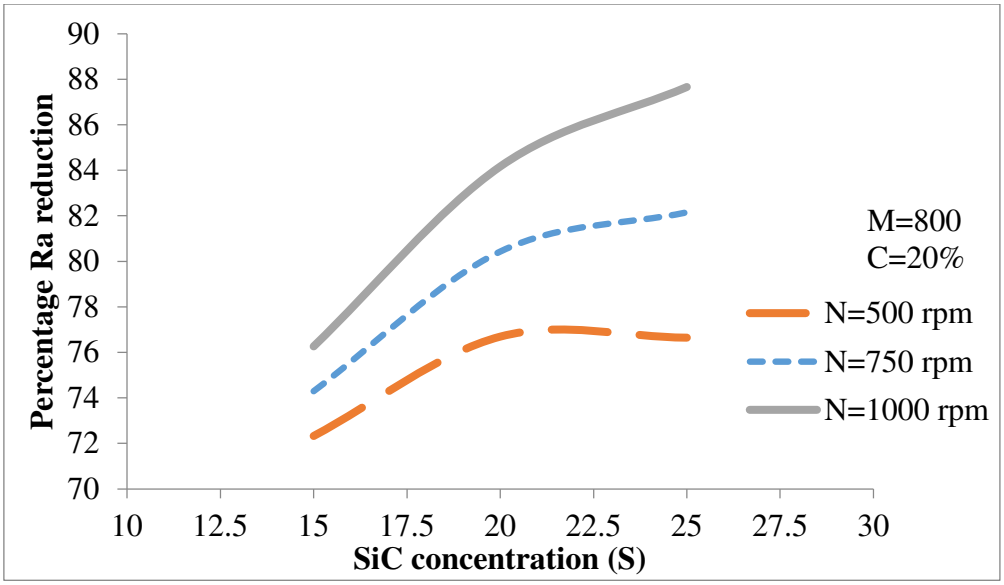

Figure 5.3: Effect of abrasive concentration on percentage change in roughness value.

5.4.4 Effect of Carbonyl Iron Particle Concentration (C)

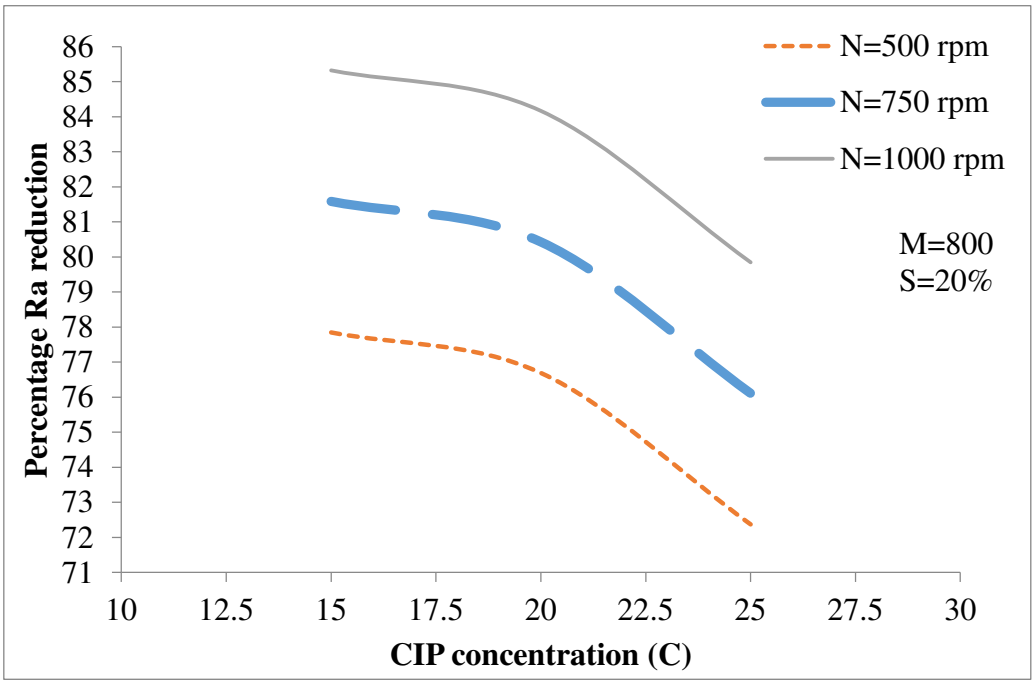

Figure 5.4: Effect of carbonyl iron particle concentration on percentage change in roughness value.

Carbonyl iron particle (CIP) concentration is a vital parameter for magnetorheological effect in MR polishing fluid assisted finishing processes. The main function of CIPs is to grip the abrasive particles in between chains that are formed under the influence of magnetic field. But as shown in Fig. 5.4, $\%\Delta R_a$ decreases as the CIP concentration increases, where abrasive concentration was kept constant as 20% of mesh size 800. This happened mainly due to

relative decrease in abrasives concentration in the MRP fluid at higher concentration of CIPs. Dense column of MR polishing fluid is formed at higher concentration of CIPs that strongly grips the abrasive particles but due to overall decrease in abrasive concentration, less removal of material occurs during finishing process. However with the increase in tool rotation speed, increase in reduction of surface roughness value is observed as shown in Fig. 5.4.

5.5 Optimization of the Process Parameters

From the study it is observed that the optimum independent variable values for best finishing on diamagnetic copper alloy workpiece are tool rotation speed is 1250 rpm, abrasive mesh size of 800 with abrasive concentration 24% and carbonyl iron particles (CIPs) concentration of 19%. Initial surface roughness parameters (R_a, R_q and Rz) of the copper alloy workpiece have been measured with Mitutoyo Surftest SJ- 400 instrument and are found as R_a= 198 nm, R_q= 254 nm and R_z= 1173 nm. Using optimum parameters of 1250 rpm of tool speed rotation, fluid composition as 24% abrasive concentration of 800 mesh size and 19% iron powder concentration, finishing was done with respect to finishing cycles of 2.5 minutes. The same workpiece was used for all experiments and successive polishing was done. The surface roughness obtained after previous experiment was taken as initial roughness value for next experiment. The surface roughness value R_a with respect to finishing cycle of 2.5 minutes is shown in Fig. 5.5. Initially for the first three cycles i.e. upto 7.5 minutes, high reduction in R_a value is observed, as in these cycles shearing of peak edges of the surface. But at 10 minutes, there is less decrease in surface roughness value as shown in Fig. 5.6. The reason behind less decrease in R_a value is the flattened peaks on the workpiece surface and it becomes difficult to shear out the flattened surface by the abrasives in same condition because of higher shear modulus of flattened surface. The surface roughness parameters (R_a, R_q and Rz) after finishing of 10 minutes with optimum parameters, are found as R_a= 18.3 nm, R_q= 24 nm and R_z= 153 nm. Surface roughness reduction ($\%\Delta R_a$) after the finishing with optimum parameters for 10 minutes is found to be 90.75% whereas from the Eq. 5.3 it was expected to be 93.25%. Error upto 5% is accepted during confirmation of theoretical value to experimental value. This also validates the experimental results and Eq. of roughness reduction derived from the plan of experiments.

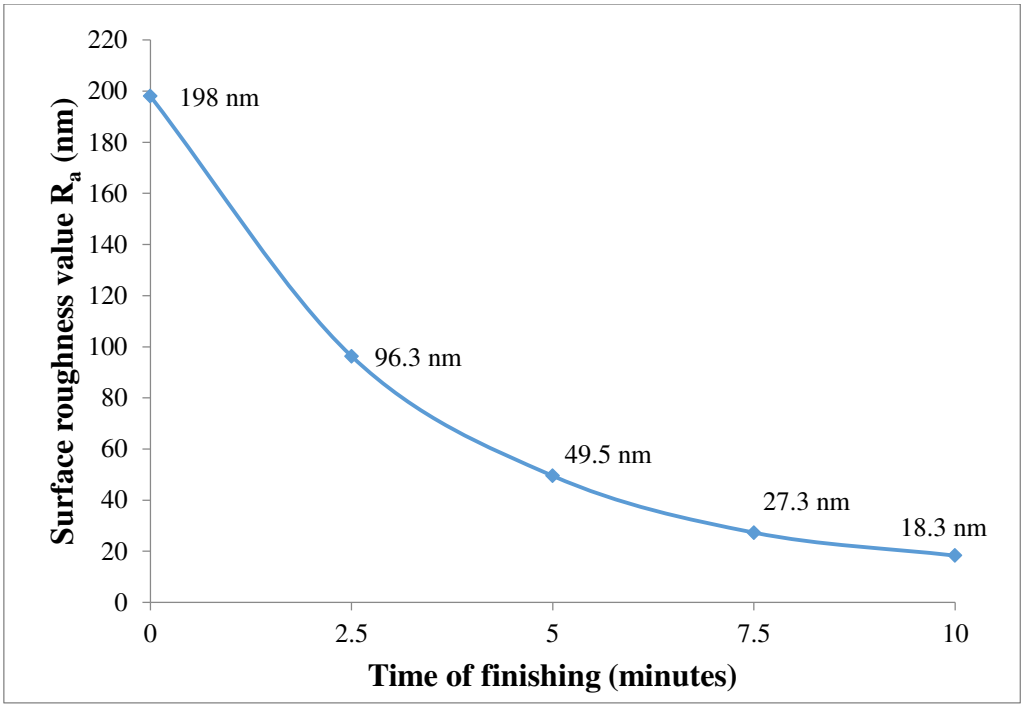

Figure 5.5: Surface roughness value R_a of workpiece with respect to time with optimum parameters N=1250 rpm, S=24%, M=800 mesh size and C=19%.

Surface roughness profile of the initial surface of the workpiece before the finishing cycle is shown in Fig. 5.6(a) and surface after finishing cycle of 10 minutes with optimum parameters is shown in Fig. 5.6(b). The surface roughness obtained after finishing cycle of 10 minutes at optimum condition was found to be as low as 18.3 nm. Using scanning electron microscopy (SEM), the surface morphology of the workpiece was observed for initial surface of the workpiece before the finishing cycle is shown in Fig. 5.7(a) and surface after finishing cycle of 10 minutes with optimum parameters is shown in Fig. 5.7(b). As observed from the SEM images, the finished surface characteristics are greatly improved as compared to the initial surface of a workpiece. As observed under SEM, on the finished workpiece surface leveling of most of the peaks and valleys is done. Using optimum parameters, it is shown that there is significant change in percentage R_a value within least finishing time of 10 minutes. Such high finishing on copper surface is necessary in manufacturing of metallic mirrors for different plasma diagnostics and also mitigating the needs of electronic industries.

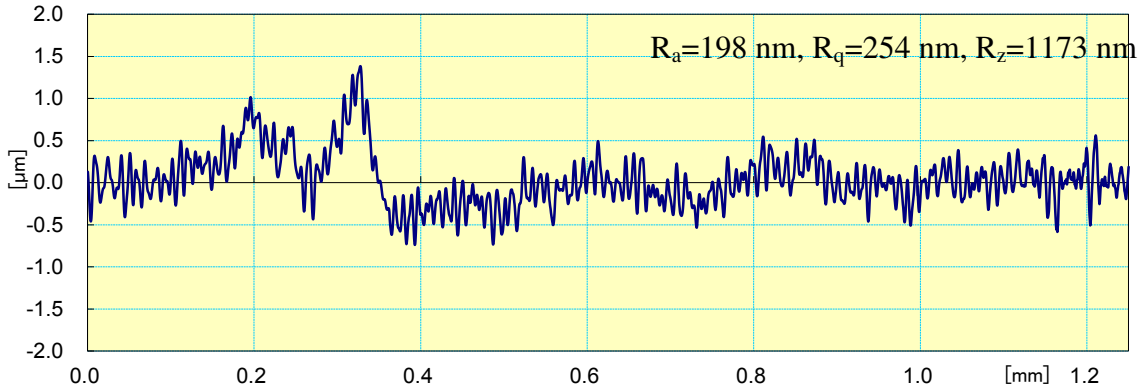

(a)

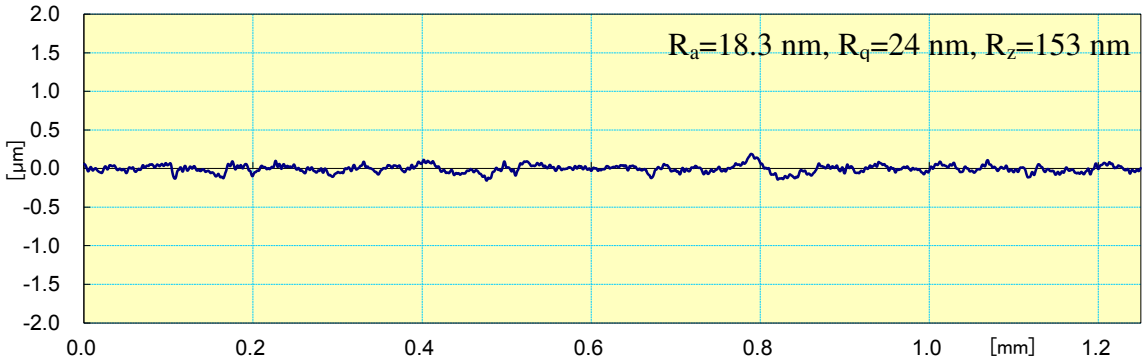

(b)

Figure 5.6: Surface roughness profiles of copper alloy workpiece (a) initial and (b) final after finishing cycle of 10 minutes with optimum parameters N=1250 rpm, S=24%, M=800 mesh size and C=19%.

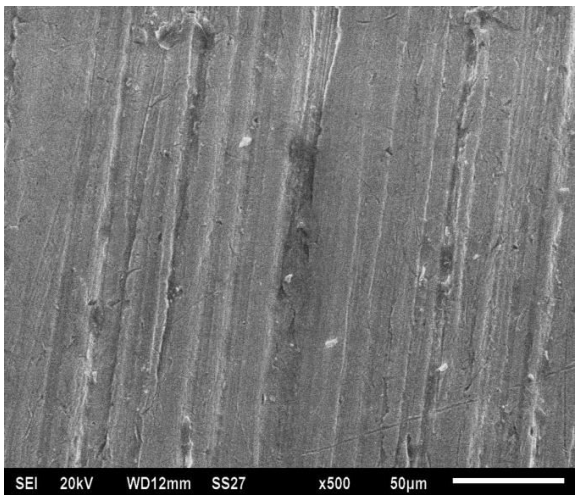

(a)

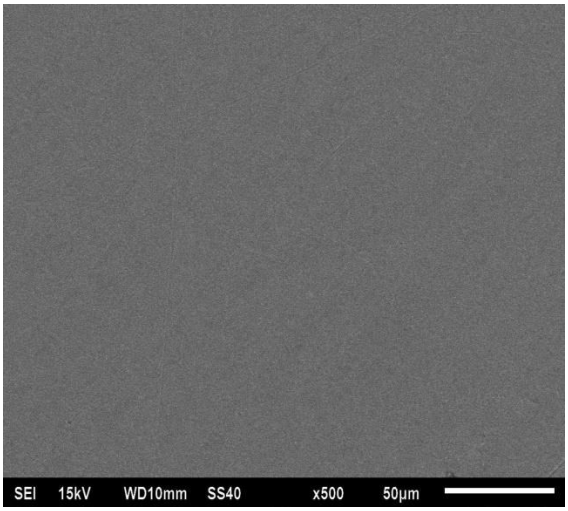

(b)

Figure 5.7: Scanning electron microscopy (SEM) of copper alloy workpiece (a) before and (b) final after finishing cycle of 10 minutes with optimum parameters N=1250 rpm, S=24%, M=800 mesh size and C=19%.

5.6 Conclusions

Effects of MR polishing fluid composition parameters and tool rotational speed on surface finish of copper have been studied using the presently developed hemispherical end magnetorheological finishing (HEMRF) process.

- It is found that abrasive concentration and tool rotation speed is the most important parameter followed by iron powder concentration and abrasive mesh size.
- Mesh size of abrasives has a significant effect in finishing, bigger size particle remove more material initially as compared to small size particle but for the proper finishing a moderate range of mesh size of the abrasive is required.
- Increase of abrasive concentration in MR polishing fluid increases the $\%\Delta R_a$ reduction but after a certain volume of abrasive, the $\%\Delta R_a$ reduces due to the weakening of the iron particles chain.
- Optimum parameters for the finishing on copper alloy workpieces were found as 1250 rpm of tool speed rotation, fluid composition as 24% abrasive concentration of 800 mesh size and 19% iron powder concentration.
- After finishing for 10 minutes with optimum parameters N=1250 rpm, S=24%, M=800 mesh size and C=19%, 90.75% reduction in R_a value was found.
- Roughness profiles and scanning electron microscopy images showed considerable improvement in surface finish. Surface characteristics examined by scanning electron microscopy of copper alloy workpiece clearly signifies that most of the peaks have been removed and surface quality has been improved by the present magnetorheological fluid assisted finishing method using permanent magnets.
- Results obtained from the experiments showed that the present technique is capable for nano-finishing of diamagnetic materials such as copper which significantly useful in industries like aerospace, dentistry, electronics and laser etc. and also for metallic mirrors.

Chapter 6

Mathematical Modeling and Simulation of Surface Roughness using HEMRF Process

6.1 Mechanism of Surface Finishing in Hemispherical End Magnetorheological Finishing (HEMRF) Process

Magnetorheological (MR) polishing fluid stick to the bottom end surface of finishing tool and gives repulsive force to the abrasive particles towards the surface of diamagnetic copper alloy workpiece. The repulsive force moves the active abrasives towards copper alloy workpiece surface. This result in active silicon carbide (SiC) abrasive particles embed on to the roughness peaks of copper alloy workpiece. These active abrasive particles are strongly gripped by carbonyl iron (CI) particles chains and rotate with the rotation of finishing tool. Due to the rotational motion of gripped SiC particles and tangential cutting force applied by them on to the peaks of workpiece surface, peaks material gets removed in the form of micro chips as shown in Fig. 6.1. As copper is diamagnetic material, its repulsive properties are helpful in the mechanism of finishing. Due to this repulsion force, CI particles get repelled from the copper workpiece surface and get attracted towards tool magnet end surface. As a result abrasive particles are pushed from the magnetic tool end surface and CI particles gripped them towards the workpiece surface. This is the basic necessity for the MR polishing fluid assisted finishing.

As depicted in the Fig. 6.1, there is simultaneous rotational and translational relative motion present between the abrasives locked in magnetically stiffened iron particle chains and workpiece surface during the finishing process. The workpiece is fixed in the precision vice. The setup of HEMRF is shown in Fig. 4.7. The movement is controlled in the computer-controlled setup by servomotors. The servomotors can have simultaneous rotational and translational motions. Stiffening of the MR polishing fluid depends on the rheological behavior of carbonyl iron particles in presence of magnetic flux density. When the MR polishing fluid is applied on the magnetic tool, the CIPs present in MR polishing fluid get aligned and make chain structures due to magnetic lines of magnetic flux density induced by

the permanent magnets. Non-magnetic SiC abrasive particles presents in the MRP fluid get locked in between the chain structures as shown in Fig. 6.1. The abrasive particles, which are in contact with the workpiece surface, are known as active abrasives particles. These active abrasives are responsible for the material removal during simultaneous translational and rotational motion of the stiffened MR polishing fluid along with the finishing tool relative to workpiece surface. The constant contact and depth of penetration of active abrasives on the workpiece surface depends on the magnetic normal force whereas the shear force on abrasive due to simultaneous relative translational and rotational motions are responsible for removal of material by abrasion action in the form of microchips during operation. Because of continuous relative motion between abrasive particle and workpiece, there is continuous change in location of active abrasive particles which results in uniform surface finishing.

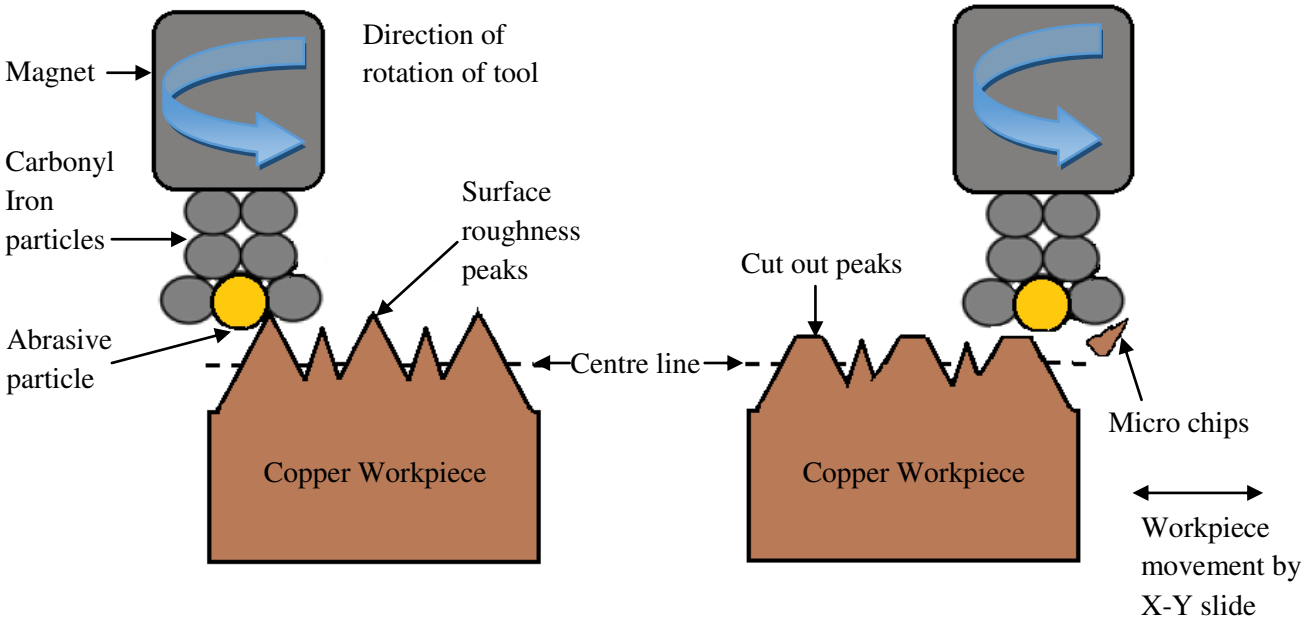

Figure 6.1: Mechanism of finishing performed by the HEMRF

6.2 Analysis of Normal Force or Magnetic Force

To understand the role of normal force in material removal mechanism and effect of magnetic field on the normal force in the present process, it is necessary to develop the mathematical model. The developed mathematical model can give complete analysis of the normal force, magnetic field and all other parameters involved in the finishing process. There are some basic assumptions have been taken into consideration for developing the model, which are as follows.

- All the abrasive particles are uniform in shape, size and uniformly distributed in the MR polishing fluid.
- All the abrasive particles are assumed spherical in shape and average diameter is 19 μm.
- All carbonyl iron particles are assumed as spherical in shape and average diameter of 21 μm.
- Gravitational forces, centrifugal force and inertial forces are neglected while finishing operation.
- Magnetic loses and leakages are not considered for the evaluation of normal force.
- Normal forces acting on active abrasive particles are responsible for indentation of abrasives into the workpiece surface and shear forces acting on the abrasives due to simultaneous motions, are responsible for the shearing of the material from the surface of workpiece.

Shear force acting due to rotational and translational relative motion between gripped active abrasives with CIP chains and workpiece surface pull out the material from the workpiece in the form of microchips [Gorodkin and Zhuravski, 2002]. The abrasive grain produces groove on the workpiece surface due to normal component of magnetic force on abrasive particle through the CIP particle. The indented groove corresponds to the profile of indented grains in the surface. Under the action of shear force due to HMI controlled external servomotor, the indented grains are given translational and rotational motion, which remove the material from workpiece surface. The material removal with abrasive grain can take place due to shearing action, which depends on average cutting edge radius and depth of indentation [Brecker et al., 1969].Therefore, the sum of the normal forces is considered as the sole cause for indentation of abrasive particles, and shear force acting on the abrasive grains is considered the sole cause for the microchip formation.

The abrasive particle produced indentation on the surface of copper workpiece due to magnetic normal force. As the abrasive particle trapped in the chains of CI particles, the magnetic normal force is transferred from CI particles to the abrasive particle. The profile of the penetrated portion of the abrasive particle is corresponded by the cross-section of indentation occurred. The removal of workpiece material in the form of chips takes place when the penetrated abrasive particle is rotated over the workpiece surface. The removal mechanism occurs only when the reaction force (F_{RS}) on the projected area of indent abrasive is lesser than the shear force (F_S) exerted by the stiffened MR polishing fluid as shown in Fig. 6.2. Due to average cutting edge radius [Jha and Jain, 2006] and depth of indentation, micro

chip formation taken place by the shearing action through the abrasive particle. This results in removal of material from the copper workpiece surface. During the indentation on the workpiece surface by the active abrasive particle, magnetic force acting on CI particle just adjacent to the active abrasive has the maximum contribution to make the indentation. F_N is the normal force acting on the abrasive particle due to all CI particles present in the chains.

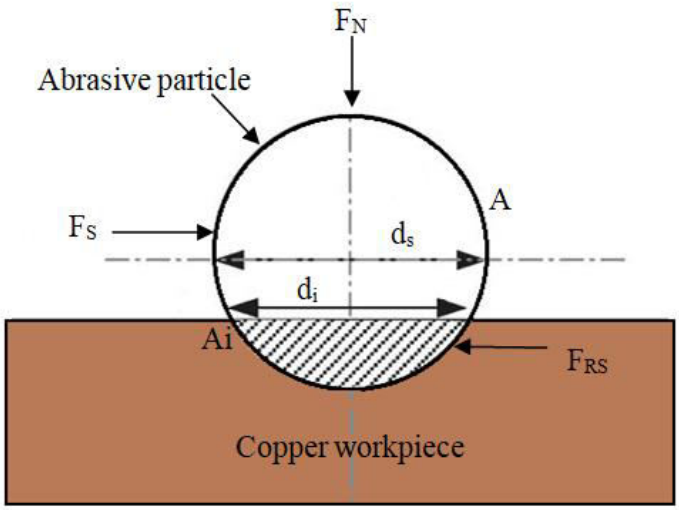

Figure 6.2: Forces acting on a abrasive particle

6.2.1 Analysis of MR Polishing Fluid and Chain Structures

The gap between the tip of finishing tool and workpiece is filled with MR polishing fluid. To know about the surface finish mechanism using MR polishing fluid, it is necessary to know the volume of the fluid in any one of the gap, and concentration of consisting component in MR polishing fluid. The aim of this HEMRF tool is to achieve nano finish on flat non magnetic soft material workpiece. The tip of the tool is circular shaped such that the active abrasive of MR polishing fluid in the gap uniformly interacts with workpiece surface.

6.2.1.1 Number of Carbonyl Iron Particle Chains in the Working Gap

The MR polishing fluid is filled the working gap between the outer surface of the finishing tool and the workpiece surface. This is the layer of MR polishing fluid which gets stiffened over the finishing tool end surface to perform the finishing action on the copper alloy workpiece surface. The end surface area (A_m) of finishing tool with diameter 'd_m' can be calculated from Eq. 6.1.

$$A_m = \frac{\pi}{4} d_m^2 \text{ mm}^2 \qquad (6.1)$$

where, d_m=30 mm.

Hence, $A_m = 706.858\ mm^2$ (6.2)

Total volume of MR polishing fluid (V) in working gap is calculated from Eq. 6.3.

$V = A_m z\ mm^3$ (6.3)

where, z = thickness of MR polishing fluid in working region in mm.

The value of thickness of MR polishing fluid in working region, z=1.5 mm. The value V can be calculated by using Eq. 6.2 and Eq. 6.3.

$Volume, V = 1060.28\ mm^3$ (6.4)

Diameter of a CI particle of 600 mesh size = 21 μm = 21×10^{-3}mm

So, volume of single carbonyl iron particle = $\frac{4}{3}\pi(\frac{d_c}{2})^3 = 4.849\times10^{-6}mm^3$

Fraction of CIP present in MR polishing fluid (optimum concentration) = 19%

The count of carbonyl iron particles (CIPs) in volume V of MR polishing fluid is calculated by using Eq. 6.5.

$$N_C = \frac{\%\ \text{volume fraction of CIP in MR polishing fluid} \times V}{\text{Volume of single CIP particle}} \quad (6.5)$$

Therefore, N_C= 41545308

Number of CI particles in one chain, $n = \frac{z-d_s}{d_c} = 71\ (approx)$

Here, d_s is diameter of single SiC particle in mm = 0.019 mm.

The number of CI particles chain formed in working region can be calculated by Eq. 6.6.

$$N_{CC} = \frac{N_C}{\text{Number of CIPs in one chain}} = \frac{41545308}{71} = 585145 \quad (6.6)$$

6.2.1.2 Number of Active Abrasives per CIP Chain

Volume of single abrasive particle = $\frac{4}{3}\pi(\frac{d_s}{2})^3 = 3.591\times10^{-6}mm^3$

$d_s =$ diameter of single SiC particle $= 19\ \mu m = 19\times10^{-3}mm$

Fraction of SiC present in MR polishing fluid (optimum concentration) = 24%

Total numbers of active SiC abrasive particles of 800 mesh size in the MR polishing fluid that remove material during finishing are given by Eq. 6.7.

$$N_a = \frac{\text{percentage volume of SiC in MR polishing fluid} \times A_m \times \text{diameter of abrasive}}{\text{Volume of single SiC particle}} \quad (6.7)$$

Therefore $N_a = 897508$ (6.8)

Number of active SiC abrasives per CIP chain is calculated by Eq. 6.9.

$$N_{acc} = \frac{\text{Number of active abrasive particles } (N_a)}{\text{Number of CIP chains } (N_{CC})} \quad (6.9)$$

Using Eqs. 6.6, 6.8 and 6.9, the number of active silicon carbide particles (SiC) per chain of CIPs on the workpiece surface is evaluated as

$$N_{acc} = \frac{897508}{585145} = 1.533 \sim 1.5 \quad (6.10)$$

It means that for two active abrasive particles, there are three chains of CIPs over it as shown in Fig. 6.3. Due to higher magnetic flux density on the outer surface of the finishing tool, the magnetic CI particles align in chains over it and non-magnetic SiC abrasive particles are pushed by these CIPs towards the workpiece surface.

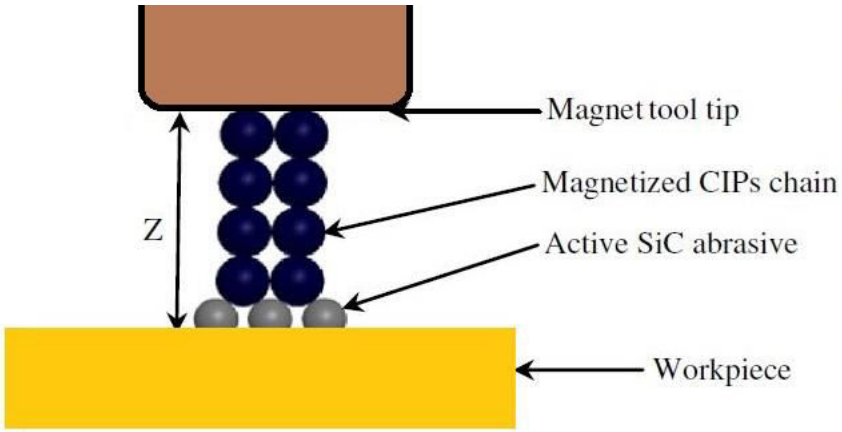

Figure 6.3: Structure in the MR polishing fluid of abrasives w.r.t. CIP chains

6.2.2 Calculation of Magnetic Flux Density of MR Polishing Fluid in Working Gap

Magnetic flux density in the MR polishing fluid region can be calculated as given in Eq. 6.11.[Camacho and Sosa, 2013]

$$B_Z = \frac{Br}{2}\left[\frac{L+Z}{\sqrt{R^2+(l+Z)^2}} - \frac{Z}{\sqrt{R^2+Z^2}}\right] \quad (6.11)$$

where,

L = total length of the magnetic tool = 35 mm

R = radius of the magnetic tool = 15 mm

Z = working gap distance from tool end surface to workpiece surface through the MR polishing fluid, mm

Br = Remanence field = 1.21 tesla (for NdFeB35)

Variation of magnetic flux density in the working gap according to Eq. 6.11 is shown in Fig 6.4. Negative slope for the distribution of magnetic flux density in working gap ensured that the carbonyl iron particles present in the MR polishing fluid are attracted towards magnetic tool end surface (higher magnetic flux density) while finishing performed by the present newly developed process.

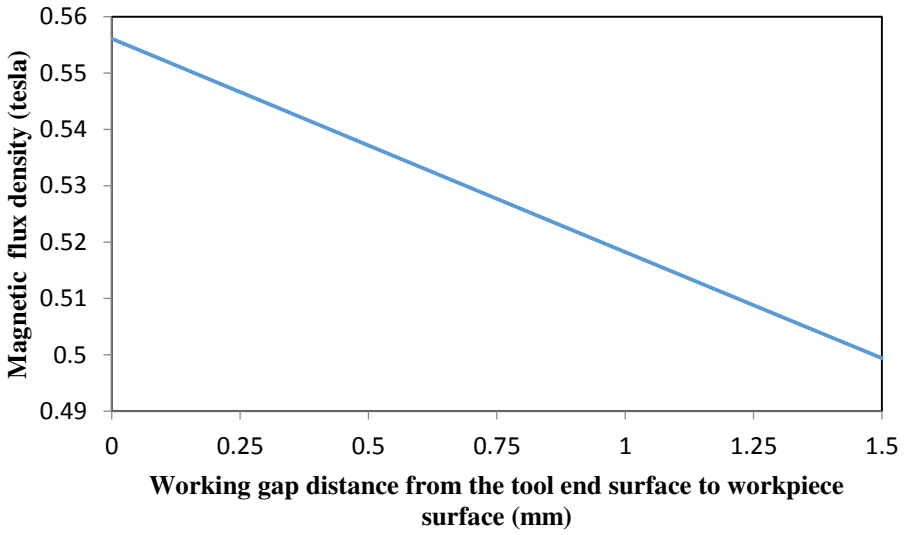

Figure 6.4: Variation of magnetic flux density in the working gap

6.2.3 Calculation of Average Normal Magnetic Force F_a with respect to Variable Working Gap

The variation in normal magnetic force F_n depends on the variation of magnetic flux density B_z with variable working gap Z.

Therefore, the normal magnetic force on the workpiece surface is given in Eq. 6.12.

$$F_n = P \times A_m \tag{6.12}$$

where, P = polishing pressure depends on the variation of magnetic flux density Bz and these relation can be expressed using the following Eq. 6.13. [Singh et al., 2013]

$$P = \frac{B_Z^2}{2\mu_0}\left(1 - \frac{1}{\mu_{mr}}\right) \text{N/m}^2 \tag{6.13}$$

where,

μ_{mr}= 5, relative permeability of MR polishing fluid

$\mu_0 = 4\,\pi\, \times 10^{-7}$ H/m, absolute permeability of free space.

Using Eqs. 6.2, 6.11 and 6.12, value of F_n is represented in the Eq. 6.14.

$$F_n = 225\, B_Z^2 \quad \text{Newton} \tag{6.14}$$

Force acting on workpiece by each CIP chain (F_N) is expressed in Eq. 6.15.

$$F_N = \frac{F_n}{N_{CC}} = 3.868 \times 10^{-4}\, B_Z^2 \tag{6.15}$$

Using Eq. 6.10, force exerted by each active abrasive particle on the workpiece surface (F_{NA}) is calculated in Eq. 6.16.

$$F_{NA} = \frac{F_N}{1.5} = 2.5789 \times 10^{-4}\, B_Z^2 \tag{6.16}$$

Varying the value of Z in Eq. 6.11 from 0 mm to 1.5 mm, and substituting it in Eq. 6.16, the variation in F_{NA} is obtained. Hence, taking mean of these different values of F_{NA}, the average normal magnetic force (F_a) is given in Eq. 6.17.

$$F_a = 7.1906 \times 10^{-5} \text{ Newton} \tag{6.17}$$

6.3 Modeling and Simulation of Surface Roughness

The grain of the abrasive produces a groove on the surface of copper workpiece, as CIPs produces magnetic normal forces under the action of magnetic field. As the abrasive particle trapped in the chains of CIPs, this force is transferred from CIPs to the abrasive particle. The profile of the penetrated portion of the grain is corresponded by the cross-section of indentation occurred. The removal of workpiece material in the form of chips takes place when the penetrated abrasive grain is rotated or translated horizontally over the

workpiece surface. The removal of material occurs only when the reaction force (F_{RS}) on the projected area of indent by the abrasive is lesser than the shear force exerted by the MR polishing fluid (F_S) on the projected area of the abrasive penetrating (above the portion indented into the surface) as shown in Fig. 6.2. Due to average cutting edge radius [Jha and Jain, 2006] and depth of indentation, chip formation takes place by the shearing action in front of the abrasive grain and hence the removal of material. During the indentation on the workpiece surface by the active abrasive, magnetic force acting on CI particle just adjacent to the active abrasive has the maximum contribution to make the indentation [Grover and Singh, 2017]. The average normal magnetic force acting on active abrasive is calculated as $F_a = 7.1906 \times 10^{-5} N$. This normal force on active abrasive is the indenting force (F_i) acting on it.

The shear force exerted by the fluid (F_S) can be calculated by Eq. 6.18 [Jha and Jain, 2006].

$$F_S = (A - A_i)\,\tau \tag{6.18}$$

where, A_i is the penetrated cross-sectional area with diameter of the indent d_i and A is the total cross sectional of indented abrasive with diameter d_s. τ is shear stress of MR polishing fluid and has the value 0.0525 MPa [Jha and Jain, 2006]. The reaction force (F_{RS}) exerted by the workpiece material as shown in Fig. 6.2 and can be calculated by Eq. 6.19.

$$F_{RS} = A_i \sigma \tag{6.19}$$

Here, σ is the yield stress of copper workpiece in shear having value 70 MPa.

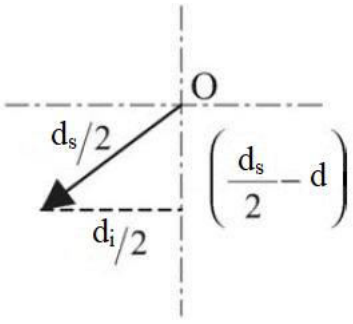

Figure 6.5: Relation between depth of indentation and indentation diameter

From the Fig. 6.5, it is clear to understand that if any one of depth of indentation d and indentation diameter d_i is known then another one can be calculated by applying the

Pythagoras theorem. The average value of depth of indentation is treated as average roughness of the surface. Relation between d, d_i, and d_s is as shown below.

$$d = \frac{d_s}{2} - \frac{1}{2}\sqrt{d_s^2 - d_i^2} \quad (6.20)$$

where d_s diameter of SiC abrasive grains which $19 \times 10^{-6}\, m$, and d_i is calculated from the relation of Hardness Brinell number.

Indentation diameter can be calculated from the Brinell hardness number kgf/mm^2 using Eq.6.21 [Jha and Jain, 2006].

$$H_{BHN} = \frac{2F_i}{\pi D_g(D_g - \sqrt{D_g^2 - D_i^2})} \quad (6.21)$$

So on rearrainging the Eq.6.21, we will have the diameter of indentation profile made by the abrasive indented.

$$d_i = \sqrt{d_s^2 - (d_s - \frac{2\times10^{-6}F_i}{9.81 H_{BHN}\pi d_s})^2} \quad (6.22)$$

Value of diameter of the indent d_i can be calculated by using Eq. 6.22, where H_{BHN} is the brinell hardness number of the copper workpiece i.e. 35 kgf/mm^2 and normal force (F_N) acting on the active abrasive is the indenting force (F_i). Substituting all these values in Eq. 6.22, value of diameter of the indent is $d_i = 5.16332 \times 10^{-7}\, m$.

Substituting the values of σ, τ, A and A_i in Eq. 6.18 and Eq. 6.19, values obtained are $F_S = 2.18 \times 10^{-4} N$ and $F_{RS} = 6.58 \times 10^{-7} N$.

It is clearly visible that shear force (F_S) exerted by the fluid is greater than the reaction force (F_{RS}) exerted by copper material i.e. $F_S > F_{RS}$. Hence, this confirms the chipping of roughness peaks and finishing action performed by active abrasive present in the newly developed finishing tool on the copper workpiece. It is also observed that indentation force is very low in the present case and the other MR based finishing processes. Hence, there is rare or no chances of having subsurface damage.

On substituting the value of diameter of abrasive and diameter of indentation in Eq. 6.20, value of depth of indentation is $d = 3.5085 \times 10^{-9} m$.

Numbers of active silicon carbide (SiC) abrasive particles present on the workpiece surface, which are responsible for removal of material during the finishing operation is mentioned in Eq. 6.8, i.e. N_a= 897508.

Let the workpiece used for finishing action, has initial roughness profile is as like shown in figure. In the Fig. 6.6 (a), P_1, P_2, P_3, P_4, P_5 and P_6 are the peaks and valleys on the initial surfcae surface. If N_a is the numbers of active abrasive particle per stroke indent depth d, then the resultant profile is P_1', P_2, P_3', P_4, P_5' and P_6' which is as shown in Fig. 6.6 (b). From Fig. 6.6 (b) it is clealy observed that the finishing action at valley positions doesn't take palce due to which before the start of next stroke, corresponding to valley profile initial reading is taking palce. Therefore after completion of first stroke of finishing genralized representation of the profile is as given below in Eq. 6.23.

$$P_i^{'} = P_i - N_a \times d \tag{6.23}$$

where 'i' subscripts on P reperesnets the data points of roughness profile height.

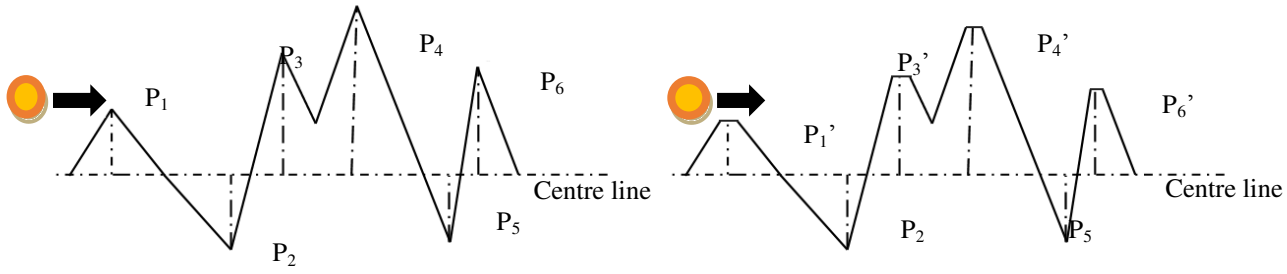

(a) (b)

Figure 6.6: (a) Abrasive grain approaching initial peaks/valleys of height/depth and (b) new peak heights updated after one indentation depth.

The initial roughness profile data was measured with Mitutoyo SJ-400 Surftest. All the sampled roughness profile data obatained from the surface roughness measuringinstruement were applied into the model with the help of MATLAB programme. A program flow chart of the MATLAB programme for final change in surface roughness profile is shown in Fig. 6.7.

After one stroke, the resultatnt roughness profile was as shown in Fig. 6.6 (b), profile P_1 and P_4 are same as initial because these are already below the centre line, hence only profile above the centre line were cutout and resultant to Fig. 6.6 (b). More clearly, it can be said that the peak values are checked from the sample data, and model was applied on it the data which are not peak that are proceed for next stroke by updating the new centreline. Again new peak data are operated and valleys data are sent for next stroke operation by updating new centreline in this way the operation goes on till desired result is found.

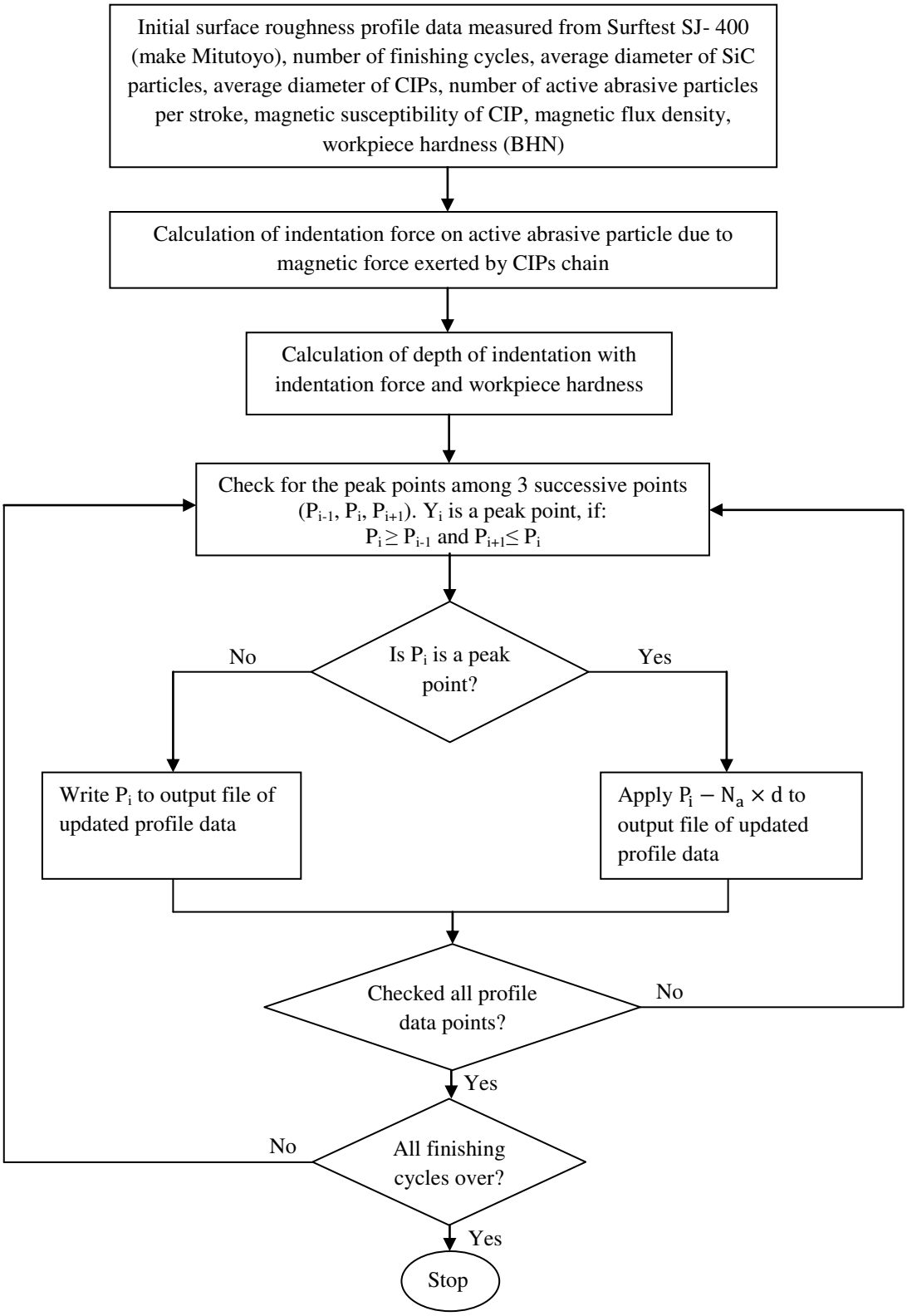

Figure 6.7: A program flow chart of the MATLAB programme for final change in surface roughness profile

After and before the start of each stroke calculation new centre line average surface roghness values (R_a) is calculated from the previous profile data with the help of Eq. 6.24.

$$R_a = \frac{\sum_{1=1}^{N} |P_i|}{N} \quad (6.24)$$

where N= number of profile data, P_i = profile data at i^{th} position on workpiece surface.

While calculation through MATLAB programme of roughness it is assumed that continous removal of material takes place till the height of profile touches zero or non negative height after which no further material removal takes palce on that point. Because of assumption in theoretical calculation final data is either zero or very small positive height or valley height so further calculation is not possible on those resultant data. Therefore for the each step of theoretcal calculation profile data is taken from the experimental data.

6.4 Results and Discussion

To ensure the validity of mathematical model for the present MR fluid based finishing process, comparison of theoretical calculated surface roughness with the experimental values. The experimentation was conducted with 1440 numbers of finishing cycles by using the MR fluid based honing process. The experimental change in surface roughness values was measured with Surftest SJ-400 (make Mitutoyo). The initial surface roughness of workpiece R_a value= 211.5 nm. The experimental conditions used during finishing are given in Table 6.1. The MR polishing fluid used during experimentation consists (by volume) of 24% SiC abrasives, 19% CIPs and 57% base fluid (80% heavy paraffin and 20% AP3 grease).

Table 6.1 Experimental parameters and conditions.

Parameters	Conditions
Total finishing cycles	1400
Tool rotational speed	1250 rpm
X- axis feed distance	9 mm
Working gap	1.5 mm

The total number of finishing cycle can be calculated by using Eq. 6.25.

$$\text{Total number of finishing cycles} = \frac{\text{Tool rotational speed} \times \text{finishing cycle time}}{\text{linear motion distance}} \quad (6.25)$$

Subtituting the values of finishing cycle time 2.5 minutes, tool rotational speed 1250 rpm and linear motion distance of X-axis 9 mm in Eq. 6.25, value of total number of finishing cycles comes out to be 350 (approx.).

The change in surface roughness profiles during different finishing cycles are shown in Figs. 6.8 (a-e).

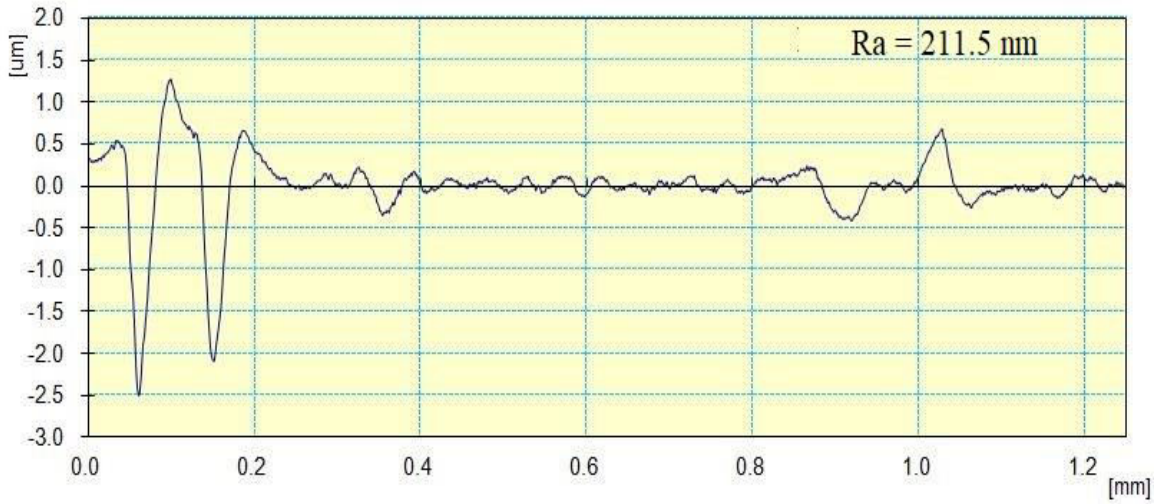

(a)

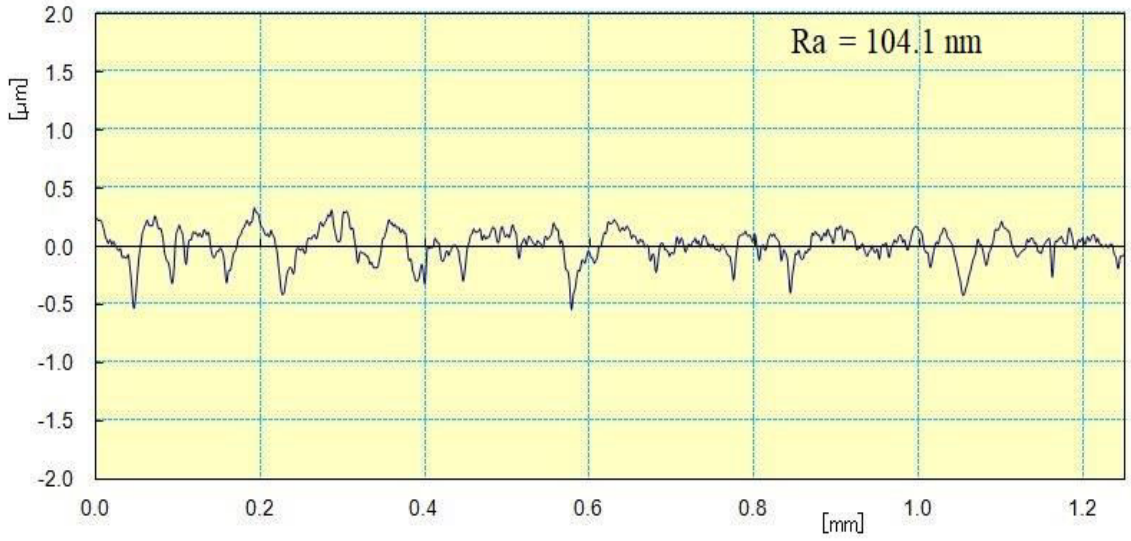

(b)

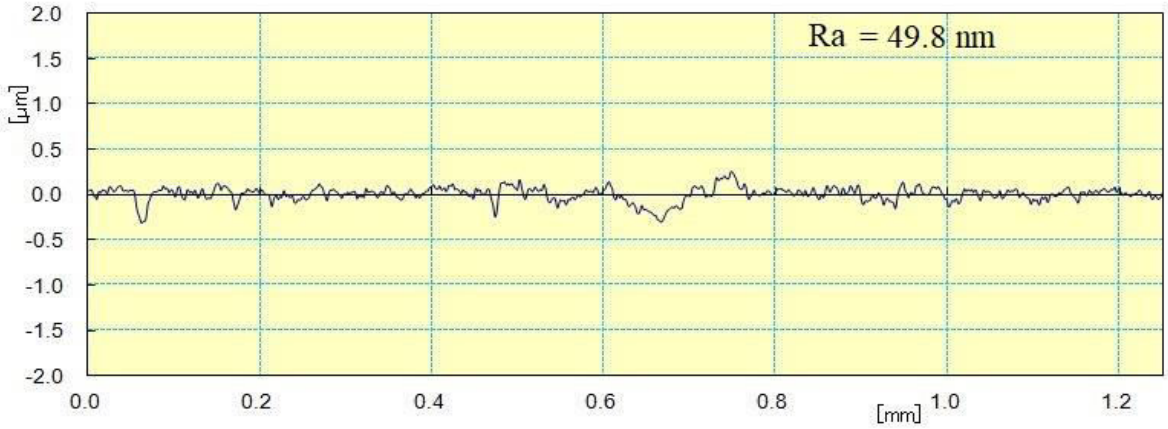

(c)

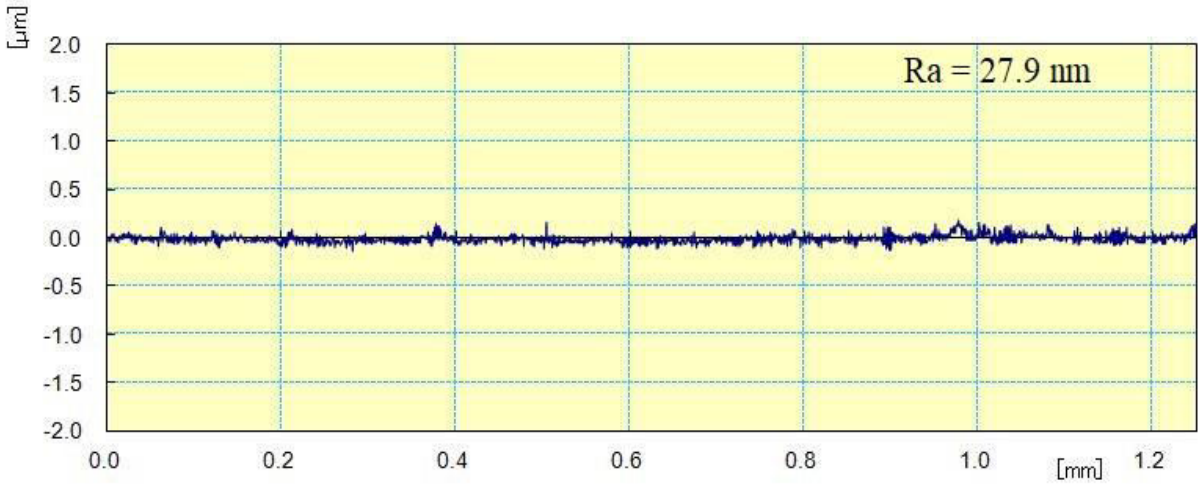

(d)

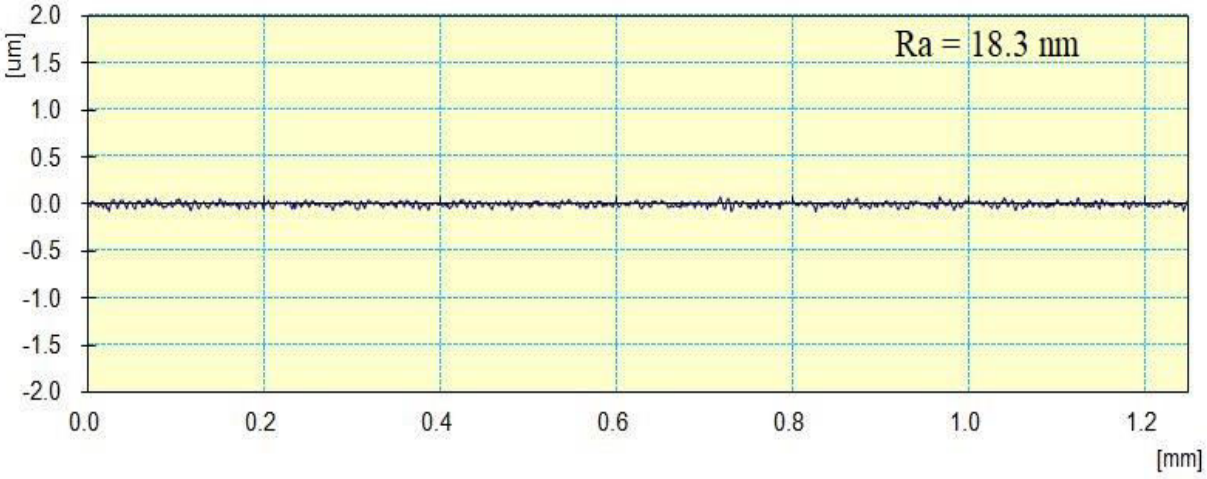

(e)

Figure 6.8: Surface roughness profiles (a) initial, (b) after 350 finishing cycles, (c) after 700 finishing cycles, (d) after 1050 finishing cycles and (e) after 1400 numbers of finishing cycles.

The surface roughness profiles data measured from Surftest SJ-400 roughness tester were applied into the mathematical model in order to calculate the final change in surface roughness by using a MATLAB programme. The theoretically calculated surface roughness value was found as 105.3 nm while experimental roughness value was 104.1 nm with the first 350 finishing cycle. In next 350 finishing cycle, the theoretical roughness value was found as 49.4 nm while experimental roughness value was 49.8 nm. In next 350 finishing cycle i.e. third cycle, the theoretical roughness value was found as 28.75 nm while experimental roughness value was 27.9 nm. With the final finishing cycle of total 1400 cycles, the theoretical surface roughness was found as 17.4 nm, while experimental roughness value was 18.3 nm. Therefore, it can be seen that the experimental surface roughness value has been reduced from 211.5 nm to 18.3 μm and theoretically value reduced from 211.5 nm to 17.4 nm. This shows a significant change in surface roughness around 91.3% experimentally and 91.7% theoretically. This clearly revealed that the theoretical and experimental results are in closer agreement with each other. In Table 5, the % error column shows how deviation in surface roughness from the experimental value to the theoretical value takes place. Therefore percentage (%) error has been calculated by using the Eq. 6.26. The theoretical calculated values of surface roughness with number of finishing cycles are validated with experimentally obtained surface roughness values for the same number of finishing cycles and conditions. Both were found in close agreement within 4.92% as reported in Table 6.2. Thus, the present developed finishing process is found suitable to reduce wear and improve functional application of cylindrical components.

$$\text{Percentage (\%) error} = \frac{(\text{Experimental surface roughness} - \text{Theoretical surface roughness})}{\text{Experimental surface roghness}} \times 100 \quad (6.26)$$

Further for microscopy study on mechanism of material removal during the present MR fluid based finishing process, the scanning electron microscopy (SEM) analysis was carried out at 1000x for initial and finished surface after 1400 finishing cycles as shown in Fig. 6.9 (a) and (b), respectively. It can be seen that the initial surface of copper alloy workpiece showed various surface defects such as deeper grooves and cavity. But, final finished surface after 1400 finishing cycles showed the significant improvement in surface quality which is almost defect free surface.

Table 6.2. Theoretical and experimental results of surface roughness corresponding to the number of cycles.

Sr. No	**Number of cycles**	**Experimental R_a**		**Theoretical R_a**		**% Error**
		Initial R_a (nm)	Final R_a (nm)	Initial R_a (nm)	Final R_a (nm)	
1	350	211.5	104.1	211.5	105.3	-1.34
2	700	104.1	49.8	104.1	49.4	0.81
3	1050	49.8	27.9	49.8	28.7	-3.04
4	1400	27.9	18.3	27.9	17.4	4.92

This significant improvement in surface quality experimentally evidence that the present newly developed magnetorheological fluid based finishing process is capable to finish diamagnetic workpieces. The removal of surface defects after 1400 finishing cycles which clearly demonstrates the better surface quality on the copper alloy flat workpiece. The overall results revealed that a significant improvement in surface quality after the chipping action performed by abrasives on the workpiece by using present newly developed MR fluid based finishing process. Hence, the present developed finishing process is found suitable to nano finish the copper alloy workpiece which leads to saving in service, energy consumption and improve its functional applications as compared to traditional finishing techniques.

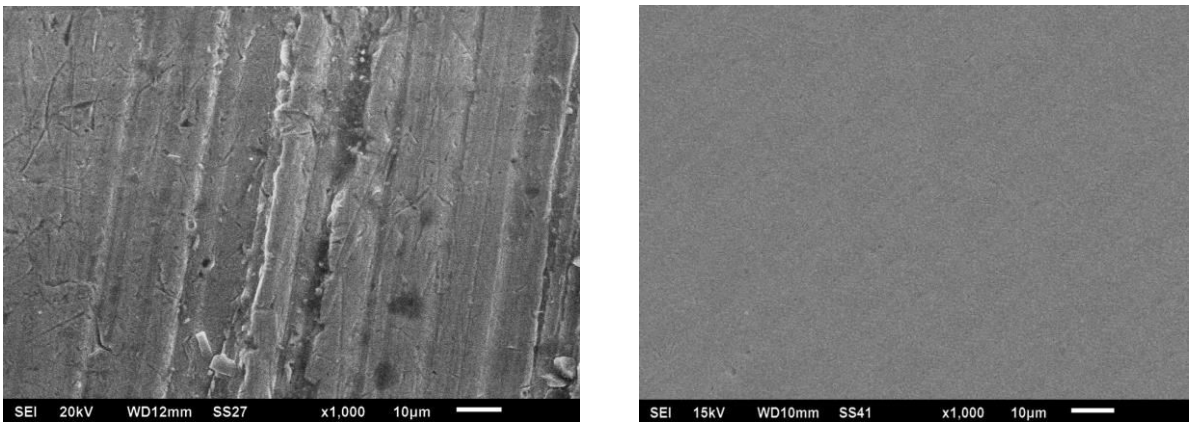

(a) (b)

Figure 6.9: Surface morphology with scanning electron microscopy at 1000x (a) initial surface and (b) final finished surface after 1400 numbers of finishing cycles on workpiece.

The atomic force microscopy (AFM) images for the copper workpiece surface before and after 10 minutes of finishing by the newly developed magnetorheological finishing process is shown in Fig. 6.10. The normal magnetic force is applied on active abrasives and its rotation on workpiece surface resulted in finishing due to abrasion action. It can be seen from Fig. 6.10 (a) that the initial surface of the copper alloy workpiece is very rough as there are many high peaks and valleys. Figure 6.10 (b) shows the finished surface after 10 minutes of finishing cycle. It is clearly visible in Fig. 6.10 (b) that the surface quality improved significantly and the workpiece surface almost flattened with some small sharp peaks and few valleys left out.

Upon the analysis of AFM image, the surface roughness values obtained are Ra = 11.7 nm, Rq= 20.4 nm and Rz= 122.85 nm. But surface roughness values obtained from the surface roughness tester are Ra = 18.3 nm, Rq= 25.6 nm and Rz= 207 nm. However, difference in the values of surface roughness is occurring because of the difference in the measuring scale in two different measuring processes. In case of surface roughness tester, the measurement of roughness was taken along a straight line for the distance of 1.25 mm whereas in case of AFM image analysis, the measurement of roughness was done on the surface area of square with edge 15 micron. The significant change in surface roughness value and surface quality demonstrates the finishing capability of newly developed finishing tool on diamagnetic workpiece.

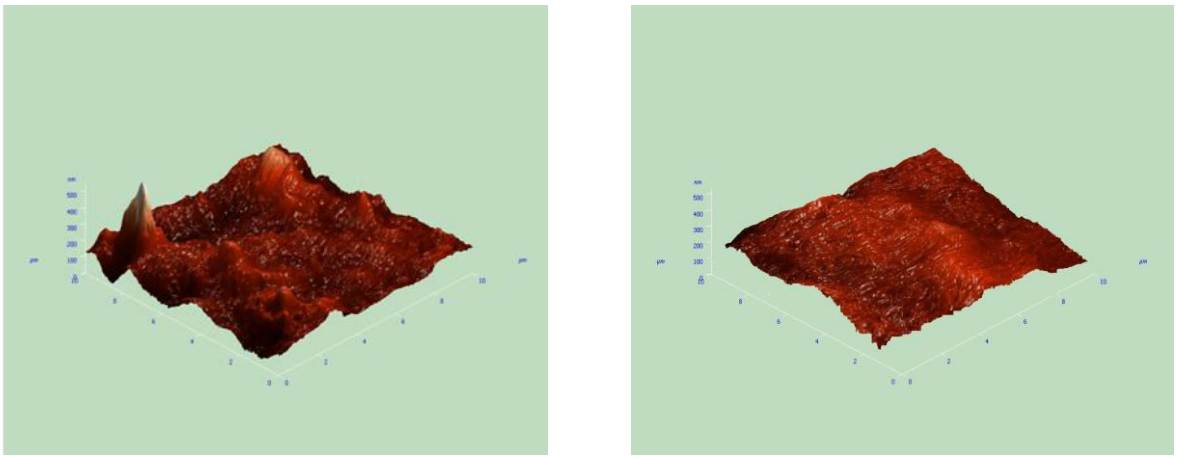

(a) (b)

Figure 6.10: Atomic force microscopy (AFM) results (a) before and (b) after finishing of 10 minutes.

6.5 Conclusions

Modeling of surface roughness with the effect magnetic normal force at different finishing cycles have been proposed for the newly developed magnetorheological fluid based finishing process. The main important conclusions related to removal of roughness peaks using present finishing process are as follows:

- Negative slope for the distribution of magnetic flux density in working gap ensured that the carbonyl iron particles present in the MR polishing fluid are attracted towards magnetic tool end surface (higher magnetic flux density) while finishing performed by the present newly developed process.
- Magnetic flux density is in direct relationship with magnetic force or indentation force which revealed that carbonyl iron particles of MR polishing get attached more strongly to the finishing tool surface than the workpiece surface. Therefore, during the finishing of the copper alloy workpiece surface, the peaks of surface roughness is removed by chipping action.
- Size of active abrasive particle effects the quality of surface as depth of indentation and diameter of SiC grains are related with each other.
- The theoretical calculated value of surface roughness was found in good agreement with experimental value within 4.92 %.
- The microscopic study with scanning electron morphology and atomic force microscopy showed the significant improvement in the surface quality by the finishing done with the newly developed hemispherical end magnetorheological finishing process (HEMRF).

Chapter 7

Conclusions and Future Scope

A new finishing tool with permanent magnets 'hemispherical end magnetorheological finishing' (HEMRF) is made for magnetorheological nanofinishing of diamagnetic and paramagnetic materials. The following conclusions are made which showed the presently developed permanent magnets tool is found suitable to finish the diamagnetic and paramagnetic workpiece surfaces.

- Surface roughness parameters R_a of the aluminum alloy workpiece get decreased from 718.2 nm to 62.7 nm in finishing time span of 20 minutes and for copper alloy workpiece R_a value decreased from 211.5 nm to 18.3 nm in finishing time span of 10 minutes. Therefore, this new technique for nano-finishing of diamagnetic and paramagnetic materials showed high productive rate.
- Simplified magnetorheological finishing setup by using permanent magnets instead of electromagnet reduced the setup cost.
- Results obtained from the experiments on paramagnetic materials showed that the present new technique is capable for nano-finishing of aluminium workpieces that is significantly useful in industries like aerospace and automobile industries. It is also useful especially in the field of micro-electronics and optics. Results obtained from the experiments on diamagnetic materials such as copper showed that the present new technique is capable for nano-finishing that is significantly useful in industries like aerospace, dentistry and laser etc. for metallic mirrors. It is also useful to nanofinish the copper electrodes of electric discharge machining and many other electronics components.
- From the optimization of the process parameters, it's found that abrasive concentration and tool rotation speed is the most important parameter followed by iron powder concentration and abrasive mesh size.
- Finishing for 10 minutes on copper workpiece with optimum parameters N=1250 rpm, S=24%, M=800 mesh size and C=19%, a significant reduction in surface roughness value R_a of 90.75% was found.

- The theoretical calculated value of surface roughness from mathematical modelling for copper workpiece was found in good agreement with experimental value within 4.92 %.
- Negative slope for the distribution of magnetic flux density in working gap ensured that the carbonyl iron particles present in the MR polishing fluid are attracted towards magnetic tool end surface (higher magnetic flux density) while finishing performed by the present newly developed process.
- Surface characteristics examined by atomic force microscopy (AFM) and scanning electron microscopy (SEM) of copper alloy workpiece clearly signified that most of the peaks have been removed and surface quality has been improved by the newly developed hemispherical end magnetorheological finishing process (HEMRF).

The future scope for the present work can be:

- The optimization of the process parameters can be done for the paramagnetic materials.
- The idea of making the flexible tool but changing the second magnet can be explored.
- Finishing on different geometries can be carried out.

References

Balasubramanian, P.; Senthilvelan, T. (2014) Optimization of Machining Parameters in EDM process using Cast and Sintered Copper Electrodes. Procedia Materials Science, 6: 1292 – 1302.

Bardamid, A.F.; Gritsyna, V.T.; Konovalov, V.G.; Orlinskij, D.V.; Borisenko, Y.N.; Shapoval, A.N.; Shtan, A.F.; Solodovchenko, S.I.; Voitsenya, V.S.; Yakimov, K.I. (1998) Ion energy distribution effects on degradation of optical properties of ion-bombarded copper mirrors. Surface and Coatings Technology, 365–369.

Barletta, M.; Guarino, S.; Rubino, G.; Tagliaferri, V., (2007) Progress in fluidized bed assisted abrasive jet machining (FB-AJM) internal polishing of aluminium tubes. International Journal of Machine tools and Manufacture, 47: 483–495.

Bayoumi, M.R.; Abdellatif, A.K. (1995) Effect of surface finish on fatigue strength. Engineering Fracture Mechanics, 51(5): 861–870.

Bedi, T.S.; Singh, A.K. (2015) Magnetorheological methods for nano finishing – a review. Particulate Science and Technology, DOI: 10.1080/02726351.2015.1081657

Brecker, J.N.; Brown, R.; Matsuo, T.; Saito, K.; Sweeney, J.A.; Vansaun, J.B.; Shaw, M. C. (1969) Fourth Annual Report of Abrasive Grain Association on Investigation of Abrasive Grain Characteristics, Carnegie Institute of Technology, USA.

Camacho J. M.; Sosa, V. (2013) Alternative method to calculate the magnetic field of permanent magnets with azimuthal symmetry. Revista Mexicana de F´ısica E, 59: 8–17

Cheng, H.; Feng, Y.; Wang, T.; Dong, Z. (2010) Magnetorheological finishing of optical surface combined with symmetrical tool function. Frontiers of Optoelectronics, 3(4): 408–412.

Cheng, H.; Yeung, Y.; Tong, H. (2008) Viscosity behavior of magnetic suspensions in fluid assisted finishing, Progress in Natural Science, 18: 91–96.

Das, M.; Jain, V.K.; Ghoshdastidar, P.S. (2010) Fluid flow analysis of magnetorheological abrasive flow finishing process. International Journal of Machine Tools and Manufacture, 48: 415–426.

Ein-Eliy; Starosvetsky, D. (2007) Review on copper chemical-mechanical polishing (CMP) and post CMP cleaning in ultra large system integrated (ULSI)- An electrochemical perspective. Electrochemica Acta, 52:1825–1838.

Gheisari, R.; Ghasemi, A.A.; Jafarkarimi, M.; Mohtaram, S. (2014) Experimental studies on the ultraprecision finishing of cylindrical surfaces using magnetorheological finishing process. Production & Manufacturing Research, 2: 550–557.

Gorana, V.V.; Jain, V.K.; Lal, G.K., (2004) Experimental investigation into cutting forces and active grain density during abrasive flow machining. International Journal of Machine Tools and Manufacture, 44: 201–211.

Gorodkin, S.; Zhuravski, N. (2002) Surface shear stress enhancement under MR fluid deformation, International Journal of Modern Physics – Part B. 16/17–18: 2745–2750.

Grover, V.; Singh, A.K., (2017) A novel magnetorheological honing process for nano-finishing of variable cylindrical internal surfaces. Materials and Manufacturing Processes, DOI: 10.1080/10426914.2016.1257801

Grover, V.; Singh, A.K., (2017) Analysis of particles in magnetorheological polishing fluid for finishing of ferromagnetic cylindrical workpiece. Particulate Science and Technology, DOI: 10.1080/02726351.2017.1302535.

Ida, N., (2000) Engineering Electromagnetics. Springer-Verlag New York Inc.,525–628.

Jain, R.K.; Jain V.K.; Dixit P.M. (1999) Modeling of material removal and surface roughness in abrasive flow machining process, International Journal of Machine Tools and Manufacture, 39: 1903–1923.

Jain, V.K. (2009) Magnetic field assisted abrasive based micro-/nano-finishing. Journal of Materials Processing Technology, 209: 6022–6038.

Jha S.; Jain, V.K. (2004), Design and development of the magnetorheological abrasive flow finishing (MRAFF) process. International Journal of Machine tools and Manufacture, 44: 1019–1029.

Jha S.; Jain, V.K. (2006), Modeling and simulation of surface roughness in magnetorheological abrasive flow finishing (MRAFF) process, Wear, 261: 856–866.

Jha, S.; Jain, V.K. (2005) Nano finishing techniques. Micro manufacturing and Nano-Technology. Mahalik, N.P. ed. Springer Verlag, New York, 171–195.

Judal, K.B.; Yadava, V.; Pathak, D. (2013), Experimental investigation of vibration assisted cylindrical magnet abrasive finishing of Aluminium workpiece. Materials and Manufacturing Processes, 28: 1196–1202.

Kang, J.; George, A.; Yamaguchi, H. (2012) High-speed internal finishing of capillary tubes by magnetic abrasive finishing. Procedia CIRP, 1: 414–418.

Khan, D.A.; Jha, S. (2016) Selection of Optimum Polishing Fluid Composition for Ball End Magnetorheological Finishing of Copper. Proceedings of 6th International & 27th All India Manufacturing Technology, Design and Research Conference, 316–319.

Khanna, O.P.; Lal, M. (2010) A text book of Production Technology. Dhanpat Rai publication: New Delhi, India.

Komanduri, R.; Lucca, D.A.; Tani, Y. (1997) Technological advances in fine abrasive processes. Annals of CIRP 46(2): 545-596.

Kordonski, W. I.; Shorey, A.B. (2007) Magnetorheological (MR) jet finishing technology. Journal of Intelligent Material Systems and Structures, 18(12); 1127–1130.

Kordonski, W. I.; Shorey, A.B.; Tricard, M. (2006) Magnetorheological jet finishing technology. Transactions of ASME, 128: 20–26.

Kordonski, W.I.; Golini, D. (1999) Fundamentals of magnetorheological fluid utilization in high precision finishing, Journal of Intelligent Material Systems and Structures, 10(9): 683–689.

Lynah, P.; Hoffman, P.R. (1989) Machining Metals Handbook, American Society for Metals: Metals Park.

Mori, Y.; Yamauchi, K.; Endo, K. (1987) Elastic Emission machining. Precision Engineering 9(3):123–128.

Nanz, G.; Camilletti, L.E. (1995) Modeling of chemical-mechanical polishing: A review. IEEE Transaction on Semiconductor Manufacturing 8: 382-389.

Newswander, T.; Crowther, B.; Gubbels, G.; Senden, R. (2013) Aluminum alloy AA-6061and RSA-6061 heat treatment for large mirror applications. Material Technologies and Applications to Optics, Structures, Components and Sub-Systems, 883–890.

Niranjan, M.; Jha, S.; Kotnala, R.K. (2014) Ball End magnetorheological finishing using bidisperse magnetorheological polishing fluid. Materials and Manufacturing Processes 29: 487-492.

Niranjan, M.S.; Jha, S. (2014) Flow behaviour of bidisperse MR polishing fluid and ball end MR finishing. Procedia Materials Science 6: 798-804.

Ranjan, P.; Balasubramaniam, R.; Jain, V.K. (2017) Analysis of magnetorheological fluid behavior in chemo-mechanical magnetorheological finishing (CMMRF) process. Precision Engineering, DOI: 10.1016/j.precisioneng.2017.02.001

Sadiq, A.; Shunmugam M. S. (2010) A novel method to improve finish on non-magnetic surfaces in magnetorheological abrasive honing process, Tribology International, 43:1122–1126.

Sadiq, A.; Shunmugam, M.S. (2009) Investigation into magnetorheological abrasive honing (MRAH). International Journal of Machine tools and Manufacture, 49: 554–560.

Saraeian, P.; Mehr, H.S.; Moradi, B.; Tavakoli, H.; Alrahmani, O.K. (2016) Study of magnetic abrasive finishing for AISI321 stainless steel. Materials and Manufacturing Processes: DOI: 10.1080/10426914.2016.1140195.

Saraswathamma, K.; Jha, S.; Rao, P.V. (2015) Experimental investigation into Ball end Magnetorheological Finishing of silicon. Precision Engineering 42: 218–223.

Schmitt, C.; Bahre, D. (2014) Analysis of the process dynamics for the precision honing of bores. Procedia CIRP, 17: 692–697.

Schmitt, C.; Moos, U.; Bahre, D. (2003) Comparison of different approaches to force controlled precision honing of bores. Journal of Mechanics Engineering and Automation, 3: 764–771.

Schnitzler, G. (2001) What's happening with honing. Manufacturing Engineering, 127(5): 70–72, 75–77.

Seok, J.; Kim, Y.J.; Jang, K.I.; Min, B.K.; Lee S. J. (2007) A study on the fabrication of curved surfaces using magnetorheological fluid finishing, International Journal of Machine Tools & Manufacture, 47: 2077– 2090.

Shankar, M.R.; Jain, V.K.; Ramkumar, J. (2010) Rotational Abrasive Flow Finishing (R-AFF) Process and its Effects on Finished Surface Topography. International Journal of Machine Tools and Manufacture, 50(7): 637–650.

Shaw, M.C. (1996) Principles of Abrasive Processing, Clarendon Press, Oxford: United Kingdom.

Sidpara, A.; Jain, V.K. (2013) Analysis of forces on the free form surface in magnetorheological fluid based finishing process. International Journal of Machine Tools and Manufacture, 69: 1–10.

Singh, A.K.; Jha, S.; Pandey P.M. (2011) Design and development of nano-finishing process for 3D surfaces using ball end MR finishing tool. International Journal of Machine tools and Manufacture, 51: 142–151.

Singh, A.K.; Jha, S.; Pandey P.M. (2013) Mechanism of material removal in ball end magnetorheological finishing process, Wear, 302: 180–191.

Singh, A.K.; Jha, S.; Pandey, P.M. (2012) Nano finishing of a typical 3D ferromagnetic workpiece using a ball end magnetorheological finishing process. International Journal of Machine tools and Manufacture, 63: 21–31.

Singh, A.K.; Jha, S.; Pandey, P.M. (2012) Nanofinishing of fused silica glass using ball end magnetorheological finishing tool. Materials and Manufacturing Processes, 27: 1139–1144.

Singh, A.K.; Jha, S.; Pandey, P.M. (2012) Performance Evaluation of Improved Ball End Magnetorheological Finishing Process. World Academy of Science and Technology, 6: 1193–1197.

Singh, D.K.; Jain, V.K.; Raghuram, V. (2004) Parametric study of magnetic abrasive finishing process. Journal of Materials Processing Technology, 149: 22–29.

Talwinder Singh Bedi , Anant Kumar Singh (2015): Magnetorheological methods for nanofinishing – a review, Particulate Science and Technology, DOI: 10.1080/02726351.2015.1081657

Tolinski, M. (2008) High-Performance Honing: Combination of honing process equipment and tooling create highly finished surfaces. Manufacturing Engineering, 140(6): 57–68.

Torres, A.; Luis, C.J.; Puertas, I. (2016) EDM machinability and surface roughness analysis of TiB2 using copper electrodes. Journal of Alloys and Compounds, DOI: 10.1016/j.jallcom.2016.08.110.

Voitsenya, V.S.; Bardamid, A.F.; Borisenko, Y.N.; Grigorenko, B.V.; Gritsyna, V.I.; Gritsyna, V.T.; Konovalov, V.G.; Orlinskij, D.V.; Poperenko, L.V.; Ruzhitskij, V.V.; Rybalko, V.F.; Shapoval, A.N.; Vinnichenko, N.V.; Yakimov, K.I. (1996) Imitation of effects of a fusion reactor environment on optical properties of metallic mirrors. Journal Nuclear Materials, 1239–1243.

Wang, A.C.; Lee, S.J. (2009) Study the characteristics of magnetic finishing with gel abrasive. International Journal of Machine Tools and Manufacture, 49: 1063–1069.

Wu, X.; Kita, Y.; Koku, K.I (2007) New polishing technology of freeform surface by GC, Journal of Materials Processing Technology 188: 81–84.

Zhong, Z.W. (2008) Recent advances in polishing of advanced materials. Materials and Manufacturing Processes 23 (5): 449–456.

Web References

W.1. Columbia Grinding, http://www.columbiagrinding.com/images/lapping_diagram.gif, (accessed on – 25/11/2016).

W.2. Watson Grinding, http://www.watsongrinding.com/wp-content/uploads/2011/12/Grinding.jpg, (accessed on – 25/11/2016).

List of Publications

SCI Journals:

1. **Kansal, H**.; Singh, A.K.; Grover, V. (2017) Magnetorheological nano-finishing of diamagnetic material using permanent magnets tool. Precision Engineering.
   Status: ***Published***
   Publisher: Elsevier
   Impact factor:2.77

2. **Kansal, H**.; Singh, A.K. (2017) Experimental Investigations into Magnetorheological Nano-finishing of Copper Alloy Materials. Journal of Engineering Materials and Technology *Status:* ***Submitted***
   Publisher: ASME
   Impact factor: 1.14

International Conferences:

1. **Kansal, H**.; Singh, A.K. (2016) Conceptualization of magnetorheological fluid assisted finishing process using permanent magnet. 4^{th} International conference on production and industrial engineering, CPIE-2016, December 20, 2016 at NIT Jalandhar.
   Status: ***Published***

2. **Kansal, H**.; Grover, V.; Singh, A.K. (2017) Development of New Magnetorheological Nano-finishing Tool Using Permanent Magnets for Flat Surfaces. 39^{th} MATADOR Conference on advanced manufacturing, MATADOR 2017, July 5^{th}-7^{th}, 2017 at University of Manchester.
   Status: ***Published***